Contents

Chapter 1

FIRST PASSAGE FUNDAMENTALS

We will study the following general questions about first-passage processes: (1) What is the time dependence of the first-passage probability – the probability that a random walk hits a specified point $\vec{r}$ *for the first time* at time t, $F(\vec{r},t)$? (2) What is the survival probability $S(t)$ – the probability that a diffusing particle has not hit the absorbing boundary by time t? (3) How long does it take for absorption to occur as a function of the starting point? (4) Where does absorption occur? (5) For an absorbing boundary consisting of disjoint subsets B_1 and B_2, what is the splitting probability, namely, the probability that a diffusing particle will eventually be trapped on B_1 or trapped on B_2 as a function of the particle position?

1.1 Connection between First-Passage and Occupation Probabilities

Let $P(\vec{r},t)$ be the probability that a random walk is at site $\vec{r}$ at time t when it starts at the origin. Similarly, let $F(\vec{r},t)$ be the first-passage probability, namely, the probability that the random walk visits $\vec{r}$ for the first time at time t with the same initial condition.

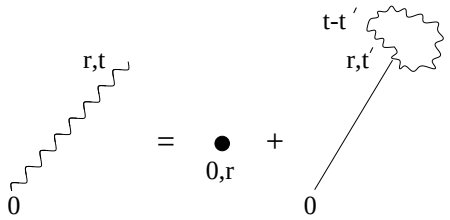

Figure 1.1: Diagrammatic relation between the occupation probability of a random walk (propagation is represented by a wavy line) and the first-passage probability (straight line).

We write $P(\vec{r},t)$ in terms of $F(\vec{r},t)$ and then invert this relation to find $F(\vec{r},t)$. For a random walk to be at $\vec{r}$ at time t, the walk must *first* reach $\vec{r}$ at some earlier time step t' and then return to $\vec{r}$ after $t-t'$ additional steps (Fig. 1.1). This connection between $F(\vec{r},t)$ and $P(\vec{r},t)$ may therefore be expressed as the convolution relation

$$P(\vec{r},t) = \delta_{\vec{r},0}\delta_{t,0} + \sum_{t'\leq t} F(\vec{r},t')\,P(0,t-t'), \tag{1.1.1}$$

where $\delta_{t,0}$ is the Kronecker delta function. The delta function accounts for the initial condition that the walk starts at $\vec{r}=0$. We solve (c1:fund) by introducing the generating functions, $P(\vec{r},z) = \sum_{t=0}^{\infty} P(\vec{r},t)z^t$

and $F(\vec{r},z)=\sum_{t=0}^{\infty}F(\vec{r},t)z^t$. Multiplying Eq. (1.1.1) by z^t, summing over all t, and solving for F gives

$$F(\vec{r},z)=\begin{cases}\dfrac{P(\vec{r},z)}{P(0,z)}, & \vec{r}\neq 0\\[2ex] 1-\dfrac{1}{P(0,z)}, & \vec{r}=0\end{cases}. \tag{1.1.2}$$

1.2 Transience and Recurrence

For diffusion that starts at the origin, $P(\vec{r}=0,t)=(4\pi Dt)^{-d/2}$, and the generating function is

$$P(0,z)\approx\int^{\infty}P(0,t)\,z^t\,dt\sim\int^{\infty}(4\pi Dt)^{-d/2}z^t\,dt. \tag{1.2.1}$$

This integral has two different behaviors, depending on whether $\int^{\infty}P(0,t)\,dt$ diverges or converges. In the former case, we obtain

$$P(0,z)\propto\int^{t*}(4\pi Dt)^{-d/2}\,dt\sim\begin{cases}(t^*)^{1-d/2}=(1-z)^{d/2-1}, & d<2\\[2ex] \ln t^*=-\ln(1-z), & d=2\end{cases}. \tag{1.2.2}$$

For $d>2$, the integral $\int^{\infty}P(0,t)\,dt$ converges and we compute the asymptotic behavior of $P(0,1)-P(0,z)$. By definition, $F(0,1)=\sum_t F(0,t)=1-(P(0,1))^{-1}$. Further, $\sum_t F(0,t)$ is just the eventual probability $\mathcal{R}$ that a random walk reaches the origin, so that $P(0,1)=(1-\mathcal{R})^{-1}$. In the asymptotic limit $z=1-s$, with $s\to 0$, $P(0,1)-P(0,z)$ may therefore be written as

$$P(0,1)-P(0,z)\propto\sum_{t=1}^{\infty}t^{-d/2}(1-z^t)\sim(1-z)^{d/2-1}. \tag{1.2.3}$$

Thus $P(0,z)$ has the asymptotic behavior

$$P(0,z)\sim(1-\mathcal{R})^{-1}+(1-z)^{d/2-1}+\ldots,\qquad d>2. \tag{1.2.4}$$

Thus the generating function for the first-passage probability has the asymptotic behaviors

$$F(0,z)\sim\begin{cases}1-(1-z)^{1-d/2}, & d<2\\[2ex] 1+\dfrac{1}{\ln(1-z)}, & d=2\\[2ex] \mathcal{R}+(1-\mathcal{R})^2(1-z)^{d/2-1}, & d>2\end{cases}, \tag{1.2.5}$$

From this generating function, we determine the time dependence of the survival probability by

$$F(0,z=1-1/t^*)\sim\int_0^{t^*}F(0,t)\,dt\equiv T(t^*)=1-S(t^*), \tag{1.2.6}$$

where $S(t)$ is the survival probability and $T(t)$ is the probability that the particle reaches the origin by time t. From Eqs. (1.2.5) and (1.2.6) we thus find

$$S(t)\sim\begin{cases}\dfrac{1}{t^{1-d/2}}, & d<2\\[2ex] \dfrac{1}{\ln t}, & d=2\\[2ex] (1-\mathcal{R})+(1-\mathcal{R})^2t^{1-d/2}, & d>2\end{cases}. \tag{1.2.7}$$

The time dependence of the first-passage probability may be obtained from $1 - S(t) \sim \int^t F(0,t)\,dt$ to give

$$F(0,t) = -\frac{\partial S(t)}{\partial t} \propto \begin{cases} t^{d/2-2}, & d<2 \\ \dfrac{1}{t\ln^2 t}, & d=2 \\ t^{-d/2}, & d>2 \end{cases}. \tag{1.2.8}$$

For $d \leq 2$, the survival probability $S(t)$ ultimately decays to zero – a random walk is *recurrent* – certain to eventually return infinitely often to its starting point, and indeed visit *any* site of an infinite lattice.

There is a simple argument for recurrence. After a time t, a random walk explores a domain of radius $\sqrt{Dt}$. The total number of sites visited during this exploration is also proportional to t. Consequently in d dimensions, the density of visited sites within this exploration domain is $\rho \propto t/t^{d/2} \propto t^{1-d/2}$. Since this diverges as $t \to \infty$ for $d < 2$, a random walk visits each site within the sphere infinitely often. On the other hand, for $d > 2$, Eq. (1.2.7) predicts that there is a non-zero probability for a diffusing particle to not return to its starting point. This behavior is known as *transient*.

1.3 Connection between First-Passage and Electrostatics

We now outline fundamental connections between the first-passage properties and electrostatics. Basic questions of first-passage include *where* a diffusing particle is absorbed and *when* absorption occurs. These are *time-integrated* attributes, obtained by integration of a time-dependent observable over all time. For example, to determine when a particle is absorbed, we compute the first-passage probability to the boundary and then integrate over all time to obtain the *eventual hitting probability*. However, it is more elegant to first integrate the equation of motion over time and then compute the outgoing flux at the boundary. The first step transforms the diffusion equation to the simpler Laplace equation. Then, in computing the flux, the exit probability is just the electric field at the boundary point. Thus there is a complete correspondence between a first-passage and electrostatics in the same geometry.

1.3.1 The Green's Function Formalism

Consider a diffusing particle that starts at $\vec{r}_0$ within a domain with boundary B. The conventional way to compute first-passage properties is to solve for the Green's function for the diffusion equation

$$\frac{\partial c(\vec{r},t;\vec{r}_0)}{\partial t} = D\nabla^2 c(\vec{r},t;\vec{r}_0), \tag{1.3.1}$$

with the initial condition $c(\vec{r},0;\vec{r}_0) = \delta(\vec{r}-\vec{r}_0)$ and the absorbing boundary condition $c(\vec{r},t;\vec{r}_0)|_{\vec{r}\in B} = 0$. This condition accounts for the fact that once a particle reaches the boundary it leaves the system. The outgoing flux at $\vec{r}_B$, $j(\vec{r}_B,t)$, is simply

$$j(\vec{r}_B,t) = -D\frac{\partial c(\vec{r},t)}{\partial \hat{n}}\Big|_{\vec{r}=\vec{r}_B}, \tag{1.3.2}$$

where $\hat{n}$ is a unit outward normal at $\vec{r}_B$. Finally, the eventual hitting probability at $\vec{r}_B$ is

$$\mathcal{E}(\vec{r}_B) = \int_0^\infty j(\vec{r}_B,t)\,dt. \tag{1.3.3}$$

In this direct approach, we first solve the diffusion equation, which has a first derivative in time, and then effectively "undo" the differentiation by integrating over all time to find the eventual hitting probability.

We now re-derive this hitting probability by mapping the problem to electrostatics. First we integrate Eq. (1.3.1) over all time to give

$$c(\vec{r},t=\infty) - c(\vec{r},t=0) = D\nabla^2 \mathcal{C}_0(\vec{r}), \tag{1.3.4}$$

where $\mathcal{C}_0(\vec{r}) = \int_0^\infty c(\vec{r},t)\,dt$ is the time integral of the Green's function. At $t=0$ the Green's function reduces to the initial condition $c(\vec{r},t=0) = \delta(\vec{r}-\vec{r}_0)$. Thus $\mathcal{C}_0(\vec{r})$ obeys the Laplace equation

$$D\nabla^2\mathcal{C}_0(\vec{r}) = -\delta(\vec{r}-\vec{r}_0), \tag{1.3.5}$$

with homogeneous Dirichlet boundary conditions. This defines an electrostatic system with a point charge of magnitude $1/(D\Omega_d)$ at $\vec{r}_0$ (where Ω_d is the surface area of a d-dimensional unit sphere). The absorbing boundaries in the diffusive system are equivalent to grounded conducting surfaces in the corresponding electrostatic problem.

In terms of $\mathcal{C}_0$, the eventual hitting probability $\mathcal{E}(\vec{r}_B)$ is given by

$$\mathcal{E}(\vec{r}_B) = \int_0^\infty j(\vec{r}_B,t)\,dt = -D\int_0^\infty \frac{\partial c(\vec{r},t)}{\partial \hat{n}}\,dt = -D\frac{\partial \mathcal{C}_0}{\partial \hat{n}}. \tag{1.3.6}$$

On the other hand, from Eq. (1.3.5) this normal derivative is just the electric field associated with the initial charge distribution. This leads to the following fundamental conclusion:

- For a diffusing particle that is initially at $\vec{r}_0$ inside a domain with absorbing boundary conditions, the eventual hitting probability to a boundary point $\vec{r}_B$ equals the electric field at this same location when a point charge of magnitude $1/(D\Omega_d)$ is placed at $\vec{r}_0$ and the domain boundary is grounded.

The electrostatic formalism can be extended to integer moments of the mean hitting time. By definition, the n^{th} moment of this time is

$$\langle t^n\rangle = \int_0^\infty t^n F(t)\,dt, \tag{1.3.7}$$

where $F(t)$ is the first-passage probability to the boundary. Here we tacitly consider situations for which the particle is certain to exit. Using $F(t) = -\frac{\partial S(t)}{\partial t}$, we integrate by parts to obtain

$$\begin{aligned}\langle t^n\rangle = -\int_0^\infty t^n\,\frac{\partial S(t)}{\partial t}\,dt &= -t^n\,S(t)\Big|_0^\infty + n\int_0^\infty t^{n-1}\,S(t)\,dt \\ &= n\int_0^\infty t^{n-1}\,dt\int_V c(\vec{r},t)\,d\vec{r}.\end{aligned} \tag{1.3.8}$$

In the special case of $n=1$, the mean exit time is simply $\langle t\rangle = \int_0^\infty S(t)\,dt$.

We now recast this derivation for $\langle t^n\rangle$ as a time independent problem by reversing the order of the temporal and the spatial integrations. First, we define the time-integrated moments of the probability distribution

$$\mathcal{C}_n(\vec{r}) = \int_0^\infty c(\vec{r},t)\,t^n\,dt. \tag{1.3.9}$$

Then from Eq. (1.3.8), the n^{th} moment of the mean exit time is just the time-independent expression

$$\langle t^n\rangle = n\int_V \mathcal{C}_{n-1}(\vec{r})\,d\vec{r}. \tag{1.3.10}$$

Each of these integrated moments satisfies the Poisson equation with an n-dependent source term. Consider

$$\int_0^\infty t^n\,\left[\frac{\partial c(\vec{r},t)}{\partial t} = D\nabla^2 c(\vec{r},t)\right]\,dt. \tag{1.3.11}$$

Integrating the left-hand side by parts, the integrated term, $t^n c(\vec{r},t)\big|_0^\infty$, vanishes, except for $n=0$, where the lower limit coincides with the initial condition. The remaining term, $-\int_0^\infty n\,t^{n-1}c(\vec{r},t)\,dt$, is proportional to the time-integrated moment of order $n-1$. Therefore $\mathcal{C}_n(\vec{r})$ obeys the equation hierarchy

$$\begin{aligned} D\nabla^2\mathcal{C}_0(\vec{r}) &= -\delta(\vec{r}-\vec{r}_0),\\ D\nabla^2\mathcal{C}_1(\vec{r}) &= -\mathcal{C}_0(\vec{r}),\\ D\nabla^2\mathcal{C}_2(\vec{r}) &= -2\mathcal{C}_1(\vec{r}),\\ &\vdots \end{aligned} \tag{1.3.12}$$

Thus each $\mathcal{C}_n$ is the electrostatic "potential" generated by the "charge" distribution $\mathcal{C}_{n-1}$. This provides all moments of the first-passage time in terms of an associated hierarchy of electrostatic potentials.

1.3.2 Laplacian Formalism

Another useful version of the correspondence between diffusion and electrostatics is based on encoding the initial condition as the spatial argument of an electrostatic potential rather than as an initial condition. This Laplacian approach gives the splitting probability for composite domain boundaries in a natural fashion and also provides *conditional* hitting times.

For simplicity, we start with a symmetric nearest-neighbor random walk in the finite interval $[x_-, x_+]$ and then take the continuum limit after developing the formalism. We define $\mathcal{E}_-(x)$ as the probability for a particle, that starts at x, to eventually hit x_- *without* hitting x_+. Pictorially, we obtain the eventual hitting probability $\mathcal{E}_-(x)$ by summing the probabilities for all paths that start at x and reach x_- without touching x_+ (Fig. 1.2). A parallel statement holds for $\mathcal{E}_+(x)$. Thus

$$\mathcal{E}_\pm(x) = \sum_{p_\pm} \mathcal{P}_{p_\pm}(x), \tag{1.3.13}$$

where $\mathcal{P}_{p_\pm}(x)$ denotes the probability of a path from x to $x_\pm$ that avoids $x_\mp$. As illustrated in Fig. 1.2, the sum over all such restricted paths can be decomposed into the outcome after one step and the sum over all path remainders from the intermediate point x' to $x_\pm$. This gives

$$\mathcal{E}_\pm(x) = \sum_{p_\pm} \left[\frac{1}{2}\,\mathcal{P}_{p_\pm}(x+\delta x) + \frac{1}{2}\,\mathcal{P}_{p_\pm}(x-\delta x)\right] = \frac{1}{2}[\mathcal{E}_\pm(x+\delta x) + \mathcal{E}_\pm(x-\delta x)]. \tag{1.3.14}$$

By a simple rearrangement, this is equivalent to $\Delta^{(2)}\mathcal{E}_\pm(x) = 0$, where $\Delta^{(2)}$ is the discrete second-difference operator.

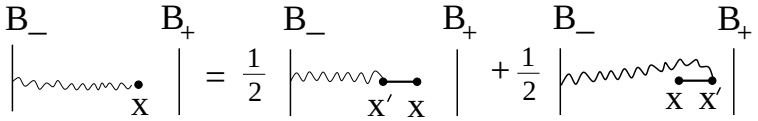

Figure 1.2: Decomposition of random walk paths from x to the absorbing subset B_- (the point x_-) into the outcome after one step and the remainder from x' to B_-. The factors 1/2 account for the probabilities associated with the first step of the decomposed paths.

This basic equation for $\mathcal{E}$ is subject to the boundary conditions $\mathcal{E}_-(x_-) = 1$, $\mathcal{E}_-(x_+) = 0$, and correspondingly $\mathcal{E}_+(x_-) = 0$, $\mathcal{E}_+(x_+) = 1$. In the continuum limit, we obtain the Laplace equation $\nabla^2\mathcal{E}_\pm(\vec{r}) = 0$, subject to the boundary conditions $\mathcal{E}_-(x_-) = 1$ and $\mathcal{E}_-(x_+) = 0$; that is $\mathcal{E}_- = 1$ on the exit subset of the absorbing boundary and $\mathcal{E}_- = 0$ on the complement of this boundary. These conditions are interchanged for $\mathcal{E}_+$. Because $\mathcal{E}_\pm$ satisfies the Laplace equation, we can transcribe well-known results from electrostatics to less familiar, but corresponding, first-passage properties.

This approach can be extended in an obvious way to more general hopping processes with both a spatially-varying bias and diffusion coefficient. As an example, consider a diffusing particle that is initially at radius r_0 exterior to a sphere of radius a centered at the origin in d dimensions. By the electrostatic formalism, the probability that this particle eventually hits the sphere is simply the electrostatic potential at r_0, $\mathcal{E}_-(r_0) = (a/r_0)^{d-2}$

We now use the Laplacian approach to determine the mean exit time from a domain with composite boundaries. Here we distinguish between the *unconditional* mean exit time, namely, the time for a particle to reach any point on an absorbing boundary B, and the *conditional* mean exit time, namely, the time for a particle to reach a specified subset of the absorbing boundary B_- *without* touching the complement boundary $B_+ = B - B_-$.

We again treat a symmetric random walk on the finite interval $[x_-, x_+]$; the generalization to higher dimensions and to general hopping processes is straightforward. Let the time increment between successive steps be δt, and let $t(x)$ denote the mean time to exit at *either* boundary component when a particle starts

at x. This quantity is simply the time for each exit path times the probability of the path, averaged over all particle trajectories. This leads to the analog of Eq. (1.3.13)

$$t(x) = \sum_p \mathcal{P}_p(x)\, t_p(x), \tag{1.3.15}$$

where $t_p(x)$ is the exit time of a specific path to the boundary that starts at x.

In analogy with Eq. (1.3.14), this mean exit time obeys the recursion formula

$$t(x) = \frac{1}{2}\left[(t(x+\delta x)+\delta t) + (t(x-\delta x)+\delta t)\right], \tag{1.3.16}$$

with the boundary conditions $t(x_-) = t(x_+) = 0$, corresponding to the exit time being equal to zero if the particle starts at the boundary. This recursion relation expresses the mean exit time starting at x in terms of the outcome one step in the future, for which the initial walk can be viewed as restarting at either $x+\delta x$ or $x-\delta x$, each with probability 1/2, but also with the time incremented by δt. In the continuum limit, the corresponding Poisson equation for the exit time is $D\nabla^2 t(\vec{r}) = -1$, subject to the boundary condition $t(\vec{r}) = 0$ for $\vec{r} \in B$.

Finally, we extend this electrostatic formalism to the conditional exit times in which we discriminate the exit time by which part of the boundary is reached. Thus let $t_-(x)$ be the conditional mean exit time for a random walk that starts at x and exits at B_- without hitting B_+. Similarly let $t_+(x)$ be the conditional mean exit time for a random walk that starts at x and exits at B_+ without hitting B_-. By its definition, $t_-(x)$ can be written as

$$t_-(x) = \frac{\sum_{p_-} \mathcal{P}_{p_-}(x)\; t_{p_-}(x)}{\sum_{p_-} \mathcal{P}_{p_-}(x)} = \frac{\sum_{p_-} \mathcal{P}_{p_-}(x)\; t_{p_-}(x)}{\mathcal{E}_-(x)}, \tag{1.3.17}$$

where the sum over paths p_- denotes only the allowed paths that start at x and reach B_- without touching B_+. By decomposing each path as the outcome after one step and its remainder, and then applying Eq. (1.3.14), we may write

$$\begin{aligned}
\mathcal{E}_-(x)t_-(x) &= \sum_{p_-} \frac{1}{2}[\mathcal{P}_{p_-}(x-\delta x)(t_{p_-}(x-\delta x)+\delta t) + \mathcal{P}_{p_-}(x+\delta x)(t_{p_-}(x+\delta x)+\delta t)] \\
&= \delta t\, \mathcal{E}_-(x) + \frac{1}{2}[\mathcal{E}_-(x-\delta x)t_-(x-\delta x) + \mathcal{E}_-(x+\delta x)t_-(x+\delta x)] \\
&\approx \delta t\, \mathcal{E}_-(x) + \left[\mathcal{E}_-(x)t_-(x) + \frac{\delta x^2}{2}\frac{\partial^2 \mathcal{E}_-(x)t_-(x)}{\partial x^2}\right].
\end{aligned} \tag{1.3.18}$$

In the continuum limit, this leads to a Poisson equation for the conditional mean first-passage time (now written for general spatial dimension)

$$D\nabla^2[\mathcal{E}_-(\vec{r})t_-(\vec{r})] = -\mathcal{E}_-(\vec{r}), \tag{1.3.19}$$

with $D = 2(\delta r)^2/2\delta t$ and subject to the boundary conditions $\mathcal{E}_-(\vec{r})t_-(\vec{r}) = 0$ both on B_- (where t_- vanishes) and on B_+ (where $\mathcal{E}_-$ vanishes). The governing equations and boundary conditions for $t_+(\vec{r})$ are entirely analogous.

1.4 Random Walks and Resistor Networks

There is a deep relation between first-passage properties of random walks and resistor networks. We shall show that the voltages at each site and the overall network resistance are directly and simply related to the exit probabilities of a corresponding random walk. To develop this network connection, consider a discrete random walk on a finite lattice graph with hopping between nearest-neighbor sites (see Fig. 1.3). We divide the boundary points into two classes, B_+ and B_-. As usual, we are interested in the exit probabilities to

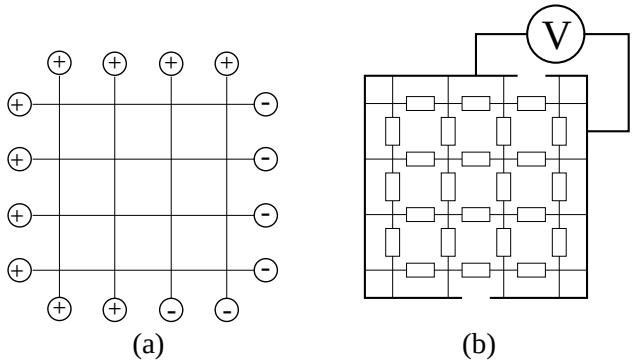

Figure 1.3: (a) A lattice graph with boundary sites B_+ or B_-. (b) Corresponding resistor network in which each bond (with rectangle) is a 1-Ω resistor. The sites in B_+ are all fixed at potential $V = 1$, and sites in B_- are all grounded.

B_+ and to B_- as functions of the initial position x of the random walk. As shown in Section 1.3, these exit probabilities, $\mathcal{E}_+(x)$, and $\mathcal{E}_-(x)$, respectively, are governed by the discrete Laplace equation $\Delta^{(2)}\mathcal{E}_\pm(x) = 0$, subject to the boundary conditions $\mathcal{E}_+ = 1$ on B_+ and $\mathcal{E}_+ = 0$ on B_- and vice versa for $\mathcal{E}_-$.

This Laplace equation has a simple resistor network interpretation. The basic connection is that if all the lattice bonds are viewed as resistors (not necessarily identical), then Kirchhoff's laws for steady current flow in the network are identical to the discrete Laplace equation for $\mathcal{E}$. Suppose that the boundary sites in B_+ are fixed at unit potential while the sites in B_- are grounded. The net current at each interior site i of the network must be zero, since there is current input and output only at the boundary. This current conservation condition is

$$\sum_j g_{ij}(V_i - V_j) = 0, \tag{1.4.1}$$

where g_{ij} is the conductance of the bond between sites i and j, V_i is the voltage at site i, and the sum runs over the nearest neighbors j of site i. Solving for V_i gives

$$V_i = \frac{\sum_j g_{ij}V_j}{\sum_j g_{ij}} \to \frac{1}{4}\sum_j V_j, \tag{1.4.2}$$

where the last step applies for a homogeneous network. Thus in the steady state, the voltage at each interior site equals the weighted average of the voltages at the neighboring sites; that is, V_i is a harmonic function with respect to the weight function g_{ij}. The voltage must also satisfy the boundary conditions $V = 1$ for sites in B_+ and $V = 0$ for sites in B_-.

We can also give a random-walk interpretation for the process defined by Eq. (1.4.2). Consider a lattice random walk in which the probability of hopping from site i to site j is $P_{ij} = g_{ij}/\sum_j g_{ij}$. Then the probability that this walk eventually reaches B_+ without first reaching B_- is just given by $\mathcal{E}_+(i) = \sum_{p_+} \mathcal{P}_{p_+}(i)$. Because both V_i and $\mathcal{E}_+(i)$ are harmonic functions that satisfy the same boundary conditions, these two functions are identical. Thus we find the basic relation between random walks and resistor networks:

- Let the boundary sets B_+ and B_- in a resistor network be fixed at voltages 1 and 0 respectively, with g_{ij} the conductance of the bond between sites i and j. Then the voltage at any interior site i is the same as the probability for a random walk that starts at i to reach B_+ before reaching B_- when the hopping probability from i to j is $P_{ij} = g_{ij}/\sum_j g_{ij}$.

An important extension of this relation between escape probability and site voltages is to infinite networks. This provides a simple connection between the recurrence/transience transition of random walks on a given network and the electrical resistance of this same network. Suppose that the voltage V at the boundary sites

B_+ is set to one. Then the total current entering the network is given by

$$I = \sum_j (V - V_j) g_{+j} = \sum_j (1 - V_j) P_{+j} \sum_j g_{+j}. \tag{1.4.3}$$

Here g_{+j} is the conductance between the positive terminal of the voltage source and the neighboring sites j and $P_{+j} = g_{+j}/\sum_j g_{+j}$. Because the voltage V_j also equals the probability for the corresponding random walk to reach B_+ without reaching B_-, the term $V_j P_{+j}$ is just the probability that a random walk starts at B_+, makes a single step to the sites j (with hopping probabilities P_{ij}), and then returns to B_+ without reaching B_-. We therefore deduce that

$$I = \sum_j g_{+j} \sum_j (1 - V_j) P_{+j} = \sum_j g_{+j} \times (1 - \text{return probability}) = \sum_j g_{+j} \times \text{escape probability}. \tag{1.4.4}$$

Here "escape" means reaching the opposite terminal of the voltage source without returning to the starting point.

On the other hand, the input current and the voltage drop across the network are simply related to the conductance G between the two boundary sets by $I = GV = G$. From this and Eq. (1.4.4) we obtain

$$\text{escape probability} \equiv P_{\text{escape}} = \frac{G}{\sum_j g_{+j}}. \tag{1.4.5}$$

Perhaps the most interesting situation is when a current I is injected at a single point of an infinite network with outflow at infinity (see Fig. 1.4). Then the escape probability for a random walk starting at this input point, that is, never return to its starting point, is simply proportional to the network conductance G.

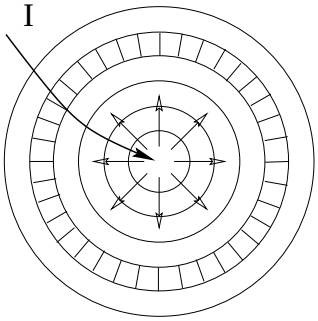

Figure 1.4: Decomposition of a conducting medium into concentric shells, each of which consists of fixed-conductance blocks. A current I is injected at the origin and flows radially outward through the medium.

In one dimension, the conductance of an infinitely long chain of identical resistors is zero. Thus $P_{\text{escape}} = 0$ or, equivalently, $P_{\text{return}} = 1$; a random walk in one dimension is recurrent. In higher dimensions, a crude physical estimate suffices to determine the recurrence or transience of a random walk. The basic idea of this estimate is to replace the discrete lattice with a continuum medium of constant conductivity. We then compute the conductance of the infinite system by further decomposing the medium into a series of concentric shells of fixed thickness dr. A shell at radius r can be regarded as a parallel array of r^{d-1} volume elements, each of which has a fixed conductance. The conductance of one such a shell is then simply proportional to its surface area, and the overall resistance is the sum of the shell resistance. This gives

$$R \sim \int^{\infty} R_{\text{shell}}(r)\, dr \sim \int^{\infty} \frac{dr}{r^{d-1}} = \begin{cases} \infty & \text{for } d \leq 2 \\ (P_{\text{escape}} \sum_j g_{+j})^{-1} & \text{for } d > 2 \end{cases} \tag{1.4.6}$$

For $d \leq 2$, the conductance to infinity is zero, essentially because there are an insufficient number of independent paths from the origin to infinity. Correspondingly, the escape probability is zero and the

random walk is recurrent. The case $d = 2$ is more delicate because the integral in expression (1.4.6) diverges only logarithmically at the upper limit. Nevertheless, the conductance to infinity slowly goes to zero as the radius of the network diverges and the corresponding escape probability is still zero.

Chapter 2

FIRST PASSAGE IN AN INTERVAL

For a particle in the interval $[0, L]$ with absorbing endpoints we wish to characterize the time dependence of the trapping. We study the following questions: (1) What is the the survival probability $S(t)$? (2) What are the first-passage and *eventual* probabilities to hit 0 and L as a function of starting position? (3) What is the mean exit time to either of the absorbing boundaries and the conditional exit times to hit a specified boundary as a function of starting position?

2.1 Survival and First-Passage Probabilities. Mean Exit Times

For a normalized initial concentration, the survival probability equals the spatial integral of the concentration $c(x, t)$ over the interval

$$S(t) \equiv \int_0^L c(x, t)\, dx. \tag{2.1.1}$$

In general, the solution to the diffusion equation may be written as the eigenfunction expansion

$$c(x, t) = \sum_{n=1}^{\infty} A_n \sin\left(\frac{n\pi x}{L}\right)\, e^{-(\frac{n\pi}{L})^2 Dt}, \tag{2.1.2}$$

where the constants A_n are determined by the initial condition. Each eigenmode decays exponentially in time, with a numerically different decay time $\tau_n = k_n^{-1} = L^2/n^2\pi^2 D$. Only the most slowly decaying eigenmode remains in the long time limit. As a result, the asymptotic survival probability is

$$S(t) \propto e^{-D\pi^2 t/L^2}. \tag{2.1.3}$$

At a finer level of description, we now investigate where a particle is trapped, as embodied by the first-passage probability to a specified boundary. We derive the first-passage probability by solving for the Green's function of the diffusion equation. Using the Laplace transform, the diffusion equation becomes $sc(x, s) - c(x, t = 0) = Dc''(x, s)$. In each subdomain $(0, x_0)$ and (x_0, L), the resulting homogeneous equation has the solution $c(x, s) = Ae^{x\sqrt{s/D}} + Be^{-x\sqrt{s/D}}$. We simplify the algebra by choosing the appropriate linear combination of exponential solutions that manifestly satisfies the boundary conditions at the outset. Thus:

$$c_<(x, s) = A \sinh\left(\sqrt{\frac{s}{D}}x\right), \quad x < x_0 \qquad c_>(x, s) = B \sinh\left(\sqrt{\frac{s}{D}}(L - x)\right), \quad x > x_0. \tag{2.1.4}$$

When continuity $c_<(x_0, s) = c_>(x_0, s)$ is imposed, the Green's function reduces to

$$c(x, s) = A \sinh\left(\sqrt{\frac{s}{D}}x_<\right) \sinh\left(\sqrt{\frac{s}{D}}(L - x_>)\right), \tag{2.1.5}$$

with $x_> = \max(x, x_0)$ and $x_< = \min(x, x_0)$. We determine the remaining constant A by the joining condition

$$c'(x, s)\big|_{x=x_0^+} - c'(x, s)\big|_{x=x_0^-} = -\frac{1}{D}.$$

to give

$$c(x,s) = \frac{\sinh\left(\sqrt{\frac{s}{D}}x_<\right)\sinh\left(\sqrt{\frac{s}{D}}(L-x_>)\right)}{\sqrt{sD}\sinh\left(\sqrt{\frac{s}{D}}L\right)}. \tag{2.1.6}$$

From this Green's function, first-passage properties follow directly. For example, the Laplace transform of the flux at $x = 0$ and at $x = L$ are

$$j_-(s;x_0) = \frac{\sinh(\sqrt{\frac{s}{D}}(L-x_0))}{\sinh(\sqrt{\frac{s}{D}}L)} \qquad j_+(s;x_0) = \frac{\sinh(\sqrt{\frac{s}{D}}x_0)}{\sinh(\sqrt{\frac{s}{D}}L)}. \tag{2.1.7}$$

Since the initial condition is normalized, the flux is identical to the first-passage probability to the boundaries. For $s = 0$, these Laplace transforms reduce to the time-integrated first-passage probabilities at 0 and at L. These quantities therefore coincide with the respective splitting probabilities, $\mathcal{E}_-(x_0)$ and $\mathcal{E}_+(x_0)$, as a function of the initial position x_0. Thus

$$\mathcal{E}_-(x_0) = j_-(s=0;x_0) = 1 - \frac{x_0}{L}, \qquad \mathcal{E}_+(x_0) = j_+(s=0;x_0) = \frac{x_0}{L}. \tag{2.1.8}$$

We now determine the lifetime of a particle in the interval, that is, the mean time until one of the boundaries is hit. We obtain this lifetime from the following power-series expansion of the flux in the Laplace domain

$$\begin{aligned} j_\pm(s;x_0) &= \int_0^\infty j_\pm(t;x_0)e^{-st}\,dt \\ &= \int_0^\infty j_\pm(t;x_0)\Big(1 - st + \frac{s^2t^2}{2!} - \frac{s^3t^3}{3!} + \ldots\Big)\,dt \\ &= \mathcal{E}_\pm(x_0)\Big(1 - s\langle t(x_0)\rangle_\pm + \frac{s^2}{2!}\langle t(x_0)^2\rangle_\pm - \frac{s^3}{3!}\langle t(x_0)^3\rangle_\pm + \ldots\Big), \end{aligned} \tag{2.1.9}$$

where $\mathcal{E}_\pm(x_0) = \int_0^\infty j_\pm(t;x_0)\,dt$ is the exit probability to $x = 0$ or $x = L$, respectively, starting at x_0, and

$$\langle t^n(x_0)\rangle_\pm = \frac{\int_0^\infty t^n\, j_\pm(t;x_0)\,dt}{\int_0^\infty j_\pm(t;x_0)\,dt} \tag{2.1.10}$$

are the corresponding moments of the mean first-passage time to these boundaries.

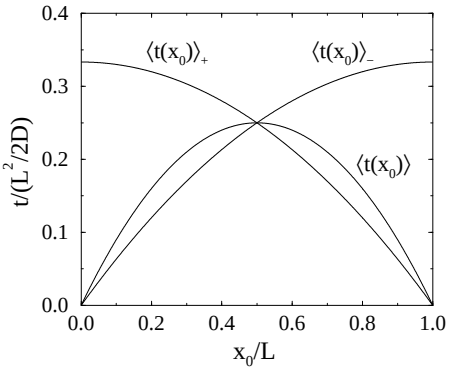

Figure 2.1: Unconditional and conditional mean exit times from the finite interval $[0, L]$ as a function of the dimensionless initial position x_0/L. The exit times are of the order of L for a particle that starts a distance of the order of one from an absorbing boundary and of the order of L^2 for a particle that starts near the middle.

Expanding the first-passage probabilities in Eqs. (2.1.7) in power series in s the conditional mean exit times to the left and right boundaries are, respectively,

$$\langle t(x_0)\rangle_- = \frac{2Lx_0 - x_0^2}{6D} \qquad \langle t(x_0)\rangle_+ = \frac{L^2 - x_0^2}{6D}. \tag{2.1.11}$$

Finally, the unconditional mean exit time (independent of which side is exited) is just the appropriately weighted average of the conditional mean exit times to each boundary,

$$\langle t(x_0)\rangle = \mathcal{E}_-(x_0)\langle t(x_0)\rangle_- + \mathcal{E}_+(x_0)\langle t(x_0)\rangle_+ = \frac{1}{2D}x_0(L - x_0). \tag{2.1.12}$$

2.2 Time Integrated Formulation

It is much simpler to first integrate the equation of motion over time to obtain the Laplace equation as the governing equation for the time-integrated concentration. Then exit probabilities, mean exit times, and related properties can be found from suitable moments of this integrated concentration.

We start by determining the exit probabilities to $x = 0$ or at $x = L$, as well as the corresponding exit times, as functions of starting position, by exploiting the electrostatic formulation of Section 1.3. Thus we compute the electrostatic potential in the interval with grounded endpoints due to a point charge of magnitude $1/2D$ at $x = x_0$. We solve $D\mathcal{C}_0''(x) = -\delta(x - x_0)$, subject to the boundary conditions $\mathcal{C}_0(0) = \mathcal{C}_0(L) = 0$. Here $\mathcal{C}_0(x)$ is the time integrated concentration $\mathcal{C}_0(x) = \int_0^\infty c(x,t)\,dt$. The Green's function is

$$\mathcal{C}_0(x) = \frac{1}{D}\,x_<\left(1 - \frac{x_>}{L}\right), \tag{2.2.1}$$

From this, the electric fields at each end are

$$\mathcal{E}_-(x_0) = +D\frac{\partial \mathcal{C}_0}{\partial x}\Big|_{x=0} = 1 - \frac{x_0}{L}, \qquad \mathcal{E}_+(x_0) = -D\frac{\partial \mathcal{C}_0}{\partial x}\Big|_{x=L} = \frac{x_0}{L}. \tag{2.2.2}$$

These are the exit probabilities to each end, thus reproducing Eqs. (2.1.8). The unrestricted exit time is obtained by integrating the potential over the interval. Thus

$$t(x_0) = \int_0^L \mathcal{C}_0(x)\,dx = \frac{1}{2D}x_0(L - x_0). \tag{2.2.3}$$

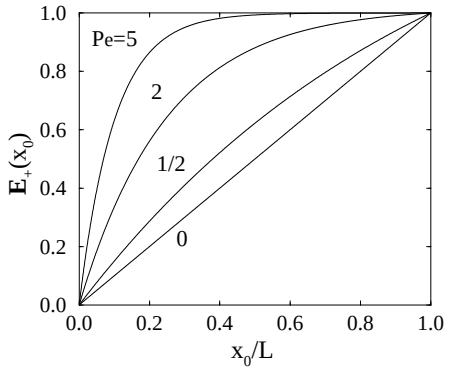

Figure 2.2: Dependence on $u_0 = x_0/L$ for the exit probability to the right boundary of a finite absorbing interval for various Péclet numbers Pe.

For biased diffusion, the exit probabilities at $x = 0$ and $x = L$ are

$$\mathcal{E}_-(x_0) = \frac{e^{-vx_0/D} - e^{-vL/D}}{1 - e^{-vL/D}} = \frac{e^{-2u_0Pe} - e^{-2Pe}}{1 - e^{-2Pe}}, \quad \mathcal{E}_+(x_0) = \frac{1 - e^{-vx_0/D}}{1 - e^{-vL/D}} = \frac{1 - e^{-2u_0Pe}}{1 - e^{-2Pe}}, \tag{2.2.4}$$

where $Pe \equiv \frac{vL}{2D}$ is the Péclet number and $u_0 = x_0/L$ the dimensionless initial position.

To appreciate this result, consider a two-person gambling game in which each person starts with the same capital, but where A wins \$1 with probability 51% in each trial. The ultimate outcome depends both on the relative initial condition *and* on the amount of capital. For this game, the Péclet number is $Pe = \frac{vL}{2D} = \frac{(p-q)L}{2}\frac{\delta x/\delta t}{\delta x^2/\delta t} = (p-q)L$. Here $\delta x = 1$ and $\delta t = 1$ are the increments in capital and in time, respectively, after each trial, and L is the sum of the capitals of both players. From Eqs. (2.2.4) the probability that B is eventually ruined is 0.622 for $Pe = 1$ (each player starting with \$25), 0.731 for $Pe = 2$ (each player starting with \$50); and 0.924 for $Pe = 5$ (each player starting with \$125). Therefore a slightly biased game leads to an overwhelming global bias if the scale of the game is sufficiently large, that is, $Pe \gg 1$.

Continuing with the electrostatic formulation, the unrestricted mean exit time when starting at x_0 is just the integral of $\mathcal{C}_0(x)$ over the interval. After some algebra,

$$t(x_0) = \frac{L^2}{2D}\frac{1}{Pe}\frac{(1-e^{-2u_0 Pe}) - u_0(1-e^{-2Pe})}{(1-e^{-2Pe})}. \tag{2.2.5}$$

This reduces to the limits $t(x_0) \to \frac{L-x_0}{v}$ as $v \to \infty$ and to $t(x_0) \to \frac{x_0(L-x_0)}{2D}$ as $v \to 0$ (Eq. (2.1.12)).

If we are interested in *only* the mean time until the particle reaches a boundary, the Laplacian formalism of Chap. 1 is the best approach. There are again two basic situations to consider: (a) the unconditional mean first-passage time to *either* boundary, and (b) the conditional mean first-passage time to a *specific* boundary, in which visits to the other boundary not allowed. As a preliminary, we reconsider the unconditional exit time $t(x)$ for a particle that starts at x with bias velocity v and diffusion coefficient D. As shown previously, $t(x)$ satisfies $Dt''(x)+vt'(x) = -1$ with boundary conditions $t(0) = t(L) = 0$. The solution is just Eq. (2.2.5).

The conditional mean exit times are more subtle. To determine $\mathcal{E}_\pm(x)$ and $t_\pm(x)$, we need to solve the basic Laplace and Poisson equations for the exit probabilities and conditional exit times, respectively,

$$\begin{aligned} D\mathcal{E}_\pm(x)'' + v\mathcal{E}_\pm(x)' &= 0, \\ D\left(\mathcal{E}_\pm(x)t_\pm(x)\right)'' + v\left(\mathcal{E}_\pm(x)t_\pm(x)\right)' &= -\mathcal{E}_\pm(x), \end{aligned} \tag{2.2.6}$$

subject to the boundary conditions $\mathcal{E}_+(0) = 0$ and $\mathcal{E}_+(L) = 1$ and vice versa for $\mathcal{E}_-(x)$, as well as $\mathcal{E}_\pm(x)t_\pm(x) = 0$ for both $x = 0$ and $x = L$. The solution to the first of these equations was given in Eq. (2.2.4) while the result for $t_\pm(x)$ is (see Fig. 2.3)

$$\begin{aligned} t_+(x) &= \frac{L}{v}\left(\frac{1+e^{-vL/D}}{1-e^{-vL/D}}\right) - \frac{x}{v}\left(\frac{1+e^{-vx/D}}{1-e^{-vx/D}}\right) \\ t_-(x) &= \frac{x}{v}\left(\frac{1+e^{v(x-L)/D}}{1-e^{v(x-L)/D}}\right) - \frac{2L/v}{1-e^{v(x-L)/D}}\left(\frac{e^{vx/D}-1}{e^{vL/D}-1}\right). \end{aligned} \tag{2.2.7}$$

For $v \to \infty$, the time to exit "downstream" is $t_+(x) \to (L-x)/v$, as expected naively. On the other hand, the mean time to exit "upstream" is just the distance to the exit divided by the "wrong way" velocity; $t_-(x) \to x/v$! In the limit $v \to 0$, these conditional exit times reduce to Eqs. (2.1.11).

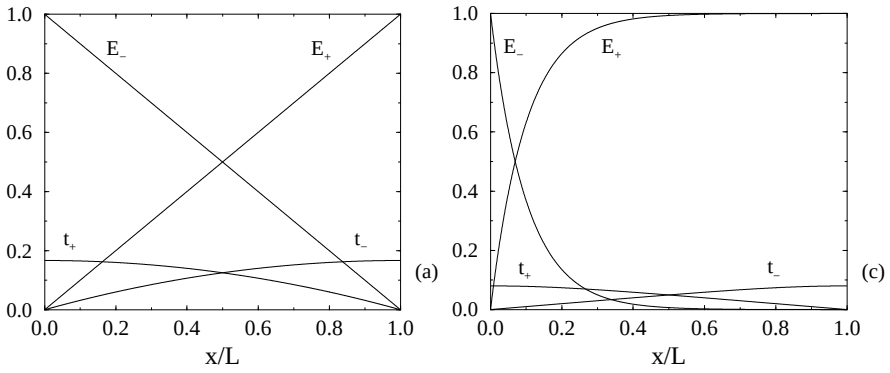

Figure 2.3: Dependence on x of the conditional exit probabilities $\mathcal{E}_{\pm}(x)$ and exit times $t_{\pm}(x)$ on the initial position x for Péclet numbers: (a) $Pe = 0$, and (b) $Pe = 10$.

Chapter 3

SEMI-INFINITE SYSTEM

3.1 Image Method

We determine the first-passage probability to the origin for a diffusing particle that starts at $x_0 > 0$, subject to the absorbing boundary condition $c(x = 0, t) = 0$. An appealing solution is based on the image method of electrostatics: a particle initially at $x = x_0$ and an image "antiparticle" initially at $x = -x_0$ that both diffuse freely on $[-\infty, \infty]$ lead to a concentration $c(x, t)$ that coincides with the concentration of the initial absorbing boundary condition system. Hence

$$c(x,t) = \frac{1}{\sqrt{4\pi Dt}} \left[e^{-(x-x_0)^2/4Dt} - e^{-(x+x_0)^2/4Dt} \right]. \tag{3.1.1}$$

It is instructive to rewrite this as

$$c(x,t) = \frac{1}{\sqrt{4\pi Dt}}\, e^{-(x^2+x_0^2)/4Dt} \left[e^{xx_0/2Dt} - e^{-xx_0/2Dt} \right] \approx \frac{1}{\sqrt{4\pi Dt}}\, \frac{xx_0}{Dt}\, e^{-(x^2+x_0^2)/4Dt}. \tag{3.1.2}$$

We see that the concentration has a linear dependence on x near the origin and a Gaussian large-distance tail, as illustrated in Fig. 3.1.

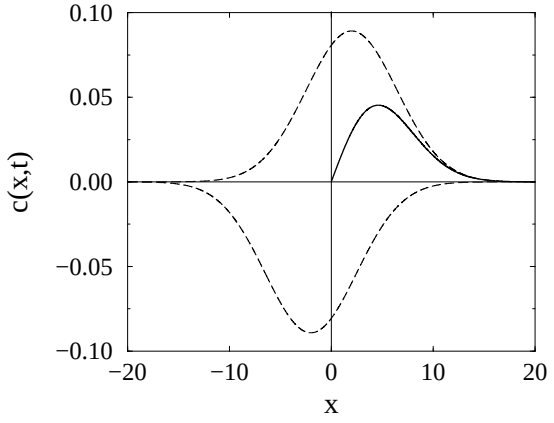

Figure 3.1: Concentration profile of a diffusing particle in the absorbing semi-infinite interval $(0, \infty)$ at $Dt = 10$, with $x_0 = 2$. Shown are the component Gaussian and image anti-Gaussian (dashed curves) and their superposition in the physical region $x > 0$ (solid curves).

The image method can be extended to various geometries. To illustrate the method, we work backward and introduce an image configuration and then determine the locus on which the concentration due to the

particle and the image vanishes. This provides the solution to a corresponding boundary value problem. Thus consider a particle that starts at x_0 and an image, with weight $-w \neq 1$, that starts at $-x_0$. The total concentration due to these two sources is

$$c(x,t) = \frac{1}{\sqrt{4\pi Dt}}\left[e^{-(x-x_0)^2/4Dt} - we^{-(x+x_0)^2/4Dt}\right] = \frac{1}{\sqrt{4\pi Dt}}\, e^{-(x-x_0)^2/4Dt}\left[1 - we^{-xx_0/Dt}\right], \quad (3.1.3)$$

that vanishes on the locus $x(t) = \frac{Dt}{x_0}\ln w$. Therefore the solution to the diffusion equation in the presence of an absorbing boundary that moves at constant speed v is given by the sum of a Gaussian and an image anti-Gaussian of amplitude $w = e^{vx_0/D}$. This approach can be extended to a wide variety of geometries.

3.1.1 First-Passage Properties

The first-passage probability to the origin at time t is just the flux to this point. From Eq. (3.1.1), we find

$$F(0,t) = +D\frac{\partial c(x,t)}{\partial x}\bigg|_{x=0} = \frac{x_0}{\sqrt{4\pi Dt^3}}\, e^{-x_0^2/4Dt} \qquad t \to \infty. \quad (3.1.4)$$

In the long time limit $\sqrt{Dt} \gg x_0$, the first-passage probability reduces to $F(0,t) \to x_0/t^{3/2}$. Due to this long-time tail, the mean time for the particle to reach the origin is infinite – $\langle t\rangle \equiv \int_0^\infty t\, F(0,t)\, dt = \infty$. On the other hand, the particle is sure to return to the origin because $\int_0^\infty F(t)\, dt = 1$. Although the mean return time is infinite, low-order moments *are* finite. The $k^{\rm th}$ moment is

$$\langle t^k\rangle = \frac{x_0}{\sqrt{4\pi D}}\int_0^\infty t^{k-3/2}\, e^{-x_0^2/4Dt}\, dt. \quad (3.1.5)$$

This integral converges for $k < 1/2$, so that moments of order less than $1/2$ are finite. Explicitly

$$\langle t^k\rangle = \frac{\Gamma(\frac{1}{2}-k)}{\sqrt{\pi}}\left(\frac{x_0^2}{4D}\right)^k. \quad (3.1.6)$$

For $k < 1/2$, the units of $\langle t^k\rangle$ are determined by the time to diffuse a distance x_0, the only time scale in the problem. The finiteness of these low-order moments is a manifestation of the dichotomy between certain return and infinite return time for one-dimensional diffusion.

From the first-passage probability, the survival probability $S(t)$ may be found directly through $S(t) = 1-\int_0^t F(0,t')\, dt'$, or it may be obtained by integrating the concentration over positive x. The former approach gives

$$S(t) = 1 - \int_0^t \frac{x_0}{\sqrt{4\pi Dt'^3}}\, e^{-x_0^2/4Dt'}\, dt' = \mathrm{erf}(\frac{x_0}{\sqrt{4Dt}}). \quad (3.1.7)$$

The survival probability is nearly constant until the diffusion length $\sqrt{Dt}$ reaches the initial distance to the boundary, x_0. Subsequently, the particle can reach the origin by diffusion, and trapping becomes significant. For $\sqrt{Dt} \gg x_0$, the asymptotic behavior of the error function then gives

$$S(t) \sim \frac{x_0}{\sqrt{\pi Dt}}. \quad (3.1.8)$$

The image method can be adapted in an elegant manner to biased diffusion. Naively, we might anticipate that if the particle has a drift velocity v, the image particle should move with velocity $-v$. However, such an image contribution would not satisfy the initial convection-diffusion equation in the domain $x > 0$. The correct solution must therefore consist of an image contribution that moves in the *same* direction as that of the original particle. By inspection, the solution is

$$c(x,t) = \frac{1}{\sqrt{4\pi Dt}}\left[e^{-(x-x_0-vt)^2/4Dt} - e^{-vx_0/D}e^{-(x+x_0-vt)^2/4Dt}\right], \quad (3.1.9)$$

where the factor $e^{-vx_0/D}$ ensures that $c(x=0,t) = 0$. Notice that by transforming to a reference frame that moves at velocity v, we map to the problem of a particle and a static image of magnitude $e^{-vx_0/D}$, together

with an absorbing boundary that moves with velocity $-v$. This is the just the problem already solved in Eq. (3.1.3)!

From the concentration profile, we determine the first-passage probability either by computing the flux to the origin, $-(vc - Dc')|_{x=0}$, or by Taylor expanding Eq. (3.1.9) in a power series in x and identifying the linear term with the first-passage probability. Either approach leads to the simple result

$$F(0,t) = \frac{x_0}{\sqrt{4\pi D t^3}} e^{-(x_0+vt)^2/4Dt}. \tag{3.1.10}$$

This first-passage probability asymptotically decays exponentially in time because of the bias. For negative bias, the particle is very likely to be trapped quickly, while for positive bias the particle very likely escapes to $+\infty$. In either case the first-passage probability should become vanishingly small in the long-time limit.

From the first-passage probability, the survival probability is

$$S(t) = 1 - \int_0^t F(0,t')\,dt = 1 - e^{-vx_0/2D} \int_0^t \frac{x_0}{\sqrt{4\pi D t'^3}}\, e^{-x_0^2/4Dt'}\, e^{-v^2 t'/4D}\, dt'. \tag{3.1.11}$$

The final result is

$$S(t) \sim \begin{cases} 1 - e^{-2Pe} = 1 - e^{-vx_0/D}, & Pe > 0 \\ \left(\dfrac{x_0}{\sqrt{Dt}}\right)^3 \dfrac{1}{\sqrt{4\pi}} \dfrac{1}{Pe^2}\, e^{-Pe^2\, Dt/x_0^2} = \sqrt{\dfrac{4}{\pi}} \dfrac{x_0\sqrt{Dt}}{(vt)^2}\, e^{-v^2 t/4D} & Pe \leq 0 \end{cases}, \tag{3.1.12}$$

and the probability to eventually be trapped as a function of the starting location, $\mathcal{E}(x_0)$, is simply

$$\mathcal{E}(x_0) = \begin{cases} e^{-vx_0/D}, & \text{for } v > 0; \\ 1 & \text{for } v \leq 0 \end{cases}. \tag{3.1.13}$$

Thus for zero or negative bias, diffusion is recurrent, while for a positive bias, no matter how small, diffusion is transient. This is the basic extension of the recurrence/transience transition to biased diffusion.

3.1.2 Arbitrary Spatial Dimension

We can easily extend our results for the semi-infinite interval to a semi-infinite slab in arbitrary spatial dimension. While the time dependence of the first-passage probability remains the same as in one dimension, we also study *where* the particle hits the boundary. Consider the semi-infinite d-dimensional slab where the last co-ordinate x_d is restricted to positive values by an absorbing boundary condition at $x_d = 0$. A diffusing particle starts at $\vec{h}_0 = (0, 0, \ldots, 0, h_0)$. What is the probability that the particle eventually hits at some point on the $(d-1)$-dimensional absorbing plane $x_d = 0$?

We may answer this question easily by the image method. First, consider the case of two dimensions. For a particle that starts at $(0, y_0)$ with the line $y = 0$ absorbing, the time-dependent concentration is

$$c(x,y,t) = \frac{1}{4\pi Dt}\left[e^{-(x^2+(y-y_0)^2)/4Dt} - e^{-(x^2+(y+y_0)^2)/4Dt}\right]. \tag{3.1.14}$$

The first-passage probability to any point along the absorbing line at time t is just the diffusive flux at $(x, 0)$,

$$j(x,0,t) = D\left|\frac{\partial c(x,y,t)}{\partial y}\right|_{y=0} = \frac{y_0}{4\pi D t^2} e^{-(x^2+y_0^2)/4Dt}. \tag{3.1.15}$$

Finally, the probability that the particle eventually hits $(x, 0)$, $\mathcal{E}(x; 0, y_0)$, is the integral of the first-passage probability at $(x, 0)$ over all time,

$$\mathcal{E}(x;0,y_0) = \int_0^\infty j(x,0,t)\,dt.$$

We evaluate this integral by changing variables to $u = (x^2+y_0^2)/4Dt$ and thus obtain the *Cauchy distribution* for the hitting probability,

$$\mathcal{E}(x;0,y_0) = \frac{1}{\pi}\frac{y_0}{x^2+y_0^2}. \tag{3.1.16}$$

Because of the x^{-2} decay of this distribution for large x, the mean transverse distance of a trapped particle, namely, $\langle x\rangle = \int_0^\infty x\mathcal{E}(x;0,y_0)\,dx$, is infinite.

For general spatial dimension, the time-dependent concentration is

$$c(\vec{x},t) = \frac{1}{(4\pi Dt)^{d/2}}\left[e^{-(\vec{x}_\perp^2+(x_d-h_0)^2)/4Dt} - e^{-(\vec{x}_\perp^2+(x_d+h_0)^2)/4Dt}\right], \tag{3.1.17}$$

where $\vec{x}_\perp^2 = x_1^2 + x_2^2 + \ldots + x_{d-1}^2$, and the first-passage probability to a point on the absorbing hyperplane is

$$j(\vec{x}_\perp,t) = \frac{1}{(4\pi Dt)^{d/2}}\frac{h_0}{t}\,e^{-(\vec{x}_\perp^2+h_0^2)/4Dt}. \tag{3.1.18}$$

Integrating over all time and using the same variable change as in two dimensions, the probability of eventually hitting $\vec{x}_\perp$ is

$$\mathcal{E}(\vec{x}_\perp;\vec{h}_0) = \frac{h_0}{\pi^{d/2}}\frac{\Gamma(d/2)}{(\vec{x}_\perp^2+h_0^2)^{d/2}}. \tag{3.1.19}$$

In greater than two dimensions, the mean lateral position of trapped particles on the absorbing hyperplane is finite. Notice, as expected from the equivalence with electrostatics, that this eventual hitting probability is also just the electric field of a point charge located at $\vec{h}_0$ in the presence of a grounded hyperplane at $x_d = 0$. We will return to this equivalence when we discuss first passage in the wedge geometry in Chap. 7.

3.2 Discrete Random Walk

3.2.1 The Reflection Principle

We now study first-passage properties of a symmetric nearest-neighbor random walk. Although the results are equivalent to those of continuum diffusion, the methods of solution are appealing and provide the starting point for treating the intriguing origin crossing properties of random walks. We start by deriving the fundamental *reflection principle* that allows us to derive first-passage properties easily in terms of the occupation probability. It is convenient to view a random walk as a directed path in space-time (x,t), with isotropic motion in space and directed motion in time (Fig. 3.2). Let $N(x,t|x_0,0)$ be the total number of random walks that start at $(x_0,0)$ and end at $(x>x_0,t)$. Typically, we will not write the starting location dependence unless instructive. This dependence can always be eliminated by translational invariance, $N(x,t|x_0,0) = N(x-x_0,t|0,0) \equiv N(x-x_0,t)$.

Consider a random walk that starts at $(0,0)$, crosses or touches a point $y>x$, and then ends at (x,t) (Fig. 3.2). Let $X_y(x,t)$ be the number of these "crossing" paths between 0 and x. The reflection principle states that

$$X_y(x,t) = N(2y-x,t). \tag{3.2.1}$$

This relation arises because any crossing path has a unique last visit to y. We may then construct a "reflected" path by reversing the direction of all steps after this last visit (Fig. 3.2). There is clearly a one-to-one mapping between the crossing paths that comprise $X_y(x,t)$ and these reflected paths. Moreover, the reflected paths are unrestricted because y is necessarily crossed in going from $(0,0)$ to $(2y-x,t)$. Thus the reflected paths constitute $N(2y-x,t)$. Parenthetically, this reflection construction could also be applied to the leading segment of the crossing path to give the equality $X_y(x,t) = N(x,t|2y,0) = N(2y-x,t)$.

We now use this reflection principle to compute the number of first-passage paths $F(x,t|0,0)$ – paths from $(0,0)$ to (x,t) that do not touch or cross x before time t (Fig. 3.3). First notice that $F(x,t)$ is the same as $F(x-1,t-1)$. Then the number of first-passage paths from $(0,0)$ to $(x-1,t-1)$ can be written as

$$F(x-1,t-1) = N(x-1,t-1) - X_x(x-1,t-1), \tag{3.2.2}$$

where again $X_x(x-1,t-1)$ is the number of paths from $(0,0)$ to $(x-1,t-1)$ that touch or cross x before $t-1$ steps. By the reflection principle, $X_x(x-1,t-1) = N(x+1,t-1)$. Consequently, the number of

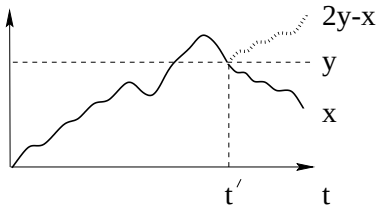

Figure 3.2: The reflection principle illustrated. The solid curve is a "crossing" path to (x,t) by way of (y,t'), with $t' < t$. The number of such restricted paths is the same as the number of unrestricted paths to $(2y-x,t)$. The reflected portion of the trajectory is shown as a dotted curve.

first-passage paths from 0 to x after t steps is

$$\begin{aligned} F(x,t) = F(x-1,t-1) &= N(x-1,t-1) - N(x+1,t-1) \\ &= \frac{(t-1)!}{\left(\frac{t+x-2}{2}\right)!\left(\frac{t-x}{2}\right)!} - \frac{(t-1)!}{\left(\frac{t+x}{2}\right)!\left(\frac{t-x-2}{2}\right)!} \\ &= \frac{x}{t}\frac{t!}{\left(\frac{t+x}{2}\right)!\left(\frac{t-x}{2}\right)!} = \frac{x}{t}N(x,t). \end{aligned} \tag{3.2.3}$$

Since the total number of paths from $(0,0)$ to (x,t) is proportional to $\frac{1}{\sqrt{4\pi Dt}}\,e^{-x^2/4Dt}$ in the continuum limit, the number of first-passage paths between these two points therefore scales as $\frac{x}{\sqrt{4\pi Dt^3}}\,e^{-x^2/4Dt}$.

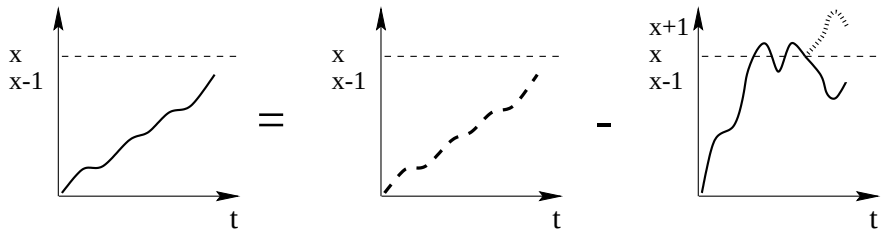

Figure 3.3: First-passage paths (solid) from $(0,0)$ to $(x-1,t-1)$ as the difference between all paths (dashed) and crossing paths. The latter are related to all paths from $(0,0)$ to $(x+1,t)$ (dotted) by the reflection principle.

If the endpoint is also at $x = 0$, then we have the first return to the origin. In this case, we apply the reflection principle in a slightly different form to obtain the number of first-passage paths. Suppose that the first step is to the right. Then the last step must be to the left, and hence $f(t) \equiv F(0,t) = F(1,t-1|1,1)$. The reflection principle now gives

$$\begin{aligned} f(t) = F(1,t-1|1,1) &= N(1,t-1|1,1) - X_0(1,t-1|1,1) \\ &= N(1,t-1|1,1) - N(1,t-1|-1,1) \\ &= \frac{(t-2)!}{[(t/2-1)!]^2} - \frac{(t-2)!}{(t/2)!\,(t/2-2)!} \\ &= \frac{1}{2(t-1)}\frac{t!}{[(t/2)!]^2} = \frac{1}{2(t-1)}N(0,t). \end{aligned} \tag{3.2.4}$$

Note that t must be even, since we are considering return to the origin.

An amusing result is the equality between the number of paths $\mathcal{N}(t)$ that *never* return to the origin *by* time t, and the number of paths $\mathcal{R}(t)$ that return to the origin *at* time t. From the binomial distribution of a random walk, the number of these return paths is

$$\mathcal{R}(t) = \frac{t!}{[(t/2)!]^2} \sim \sqrt{\frac{2}{\pi t}}\, 2^t, \tag{3.2.5}$$

where Stirling's approximation is used to obtain the asymptotic result. By reversing the direction of time, non-returning paths are the same as all first-passage paths from any starting to the origin. Therefore, by summing over all starting points (endpoints in the original problem), we have

$$\mathcal{N}(t) = \sum_{x=2}^{t}{}' F(x,t) = \sum_{x=2}^{t}{}' [N(x-1,t-1) - N(x+1,t-1)]. \tag{3.2.6}$$

Here the prime on the sum denotes the restriction to the even integers. Successive terms in the second sum cancel in pairs, leaving behind the first series term $N(1,t-1) = N(0,t|0,0)$. Thus we obtain the simple and unexpected result that the number of paths that never return by time t is the same as the number of otherwise unrestricted paths that return at time t:

$$\mathcal{N}(t) = \mathcal{R}(t). \tag{3.2.7}$$

3.2.2 Origin Crossing Statistics

Hidden within the first-passage properties of the one-dimensional random walk are fundamental properties about the statistics of crossings of the origin (Fig. 3.4). Some of these properties are sufficiently counter-intuitive that they appear to be "wrong", yet they can be derived simply and directly from the first-passage probability.

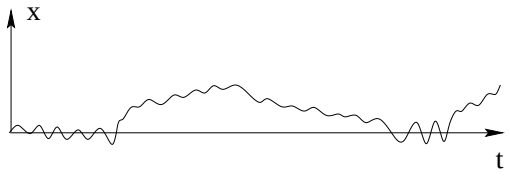

Figure 3.4: Caricature of a one-dimensional random walk trajectory. There are many quick returns to the origin and fewer, long-duration returns that take most of the elapsed time.

Consider a symmetric random walk on the infinite line for which the mean return time is infinite; on the other hand, from Eq. (3.2.4), the probability of return to the origin after a relatively small number of steps is appreciable. For example, the first-passage probabilities $f(t)$ are $\frac{1}{2}, \frac{1}{8}, \frac{1}{16}, \frac{5}{128}$, and $\frac{7}{256}$ for $t = 2, 4, 6, 8,$ and 10, respectively. Thus the probability of returning to the starting point within 10 steps is $0.7539\ldots$. This contrast between the relatively large probability of returning after a short time and an infinite mean return time is the source of the intriguing properties of origin crossings by a random walk.

One basic question is: what is the average number of returns to the origin in an n-step walk? More generally, what is the probability that there are m returns to the origin in an n-step walk? Surprisingly, the most likely outcome is *zero* returns. In fact, the probability for m returns in an n-step walk has the Gaussian form $e^{-m^2/n}$, so that the typical number of returns after n steps is of the order of $\sqrt{n}$ or less.

We also study the *lead probability*. To appreciate its meaning, consider again the coin-tossing game where player A wins \$1 from B if a coin toss is heads and gives \$1 to B if the result is tails. In a single game with n coin tosses, A will be leading for a time $n\phi$ (ϕ is the *lead fraction*), whereas B will be leading for a time $n(1-\phi)$. (In a discrete random walk, "ties" can occur; we can eliminate these by defining the leader in the previous step as the current leader.) This gives our second fundamental question: For an n-step random walk, what is the lead fraction ϕ? What is the probability distribution for this lead fraction?

Amazingly, the lead fraction is likely to be close to 0 or 1! That is, one player is in the lead most of the time, even though the average amount won is zero! Conversely, the least likely outcome is the naive expectation that each player should be in the lead for approximately one-half the time. The ultimate expression of these unexpected results is the beautiful arcsine law for the lead probability. To set the stage for this law, we first study the statistics of number of returns to the origin. We then treat the statistics of lead durations, from which the arcsine law follows simply.

It is easy to estimate the typical number of returns to the origin in an n-step walk. Since the occupation probability at the origin is $P(n,0) \propto 1/\sqrt{n}$, after n steps, there are of the order of $n/\sqrt{n} = \sqrt{n}$ returns. Thus returns to the origin should be few and far between. In fact, returns are clustered because the distribution of times between returns has a $t^{-3/2}$ tail. Thus of the $\sqrt{n}$ returns to the origin, most occur after a soon after the previous return (Fig. 3.4).

Now let's consider the probability that an n-step random walk contains m returns to the origin. This can be found conveniently in terms of the m^{th}-passage probability of a random walk. Let $F(x,n)$ be the usual first-passage probability that a random walk hits x for the first time at the n^{th} step. From Chap. 1, the generating function, $F(x,z) = \sum_n F(x,n) z^n$, is

$$F(x,z) = \frac{P(x,z) - \delta_{x,0}}{P(0,z)}, \tag{3.2.8}$$

where $P(x,z)$ is the generating function for the occupation probability $P(x,n)$.

Now define the m^{th}-passage probability $F^{(m)}(x,n)$ as the probability that a random walk hits x for the m^{th} time *at* the n^{th} step. This m^{th}-passage probability can be expressed recursively in terms of the $(m-1)^{\text{th}}$-passage probability

$$F^{(m)}(x,n) = \sum_{k=0}^{n} F^{(m-1)}(x,k) F(0,n-k). \tag{3.2.9}$$

That is, for the walk to hit x for the m^{th} time at step n, it must hit x for the $(m-1)^{\text{th}}$ time at an earlier step k and then return to x one more time exactly $n-k$ steps later. This recursion is conceptually similar to the convolution that relates the first-passage probability to the occupation probability (Eq. (1.1.1)).

We solve this recursion by substituting the generating function $F^{(m)}(x,z) = \sum_n F^{(m)}(x,n) z^n$ into the above recursion to give $F^{(m)}(x,z) = F^{(m-1)}(x,z) F(0,z) = F(x,z) F(0,z)^{m-1}$. Here we use the definition that $F^{(1)}(x,z) = F(x,z)$. We therefore find

$$F^{(m)}(x,z) = \begin{cases} \dfrac{P(x,z)}{P(0,z)} \left[1 - \dfrac{1}{P(0,z)}\right]^{m-1} & x \neq 0; \\[2ex] \left(1 - \dfrac{1}{P(0,z)}\right)^{m} & x = 0. \end{cases} \tag{3.2.10}$$

What we seek, however, is the probability that x is visited m times *sometime* during an n-step walk. This m-visit probability can be obtained from the m^{th}-passage probabilities as follows. First, the probability that x has been visited *at least* m times in an n-step walk is

$$\sum_{j=1}^{n} F^{(m)}(x,j) \quad x \neq 0, \qquad \sum_{j=1}^{n} F^{(m-1)}(0,j) \quad x = 0. \tag{3.2.11}$$

These express the fact that to visit x at least m times, the m^{th} visit must occur in $j \leq n$ steps.

The probability that there are m visits to x sometime during an n-step walk, $G^{(m)}(x,n)$, is just the difference in the probability of visiting at least m times and at least $m+1$ times. Therefore

$$G^{(m)}(x,n) = \begin{cases} \displaystyle\sum_{j=1}^{n} [F^{(m)}(x,j) - F^{(m+1)}(x,j)] & x \neq 0 \\[2ex] \displaystyle\sum_{j=1}^{n} [F^{(m-1)}(0,j) - F^{(m)}(0,j)] & x = 0. \end{cases} \tag{3.2.12}$$

In terms of the generating function for G, these relations become

$$G^{(m)}(x,z) = \begin{cases} \dfrac{1}{1-z}[F^{(m)}(x,z) - F^{(m+1)}(x,z)] & x \neq 0 \\ \dfrac{1}{1-z}[F^{(m-1)}(0,z) - F^{(m)}(0,z)] & x = 0. \end{cases} \tag{3.2.13}$$

Focusing on returns to the origin, we substitute the m^{th}-passage probability (Eq. (3.2.10), and also the relation between the first-passage and occupation probabilities (Eq. (1.1.2)) into Eq. (3.2.13), to obtain

$$G^{(m)}(0,z) = \frac{1}{1-z}\left[1 - \frac{1}{P(0,z)}\right]^{m-1} \frac{1}{P(0,z)} \tag{3.2.14}$$

We now extract the asymptotic time dependence from this generating function. Using $P(0,z) = (1-z^2)^{-1/2} \approx (2s)^{-1/2}$ as $z \to 1$ from below, with $s = 1-z$, we have

$$G^{(m)}(0,s) \approx \frac{1}{s}(1-\sqrt{2s})^m\sqrt{2s} \sim \sqrt{\frac{2}{s}}\; e^{-m\sqrt{2s}}. \tag{3.2.15}$$

This is identical to the Laplace transform of the random walk occupation probability. Thus the probability for a random walk to make m visits to the origin during the course of an n-step walk is

$$G^{(m)}(0,n) \sim \frac{1}{\sqrt{2\pi n}} e^{-m^2/2n}. \tag{3.2.16}$$

Eq. (3.2.16) has amusing consequences. First, from among all the possible outcomes for the number of returns to the origin, the most likely outcome is *zero* returns. In the context of the coin-tossing game, this means that one person would always be in the lead. The probability for $m > 0$ returns to the origin monotonically decreases with m and becomes vanishingly small after m exceeds $\sqrt{n}$. Thus the typical number of returns is of the order of $\sqrt{n}$. As a result, ties in the coin-tossing game occur with progressively lower frequency as the game continues, since it is very unlikely that the number of returns is of the order of n.

3.2.3 Lead Probability and the Arcsine Law

We now turn to the lead probability of a random walk. For a random walk of n steps, a total of k steps lie in the region $x > 0$, while the other $n-k$ steps lie in the region $x < 0$. If x happens to be zero, we again use the tie-breaker rule that a walk at the origin is considered as having $x \gtrless 0$ if the location at the previous step was positive (negative). We want to find the probability $Q_{n,k}$ for this division of the lead times in an n-step walk.

We use the fact that the occurrence probabilities for each of the first-passage segments of the walk in Fig. 3.5 are independent. Hence they can be interchanged freely without changing the overall occurrence probability of the walk. We therefore move all the negative segments to the beginning and all the positive segments to the end. This rearranged walk can be viewed as composite of a return segment of length $n-k$ and a no-return segment of length k. For convenience, we now choose n to be even while k must be even. The occurrence probability of this composite path is just the product of the probabilities for the two constituents. From Eq. (3.2.5), the probability of the return segment is $\mathcal{R}(k)/2^k$, while that of the no-return segment is $\mathcal{R}(n-k)/2^{n-k}$. Thus the probability for all paths that are decomposable as in Fig. 3.5 is

$$Q_{n,k} = 2^{-n}\,\mathcal{R}(k)\mathcal{R}(n-k) \sim \frac{2}{\pi\sqrt{k(n-k)}}. \tag{3.2.17}$$

As advertised previously, this probability is maximal for $k \to 0$ or $k \to n$ and the minimum value of the probability occurs when $k = n/2$. For large n,

$$Q_{n,k} \to Q(x) = \frac{1}{n\pi}\frac{1}{\sqrt{x(1-x)}}, \tag{3.2.18}$$

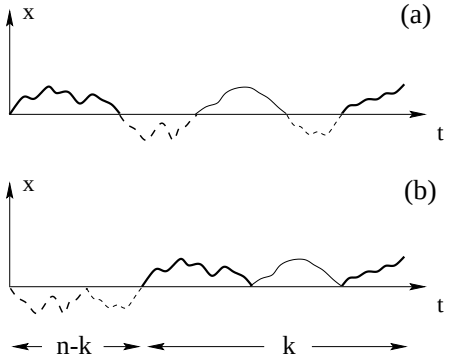

Figure 3.5: (a) A typical random walk, with k total steps in the region $x > 0$ (solid curves) and $n - k$ steps in $x < 0$ (dashed curves). (b) This configuration is in one-to-one correspondence with a walk in which all the dashed segments are at the beginning and concatenated with all the solid segments (b). The first element is a return segment of $n - k$ steps while the latter is a no-return segment of k steps.

where $Q(x)$ is the probability that the lead fraction equals x in an n-step walk.

In addition to the probability that player A is in the lead for exactly k out of n steps, consider the probability $L_{k,n}$ that A is in the lead for *at least* k steps. In the limit $k, n \to \infty$ with $x = k/n$ remaining finite, $L_{n,k} \to L(x)$ becomes

$$L(x) = \int_k^n \frac{dk'}{\pi\sqrt{k'(n-k')}} = \frac{2}{\pi}\sin^{-1}\sqrt{x}, \tag{3.2.19}$$

where $x = k/n$. This is the *continuous arcsine distribution.*

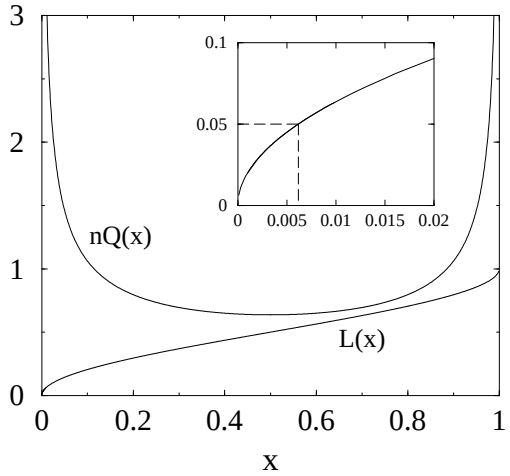

Figure 3.6: The arcsine distribution. Shown are both the underlying density $nQ(x)$ (upper curve), and the arcsine distribution itself $L(x)$ (lower curve). The inset shows $L(x)$ near $x = 0$. The dashed line highlights the numerical example that, at $x \approx 0.00615$, $L(x)$ has already risen to 0.05.

The strange consequences of this arcsine distribution arise from the fact that the underlying density $1/\sqrt{x(1-x)}$ has a square-root singularity near the extremes of $x \to 0$ and $x \to 1$, as shown in Fig. 3.6. It is easy to devise paradoxical numerical illustrations of this distribution and many are given in Feller's book.

One nice example is our two-person coin tossing game that is played once every second for 1 year. Then, with probability 1/2, the unluckier player will be leading in this game for 53.45 days or fewer – that is, less than 0.146 of the total time. With probability 1/10 (inset of Fig. 3.6), the unluckier player will be leading for 2.24 days or fewer – less than 0.00615 of the total time!

Chapter 4

EXAMPLES IN SIMPLE GEOMETRIES

4.1 Integrate-and-Fire Neuron Dynamics

In the integrate and fire model of neuron dynamics, excitatory or inhibitory inputs occur with rates λ_E and λ_I. This stimulus causes the voltage to increase by a_E or decrease by a_I. When the voltage first exceeds a value θ, the neuron emits a voltage spike and the state of the neuron quickly returns to a reference level (Fig. 4.1). The time between spikes, the *interspike interval* (ISI), is governed by the first-passage probability for the voltage to reach the threshold.

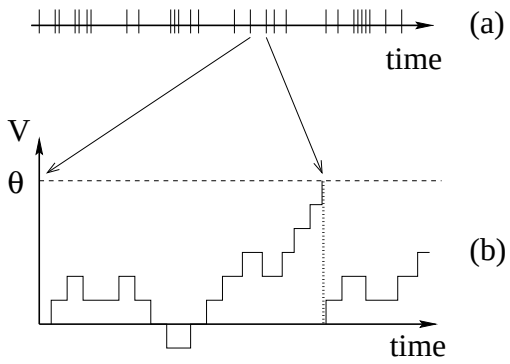

Figure 4.1: (a) Schematic spike train that is due to a sequence of neuron firing events. (b) Basic mechanism for the creation of an action potential spike for an integrate-and-fire neuron (finer time scale). The potential of a neuron fluctuates stochastically due to excitatory and inhibitory inputs. When the potential first reaches a threshold level θ, the neuron "fires" and its potential quickly returns to a resting level.

We assume that each input is sufficiently small that we can approximate the discrete evolution of the voltage by a diffusive process with bias $v = \lambda_E a_E - \lambda_I a_I$ and diffusivity $D = \sqrt{\lambda_E a_E^2 + \lambda_I a_I^2}$. The voltage first reaching the threshold θ is identical to the first passage to the origin of a biased diffusing particle that starts at $x = \theta$ in the semi-infinite system (Eq. (3.1.10)). Using this equivalence, the ISI distribution is

$$F(t) = \frac{\theta}{\sqrt{4\pi D t^3}} e^{-(\theta - vt)^2/4Dt}. \tag{4.1.1}$$

This distribution has a long-time power-law tail that gets cut off exponentially, with the characteristic time for the exponential determined by the relative bias between excitatory and inhibitory inputs (Fig. 4.2).

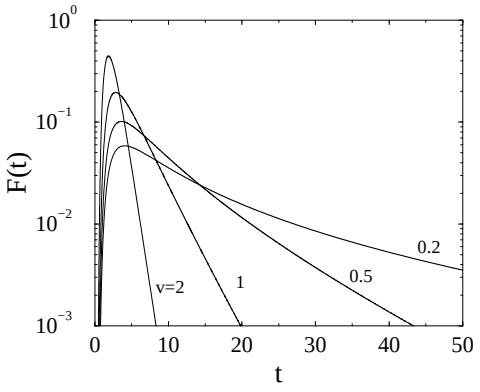

Figure 4.2: The distribution of ISIs on a semilogarithmic scale for $\theta = D = 1$ for the values of v indicated.

From the moments of the distribution $\langle t^k \rangle = \int t^k F(t)\, dt$, the mean ISI time and its variance are given by

$$\langle t \rangle = \frac{\theta}{v}, \qquad \sigma^2 = \langle t^2 \rangle - \langle t \rangle^2 = \frac{D\theta}{v^3} = \frac{\langle t \rangle^2}{Pe}, \tag{4.1.2}$$

where $Pe = v\theta/D$ is the Péclet number. Although the mean ISI time involves only the threshold and the bias, the variance also depends on the fluctuations in the inputs. Notice also that the variance is much larger than $\langle t \rangle^2$ and that the ratio $\sigma^2/\langle t \rangle^2$ diverges as the bias vanishes. This is a manifestation of the power-law tail in $F(t)$ when there is no bias.

An interesting aspect of the ISI distribution is the dependence of the most probable value of the ISI time, $t_{\rm mp}$, on basic system parameters. From Fig. 4.2, we see that $\langle t \rangle$ changes significantly as v changes, while $t_{\rm mp}$ is much more slowly varying. The location of the peak in $F(t)$ is simply given by

$$t_{\rm mp} = \frac{3D}{v^2}(\sqrt{1 + Pe^2/9} - 1). \tag{4.1.3}$$

Thus as $Pe \to \infty$, $t_{\rm mp} \to \langle t \rangle$. This reflects the relative unimportance of fluctuations in the ISI when the bias is dominant. When fluctuations are small the mean and most probable ISI times become the same. Conversely as $Pe \to 0$, $t_{\rm mp} \to \theta^2/6D$; that is, $t_{\rm mp}$ becomes roughly of the order of the time for a particle to diffuse a distance θ. On the other hand $t_{\rm mp}$ also approaches $\langle t \rangle Pe/6$. Thus $\langle t \rangle$ becomes arbitrarily large as $Pe \to 0$; this stems from the $t^{-3/2}$ tail in the ISI distribution.

4.2 Kinetics of Spin Systems

The Ising-Glauber model is a simple yet widely-applicable kinetic Ising-like spin system. Each spin can flip at a rate that is chosen to give thermodynamic equilibrium in the long-time limit. The Voter model is an even simpler interacting two-state spin system, in which we can equivalently view each site as being a "voter" with only two opinions. The dynamics involves picking a voter at random and updating it according to the following rule: a randomly-selected voter assumes the state of a randomly-chosen nearest neighbor. We can think of each voter as an individual with zero self-confidence who blindly assumes the state of its neighbor in an update. In the long-time limit, the Voter model either reaches complete unanimity for spatial dimension $d \leq 2$, or it reaches a steady state where voters change their opinion *ad infinitum*, for $d > 2$.

4.2.1 Solution to the One-Dimensional Ising-Glauber Model

The fundamental quantity is the probability distribution $P(\{\sigma\},t)$ that the spins of the system are in a particular state, denoted collectively as $\{\sigma\}$. This probability obeys the master equation

$$\frac{d}{dt}P(\{\sigma\},t)=\sum_i w(\{\sigma'\}_i\to\{\sigma\})P(\{\sigma'\}_i,t)-\sum_i w(\{\sigma\}\to\{\sigma'\}_i)P(\{\sigma\},t). \tag{4.2.1}$$

Here $\{\sigma'\}_i$ denotes the state where only the $i^{\rm th}$ spin is reversed compared to the state $\{\sigma\}$. This equation thus accounts for the gain in $P(\{\sigma\})$ due to transitions into this spin state at rate $w(\{\sigma'\}_i\to\{\sigma\})$, and for the loss in $P(\{\sigma\})$ due to transitions out of this state by the flip of a single spin σ_i, with rate $w(\{\sigma\}\to\{\sigma'\}_i)$. On physical grounds, Glauber found the following particularly convenient choice for the transition rates

$$w(\{\sigma\}\to\{\sigma'\}_i)=\frac{\alpha}{2}\left[1-\frac{\gamma}{2}\sigma_i(\sigma_{i-1}+\sigma_{i+1})\right]=\begin{cases}\frac{\alpha}{2}(1-\gamma) & \text{if } \uparrow\uparrow\uparrow\longrightarrow\uparrow\downarrow\uparrow\\ \frac{\alpha}{2} & \text{if } \uparrow\uparrow\downarrow\longrightarrow\uparrow\downarrow\downarrow\\ \frac{\alpha}{2}(1+\gamma) & \text{if } \uparrow\downarrow\uparrow\longrightarrow\uparrow\uparrow\uparrow,\end{cases}$$

with the same rates applying under an overall sign change of all these spins.

As constructed, these flip rates favor alignment. These rates must also satisfy *detailed balance* to ensure that the correct thermodynamic equilibrium is reproduced. This detailed balance condition is

$$\frac{w(\{\sigma\}\to\{\sigma'\}_i)}{w(\{\sigma'\}_i\to\{\sigma\})}=\frac{P(\{\sigma'\}_i)}{P(\{\sigma\})},$$

which translates to

$$\frac{1-\frac{\gamma}{2}\sigma_i(\sigma_{i-1}+\sigma_{i+1})}{1+\frac{\gamma}{2}\sigma_i(\sigma_{i-1}+\sigma_{i+1})}=\frac{e^{-\beta J\sigma_i(\sigma_{i-1}+\sigma_{i+1})}}{e^{+\beta J\sigma_i(\sigma_{i-1}+\sigma_{i+1})}},$$

This merely expresses the fact that in equilibrium the probability current from one state to another is the same as the current in the reverse direction for any pair of states. Writing $e^x=\cosh x+\sinh x$ and using the property that $\sinh(\epsilon x)=\epsilon\sinh(x)$ for $\epsilon=\pm1$, the transition rate reduces to,

$$w(\{\sigma\}\to\{\sigma'\}_i)=\frac{\alpha}{2}\left(1-\frac{\gamma}{2}E_i\right), \tag{4.2.2}$$

where $\gamma=\tanh(2\beta J)$ and the local spin energy is defined as $E_i=-\sigma_i(\sigma_{i-1}+\sigma_{i+1})$. Henceforth we set $\alpha=1$.

We now solve for the mean spin and the mean spin correlation function in one dimension with these flip rates. The mean spin at site j is given by

$$s_j\equiv\langle\sigma_j\rangle=\sum_{\{\sigma\}}\sigma_j P(\{\sigma\},t),$$

where the sum is over all spin configurations of the system. From the master equation for the probability distribution, s_j obeys the equation of motion

$$\begin{aligned}\frac{ds_j}{dt}&=\sum_{\{\sigma\}}\sigma_j\frac{d}{dt}P(\{\sigma\},t)\\&=\sum_{\{\sigma\}}\sigma_j\sum_i\left[(w(\{\sigma'\}_i\to\{\sigma\})P(\{\sigma'\}_i,t)-w(\{\sigma\}\to\{\sigma'\}_i)P(\{\sigma\},t))\right]\\&=\sum_{\{\sigma\}}\sigma_j\sum_i\left[\frac{1}{2}(1+\frac{\gamma}{2}E_i)P(\{\sigma'\}_i,t)-\frac{1}{2}(1-\frac{\gamma}{2}E_i)P(\{\sigma\},t)\right].\end{aligned} \tag{4.2.3}$$

We can simplify these sums by exploiting the following basic facts:

$$\sum_{\{\sigma\}}\sigma_j P(\{\sigma\})=+\langle\sigma_j\rangle,\quad \sum_{\{\sigma\}}\sigma_j P(\{\sigma'\}_j)=-\langle\sigma_j\rangle,\quad \sum_{\{\sigma\}}\sigma_j P(\{\sigma'\}_{k\neq j})=+\langle\sigma_j\rangle.$$

These identities reduce the above equation of motion (4.2.3) into a simple closed equation for the mean spin

$$\frac{ds_j}{dt} = -s_j + \frac{\gamma}{2}(s_{j-1} + s_{j+1}). \tag{4.2.4}$$

We see that s_j obeys the same type of master equation as the one-dimensional random walk. From this equivalence, the solution for $s_n(t)$ for the initial condition $s_n(t=0) = \delta_{n,0}$ is simply

$$s_n(t) = e^{-t} I_n(\gamma t), \tag{4.2.5}$$

where $I_n(x)$ is the modified Bessel function of the first kind of order n. Then

$$s_n(t) \sim \frac{1}{\sqrt{2\pi\gamma t}} e^{-(1-\gamma)t}, \tag{4.2.6}$$

i. e., exponential decay for $T > 0$ and power-law decay for $T = 0$. Although the mean value of each spin decays to zero, the average magnetization $m \equiv \sum_j s_j/N$, where N is the total number of spins, is conserved at $T = 0$! This seemingly paradoxical feature follows directly from equation of motion (4.2.4). Thus the mean magnetization does not characterize the degree of spin alignment in the system.

The two-spin correlation function, $c(i,j) \equiv \langle \sigma_i \sigma_j \rangle$, is much more useful. Since $\sigma_i \sigma_j = +1$ when the two spins are parallel and $\sigma_i \sigma_j = -1$ when the spins are antiparallel, the correlation function measures the extent to which these two spins are aligned. By translational invariance and isotropy, this function may be written as $c(i,j) = c_n$ for large n, where $n = |i - j|$ is the distance between the two spins. If c_n goes to zero rapidly as n increases, there is no long-range spin alignment, while if c_n decays as a power law in n as $n \to \infty$, long-range alignment exists. The evolution of this correlation function is described by a rate equation that is very similar to Eq. (4.2.3) for the mean spin. Following the same approach as that used to solve for the mean spin (all the details are in Glauber's original paper), the correlation function obeys

$$\frac{dc_n}{dt} = -2c_n + \gamma(c_{n-1} + c_{n+1}). \tag{4.2.7}$$

This is identical to the master equation for the mean spin (up to an overall factor of 2), but with the crucial difference that the boundary condition for the correlation function is $c_0(t) = \langle \sigma_i^2 \rangle = 1$, since $\sigma_i = \pm 1$.

The most interesting situation is the limit of zero temperature, in which the master equation for the correlation function reduces to

$$\frac{dc_n}{dt} = c_{n-1} - 2c_n + c_{n+1} \equiv \Delta^{(2)} c_n, \tag{4.2.8}$$

subject to the boundary condition is $c_0(t) = 1$. For simplicity, we assume that the spins are initially uncorrelated, $c_n = 0$ for $n > 0$. In the continuum limit, Eq. (4.2.8) describes diffusion in the half-line $x > 0$, with the concentration at the origin fixed to be one and the initial concentration equal to zero for all $x > 0$. By linearity of the diffusion equation, this is trivially related to diffusion in the same geometry with the initial concentration equal to one and the concentration at origin fixed to be zero. Solving this boundary-value problem, we conclude that the correlation function is

$$c_n(t) = 1 - \mathrm{erf}\Big(\frac{n}{\sqrt{4t}}\Big) \sim 1 - \frac{n}{\sqrt{4t}}. \tag{4.2.9}$$

The correlation function decays to one as $t^{-1/2}$ for any n. This simply means that the correlation between spins extends to the order of $\sqrt{t}$. That is, spins organize into a coarsening mosaic of aligned domains of typical length $\sqrt{t}$.

4.2.2 Solution to the Voter Model in all Dimensions

According to the dynamics of the Voter model, the transition rate between a state $\{\sigma\}$ and a state $\{\sigma'\}_i$ where only the spin (or voter) σ_i has been flipped is

$$w(\{\sigma\} \to \{\sigma'\}_i) = \frac{1}{2}\left(1 - \frac{\sigma_i}{z} \sum_{k \text{ n.n.} i} \sigma_k\right),$$

where the sum is over the z nearest-neighbors of site i on a lattice of coordination number z. The overall factor of $1/2$ is for convenience only. With these rates, a spin σ_i on the square lattice changes from -1 to $+1$ with respective rates $1, \frac{3}{4}, \frac{1}{2}, \frac{1}{4}$, and 0 when the number of neighboring up spins are 4, 3, 2, 1, and 0, respectively. Substituting these transition rates into master equation Eq. (4.2.1) and following the same steps as those developed for the Ising-Glauber model, the mean voter spin (opinion) at site j evolves as

$$\begin{aligned}\frac{ds_j}{dt} &= \sum_{\{\sigma\}} \sigma_j \frac{d}{dt} P(\{\sigma\},t) \\ &= \sum_{\{\sigma\}} \sigma_j \sum_i \left[(w(\{\sigma'\}_i \to \{\sigma\}) P(\{\sigma'\}_i,t) - w(\{\sigma\} \to \{\sigma'\}_i) P(\{\sigma\},t))\right] \\ &= \frac{1}{2}\sum_{\{\sigma\}} \sigma_j \sum_i \left[\Big(1+\frac{\sigma_i}{z}\sum_k \sigma_k\Big) P(\{\sigma'\}_i,t) - \Big(1-\frac{\sigma_i}{z}\sum_k \sigma_k\Big) P(\{\sigma\},t)\right]. \end{aligned} \tag{4.2.10}$$

By evaluating the sums in this equation we find $\frac{ds_j}{dt} = -s_j + \frac{1}{z}\sum_k s_k$, similar in form to the master equation for the mean spin in the Ising-Glauber model. However, the linear form of the transition rates allows us to factorize this equation along different coordinate axes. This gives a discrete diffusion equation in d dimensions with the boundary condition of unit concentration at the origin. This is the mechanism by which the Voter model is exactly soluble in all dimensions.

We now rewrite the master equation by labeling each site by its vector location to give

$$\frac{ds_{\vec{r}}}{dt} = \frac{1}{z}\left[(s_{\vec{r}+\hat{e}_1} + s_{\vec{r}-\hat{e}_1} - 2s_{\vec{r}}) + \ldots + (s_{\vec{r}+\hat{e}_d} + s_{\vec{r}-\hat{e}_d} - 2s_{\vec{r}})\right] \equiv \frac{1}{z}\vec{\Delta}^{(2)} s_{\vec{r}}, \tag{4.2.11}$$

where $\hat{e}_k$ denotes a unit vector in the k^{th} co-ordinate direction and $\vec{\Delta}^{(2)}$ is the vector discrete second difference operator. Following the same steps as in solving the master equation for the Ising-Glauber model, we obtain, for the initial condition $s_n(0) = \delta_{n,0}$ (*e. g.*, one "Democrat" in a sea of uncommitted voters),

$$s_{\vec{r}}(t) = e^{-2t} I_{\vec{r}}(4t/z), \quad \text{where} \quad I_{\vec{r}}(z) = \prod_{i=1}^{d} I_{x_i}(z), \tag{4.2.12}$$

and where x_i is the i^{th} Cartesian coordinate of $\vec{r}$.

By similar considerations, the master equation for the correlation function is $\frac{dc(\vec{r})}{dt} = \frac{2}{z}\vec{\Delta}^{(2)} c(\vec{r})$, subject to the initial condition that $c(0) = 1$. For the asymptotics, it is simpler to consider the continuum limit. Then the correlation function $c(\vec{r},t)$ obeys the diffusion equation with boundary condition $c(0,t) = 1$, and we choose the initial condition $c(\vec{r},0) = 0$. In one dimension, the Voter model is identical to the Ising-Glauber model and the correlation function asymptotically goes to one. In two dimensions, the survival probability of a diffusing particle in the presence of an absorbing point decays as $1/\ln t$ (Eq. (1.2.7)) and the correlation function at any r asymptotically approaches one as $1 - (\ln t)^{-1}$. Unanimity is achieved, albeit slowly. In three dimensions and greater, there is a finite probability for a diffusing particle to never reach the origin and a steady-state concentration profile develops with a $1/r^{d-2}$ deviation from the value one at large r. Correspondingly, the steady-state correlation function decays to zero as $1/r^{d-2}$ at large distances – distant voters are uncorrelated! Thus the high-dimensional Voter model reaches a steady state in which voters change opinions *ad infinitum*, with vanishing correlations at large distances.

4.3 Survival in an Expanding Cage

For a fixed-length interval, the survival probability of a diffusing particle $S(t)$ asymptotically decays as $e^{-\pi^2 Dt/L^2}$. We now consider the situation where the interval length $L(t)$ grows. There are 3 basic cases: (1) For $L(t) \propto t^\alpha$ with $\alpha < 1/2$, we apply the *adiabatic approximation*. This leads to a stretched exponential decay, $S(t) \propto \exp(-At^{(1-2\alpha)})$. (2) For $\alpha > 1/2$, the probability distribution is close to that for free diffusion. This leads to a non-zero limiting value for $S(t)$ as $t \to \infty$. (3) The most interesting case is when the cage expands at the same rate as diffusion. Here a new dimensionless parameter appears – the ratio of the diffusion

length to the cage length – that leads to $S(t)$ decaying as a non-universal power-law in time. There are still two distinct situations: either the cage expands as a power law in time, $L(t) = (At)^\alpha$ or the boundaries of the cage each diffuse. For the former situation, we will show that $S(t)$ decays as $t^{-\beta}$, with $\beta = \beta(A, D)$ diverging as D/A for $A/D \ll 1$ and approaching zero as $\exp(-A/D)$ for $A/D \gg 1$.

4.3.1 Slowly Expanding Cage: Adiabatic Approximation

For $L(t) \ll \sqrt{Dt}$, we invoke the adiabatic approximation, in which the spatial dependence of the concentration for an interval of length $L(t)$ is assumed to be identical to that of the static diffusion equation at the instantaneous value of L. Thus we write

$$c(x,t) \approx f(t)\, \cos\left(\frac{\pi x}{2L(t)}\right) \equiv c_{\rm ad}(x,t), \tag{4.3.1}$$

with $f(t)$ to be determined. The corresponding survival probability is

$$S(t) \approx \int_{-L(t)}^{L(t)} c_{\rm ad}(x,t)\, dx = \frac{4}{\pi}\, f(t) L(t). \tag{4.3.2}$$

To obtain $f(t)$, we substitute (4.3.1) into the diffusion equation, to give

$$\frac{df}{dt} = -\left(\frac{D\pi^2}{4L^2}\right) f - \left(\frac{\pi x}{2L^2}\right)\, \frac{dL}{dt}\, \tan\left(\frac{\pi x}{2L}\right)\, f. \tag{4.3.3}$$

While variable separation does not strictly hold, since the equation for $f(t)$ also involves x, the second term on the right-hand side is negligible when $L(t)$ increases as $(At)^\alpha$ with $\alpha < 1/2$. Then

$$f(t) \propto \exp\left[-\frac{D\pi^2}{4}\int_0^t \frac{dt'}{L^2(t')}\right] = \exp\left[-\frac{D\pi^2}{4(1-2\alpha)A^{2\alpha}}\, t^{1-2\alpha}\right]. \tag{4.3.4}$$

4.3.2 Rapidly Expanding Cage: Free Approximation

For a rapidly expanding cage, the absorbing boundaries eventually become irrelevant and the concentration profile approaches the Gaussian distribution of free diffusion. We then account for the slow decay of the survival probability by augmenting the Gaussian with an overall decaying amplitude as follows:

$$c(x,t) \approx \frac{S(t)}{\sqrt{4\pi D t}}\, e^{-x^2/4Dt} \equiv c_{\rm free}(x,t).$$

Although this concentration does not satisfy the absorbing boundary condition, the inconsistency is negligible at large times, since the density is exponentially small at the cage boundaries. We may now find the decay of the survival probability by equating the probability flux to the cage boundaries, $2D|\frac{\partial c}{\partial x}|$, to the loss of probability within the cage. For $L(t) = (At)^\alpha$, this flux is

$$\frac{S(t) A^\alpha}{\sqrt{4\pi D}}\, t^{\alpha - 3/2}\, \exp\left(-\frac{A^{2\alpha}}{4D} t^{2\alpha-1}\right), \tag{4.3.5}$$

that rapidly goes to zero for $\alpha > 1/2$. Since this flux equals $-\frac{dS}{dt}$, it follows that the survival probability approaches a non-zero limiting value for $\alpha > 1/2$, and that this limiting value goes to zero as $\alpha \to 1/2$.

4.3.3 Marginally Expanding Cage

For $\alpha = 1/2$, we might hope that the adiabatic and the free approximations will be use for $A/D \ll 1$ and $A/D \gg 1$. In the adiabatic approximation, the second term in Eq. (4.3.3) is, in principle, non-negligible for $\alpha = 1/2$. However, if $A \ll D$, the cage still expands more slowly than free diffusion and the error made

by neglecting the second term in Eq. (4.3.3) may still be small. The solution to this truncated equation immediately gives $f(t)$, which, when substituted into approximately (4.3.2) leads to $S_{\rm ad}(t) \approx t^{-\beta_{\rm ad}}$, with

$$\beta_{\rm ad} \approx \frac{D\pi^2}{4A} - \frac{1}{2}. \tag{4.3.6}$$

Similarly for $A \gg D$, the free approximation gives

$$\frac{dS}{dt} \approx -2D\left|\frac{\partial c(x,t)}{\partial x}\right|_{x=\sqrt{At}} = -\frac{S(t)}{t}\sqrt{\frac{A}{4\pi D}}\, e^{-A/4D}. \tag{4.3.7}$$

This again leads to the non-universal power law for the survival probability, $S_{\rm free} \sim t^{-\beta_{\rm free}}$, with

$$\beta_{\rm free} = \sqrt{\frac{A}{4\pi D}}\, e^{-A/4D}. \tag{4.3.8}$$

As shown in Fig. 4.3, these approximations are surprisingly accurate over much of the range of A/D.

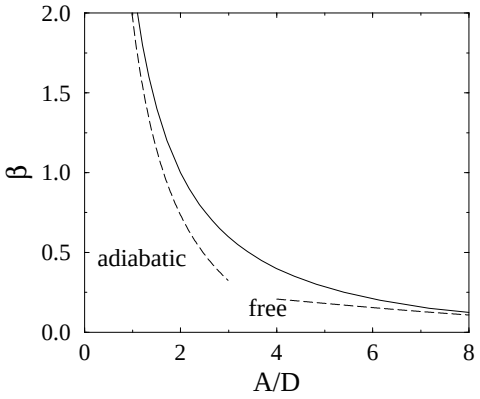

Figure 4.3: The survival probability exponent β for the marginal case $L(t) = (At)^{1/2}$. Shown is the exact value of β (solid), together with the predictions from the adiabatic and the free approximations respectively.

We now outline a first-principles analysis for the survival probability of a diffusing particle in a marginally expanding cage. We first write the density in terms of the scaling variables $\xi \equiv \frac{x}{L(t)}$ and $\rho \equiv \sqrt{\frac{A}{D}}$

$$c(x,t) = t^{-\beta-1/2}\mathcal{C}_\rho(\xi), \tag{4.3.9}$$

where $\mathcal{C}_\rho(\xi)$ is the scaling function that encodes the spatial dependence. The power law prefactor ensures that the survival probability decays as $t^{-\beta}$. When Eq. (4.3.9) is substituted into the diffusion equation, the scaling function satisfies the ordinary differential equation

$$\frac{1}{\rho^2}\frac{d^2\mathcal{C}}{d\xi^2} + \frac{\xi}{2}\frac{d\mathcal{C}}{d\xi} + \left(\beta + \frac{1}{2}\right)\mathcal{C} = 0.$$

Introducing $\eta = \xi\sqrt{\rho/2}$ and $\mathcal{C}(\xi) = e^{-\eta^2/4}\,\mathcal{D}(\eta)$, we transform this into the parabolic cylinder equation

$$\frac{d^2\mathcal{D}}{d\eta^2} + \left[2\beta + \frac{1}{2} - \frac{\eta^2}{4}\right]\mathcal{D} = 0. \tag{4.3.10}$$

For an unbounded range of η, this equation has solutions for quantized values of the energy eigenvalue $E = 2\beta + \frac{1}{2} = \frac{1}{2},\ \frac{3}{2},\ \frac{5}{2}, \ldots$. For the cage problem, the range of η is restricted to $|\eta| \le \sqrt{A/2D}$. In the

equivalent quantum mechanical system, this corresponds to a particle in a harmonic-oscillator potential for $|\eta| < \sqrt{A/2D}$ and an infinite potential for $|\eta| > \sqrt{A/2D}$. For this geometry, the appropriate solution is $\mathcal{D}(\eta) \equiv \frac{1}{2}(\mathcal{D}_{2\beta}(\eta) + \mathcal{D}_{2\beta}(-\eta))$, where $\mathcal{D}_\nu(\eta)$ is the parabolic cylinder function of order ν. Finally, the relation between the decay exponent β and $\sqrt{A/D}$ is determined implicitly by the absorbing boundary condition, namely, $\mathcal{D}_{2\beta}(\sqrt{A/2D}) + \mathcal{D}_{2\beta}(-\sqrt{A/2D}) = 0$, which can be solved numerically. In the limiting cases $A/D \ll 1$ and $A/D \gg 1$ we obtain the forms given by the heuristic approaches.

4.4 The Moving Cliff

As a complement to the expanding cage, we study the first-passage properties to an absorbing, moving boundary in a semi-infinite domain (a "cliff"). Once again, the asymptotic behavior of the survival probability depends on the relative time dependences of the cliff position $x_{\rm cl}(t)$ and the diffusion length $\sqrt{Dt}$. When $x_{\rm cl}(t) \sim t^\alpha$ with $\alpha > 1/2$, the particle motion is subdominant. Consequently $S(t)$ approaches a non-zero asymptotic value for a receding cliff and quickly goes to zero for an advancing cliff. For $\alpha < 1/2$, the cliff motion is asymptotically irrelevant and the survival probability decays as $t^{-1/2}$, as in the case of a static boundary. The interesting situation is again $x_{\rm cl}(t) \sim \sqrt{At}$, where we find that $S(t)$ decays as $t^{-\beta}$, with β dependent on A/D.

We analyze this system by the methods used for the marginally expanding interval. It is convenient to change variables from (x,t) to $(x' = x - x_0(t), t)$ to fix the absorbing cliff at the origin. The initial diffusion equation is then transformed to the convection-diffusion equation (in which the prime is now dropped)

$$\frac{\partial c}{\partial t} - \frac{x_{\rm cl}}{2t}\frac{\partial c}{\partial x} = D\frac{\partial^2 c}{\partial x^2}, \quad \text{for} \quad 0 \le x < \infty, \tag{4.4.1}$$

with the boundary condition $c(x = 0, t) = 0$. This describes biased diffusion with velocity $-x_{\rm cl}/2t$ and absorption at the origin. If the cliff in the initial system is approaching, then in the transformed problem the bias velocity is toward a fixed cliff and vice versa for the receding cliff.

We now introduce the dimensionless length $\xi = \pm x/x_{\rm cl}$, where $\pm$ refers to the approaching and the receding cliffs, respectively, and then we make the scaling ansatz $c(x,t) = t^{-\beta-1/2}\mathcal{C}_\rho(\xi)$ (see (4.3.9)) for the concentration profile. Substituting this ansatz into Eq. (4.4.1) gives

$$\frac{D}{A}\frac{d^2\mathcal{C}}{d\xi^2} + \frac{1}{2}(\xi \pm 1)\frac{d\mathcal{C}}{d\xi} + \left(\beta + \frac{1}{2}\right)\mathcal{C} = 0.$$

It is now expedient to transform variables yet again by

$$\eta = \sqrt{\frac{A}{2D}}(\xi \pm 1), \quad \mathcal{D}(\eta) = \mathcal{C}(\xi)\, e^{\eta^2/4}.$$

With these definitions, $\mathcal{D}(\eta)$ satisfies the same parabolic cylinder equation as the interval problem (Eq. (4.3.10)), but with the boundary conditions

$$\mathcal{D}_{2\beta}(\pm\sqrt{A/2D}) = 0, \tag{4.4.2a}$$

that correspond to absorption of the particle when it hits the cliff (+ sign for approaching cliff and − sign for receding), and

$$\mathcal{D}_{2\beta}(\eta = \infty) = 0, \tag{4.4.2b}$$

that ensures that $S(t) = \int_0^\infty dx\; c(x,t)$ remains bounded.

The determination of the survival exponent β and the concentration profile $\mathcal{D}(\eta)$ is therefore equivalent to finding the ground state energy and wavefunction of a quantum particle in a potential composed of an infinite barrier at $\eta = \pm\sqrt{A/2D}$ and the harmonic-oscillator potential for $\eta > \pm\sqrt{A/2D}$. Higher excited states do not contribute in the long time limit. This prescription provides a general (implicit) solution for $\beta = \beta(A/D)$ that must be solved numerically (see Fig. 4.4). However, we can obtain some of the limiting behavior for β for small and large values of A/D directly from the parabolic cylinder equation (Eq. (4.3.10)) together with elementary facts about the quantum mechanics of the harmonic oscillator.

In the limit $A \ll D$, the infinite barrier in the equivalent quantum problem is close to $\eta = 0$. When the wall is exactly at the origin, the ground state of this truncated harmonic-oscillator potential is obviously the first excited state of the pure harmonic oscillator, namely, $\mathcal{D}(\eta) = \eta e^{-\eta^2/4}$ and correspondingly $\beta = 1/2$. For $A \ll D$, it is possible to construct a perturbative solution for the concentration profile, which ultimately gives

$$\beta \approx \frac{1}{2} \pm \sqrt{\frac{A}{4\pi D}} \qquad A \ll D. \tag{4.4.3a}$$

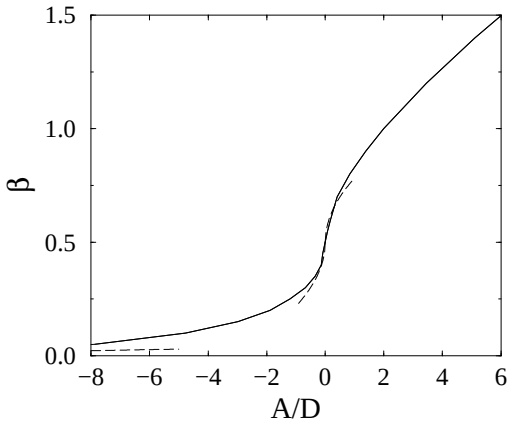

Figure 4.4: Survival probability exponent β versus A/D for the cliff geometry when its position is $L(t) = \pm(At)^{1/2}$. Positive (negative) A/D corresponds to an approaching (receding) cliff. Shown are the exact value of β from the numerical solution of Eq. (4.4.2a) and the approximate predictions (both dashed) for $|A|/D \ll 1$ (Eq.(4.4.3a)), and for $-A/D \gg 1$ (Eq. (4.4.3b)).

When $A \gg D$ and the cliff is receding, the position of the absorbing boundary goes to $-\infty$. Hence the ground state for this system is close to the harmonic-oscillator ground state, namely, $\mathcal{D}(\eta) = e^{-\eta^2/4}$ and $\beta \approx 0$. For this case, we can also apply the free approximation, but with the obvious modification that there is only a single boundary at which flux leaves the system. By this approach, the survival probability exponent is

$$\beta \approx \sqrt{\frac{A}{16\pi D}}\, e^{-A/2D}, \qquad A \gg D \text{ and receding cliff.} \tag{4.4.3b}$$

For the advancing cliff, the equivalent quantum system is the harmonic-oscillator potential for $\eta > \sqrt{A/2D}$ and an infinite barrier at $\eta = \sqrt{A/2D}$. Here, the most naive estimate for the ground state energy is simply the minimum value of the potential energy, that is, $E_0 \approx \eta^2/4 = A/8D$. This immediately gives

$$\beta \approx \frac{A}{16D}, \qquad A \gg D \text{ and advancing cliff.} \tag{4.4.3c}$$

This crude estimate turns out to be relatively inaccurate, however, even though it gives the correct asymptotic result. Part of the inaccuracy stems from the neglect of the zero-point fluctuations in the corresponding determination of the ground-state energy of a quantum particle in the truncated oscillator potential. Using the Heisenberg uncertainty principle, we obtain relatively large corrections to approximation (4.4.3c) that are of the order of $(A/D)^{1/3}$. Finally, notice that when $A/D = 2$, the survival exponent equals one. Thus the mean survival time of a diffusing particle near an advancing cliff is finite for $A/D > 2$ and infinite for $A/D \leq 2$.

Chapter 5

FRACTAL AND NON-FRACTAL NETWORKS

5.1 Cayley Tree

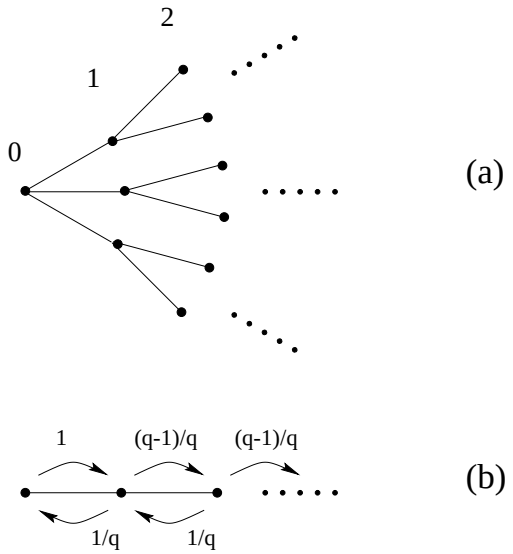

Figure 5.1: (a) A Cayley tree of co-ordination number $q = 3$ organized by generation number. (b) The rates of the effective one-dimensional random walk that are obtained when all sites in a given generation are lumped together.

To compute the first-passage probability on the Cayley tree, we first write the master equations for the occupation probability. Let $P_n(t)$ be the probability that the random walk is at a site in generation n at time t. The hopping rates are all the same, we take them to be $1/q$. The master equations for $P_n(t)$ are

$$\begin{aligned}
\frac{\partial P_0(t)}{\partial t} &= \frac{1}{q} P_1(t) - P_0(t), \\
\frac{\partial P_1(t)}{\partial t} &= \frac{1}{q} P_2(t) - P_1(t) + P_0(t), \\
\frac{\partial P_n(t)}{\partial t} &= \frac{1}{q} P_{n+1}(t) - P_n(t) + \frac{q-1}{q} P_{n-1}(t), \quad n \geq 2.
\end{aligned} \tag{5.1.1}$$

We solve these equations for the initial condition of a particle initially at site 0, $P_n(0) = \delta_{n,0}$. Laplace transforming Eqs. (5.1.1) leads to the recursion formulae for $P_n(s)$,

$$\begin{aligned}(s+1)P_0(s) &= \frac{1}{q}P_1(s) + 1,\\ (s+1)P_1(s) &= \frac{1}{q}P_2(s) + P_0(s),\\ (s+1)P_n(s) &= \frac{1}{q}P_{n+1}(s) + \frac{q-1}{q}P_{n-1}(s), \quad n \geq 2.\end{aligned} \tag{5.1.2}$$

For $n \geq 2$, the general solution to this constant-coefficient linear system of equation is $P_n \propto \lambda^n$ for $n \geq 1$. By inspection, the exponential solution continues to hold for for P_1, while P_0 is distinct. Therefore substituting $P_n \propto \lambda^n$ into Eqs. (5.1.2) for $n \geq 2$ leads to a characteristic equation for λ whose roots are

$$\lambda_\pm(s) = \frac{(s+1)q \pm \sqrt{(s+1)^2q^2 - 4(q-1)}}{2},$$

with $\lambda_\pm \gtrless 1$ for $q > 2$. The general solution is $P_n = A_+\lambda_+^n + A_-\lambda_-^n$, but the coefficient A_+ must be set to zero to have P_n finite at $n = \infty$. We may now obtain the coefficient A_-, as well as P_0, by substituting $P_1 = A_-\lambda_-$ and $P_2 = A_-\lambda_-^2$ into the first two recursion formulae to yields

$$A_- = \frac{q}{(q-1)(s+1) - \lambda_-}, \quad P_0 = \frac{q-1}{q}A_-, \quad P_n = \frac{q}{(q-1)(s+1) - \lambda_-}\lambda_-^n. \tag{5.1.3}$$

We now determine the first-passage characteristics. Let $F_n(t)$ be the probability for a random walk to reach a site in the n^{th} generation for the first time at time t. Then $F_n(t)$ may be found in terms of $P_n(t)$ by the basic convolution relation between $P_n(t)$ and $F_n(t)$ given in Chap. 1 (Eq. (1.1.1)),

$$P_n(t) = \int_0^t F_n(t')P_0(t-t')\,dt' + \delta_{n,0}\,\delta(t). \tag{5.1.4}$$

The corresponding relation in terms of Laplace transforms is

$$F_n(s) = \frac{P_n(s) - \delta_{n,0}}{P_0(s)}. \tag{5.1.5}$$

Thus for a random walk that starts at site 0, the Laplace transform of the first-return probability is

$$F_0(s) = 1 - \frac{1}{P_0(s)}. \tag{5.1.6}$$

For $s \to 0$, Eqs. (5.1.3) give $P_0(s=0) = (q-2)/(q-1)$, and we obtain the fundamental result

$$F_0(s=0) = \frac{1}{q-1} \tag{5.1.7}$$

for the Laplace transform of the first-return probability at $s = 0$. This coincides with the time integral of the first-passage probability, namely, the eventual return probability to the origin. Because this quantity is less than one, a random walk on the Cayley tree is transient.

5.2 Hierarchical Three-Tree

We now study the first-passage properties of a hierarchically-branched three-coordinated tree. This self-similar object is generated by replacing iteratively a single bond with a first-order tree (Fig. 5.2). This tree provides a simple laboratory to understand the role of branching and self-similarity on first-passage characteristics.

There are two generic transport modes on the tree – transmission and reflection. In the former, a random walk is injected at the left edge and exits at the right edge, with all other sites at the end of cul-de-sacs reflecting. At long times, the first-passage probability decays exponentially with time on a finite-order tree due to its finiteness. In reflection mode, a particle is injected at one end and leaves the system only when it returns to its starting point. This leads to an intermediate-time power-law tail in the first-passage probability before the ultimate exponential decay, imposed by the finiteness of the system, sets in.

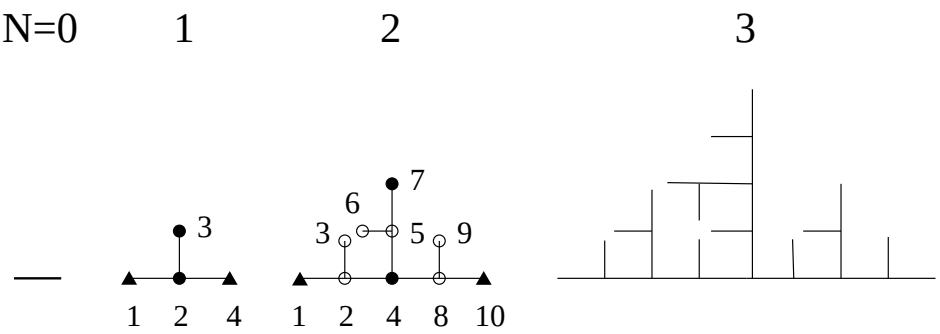

Figure 5.2: First four iterations of the hierarchical three-tree. The solid symbols – triangles for inlet and outlet sites and circles for interior sites – indicate first-order sites, and the open circles denote second-order sites. The site labels used in the master equations are written for the first- and the second-order trees.

5.2.1 Transmission in the First-Order Tree

Consider a random walk on the first-order tree that starts at site 1 and is absorbed at site 4 (Fig. 5.2) and hops equiprobably to any of its nearest-neighbor sites at each discrete time step. Let $P_i(t)$ be the probability for a random walk to be at site i at time t. We seek the first-passage probability $F(t)$ that the walk reaches the output site 4 at time t. If we view the output site as sticky, then the first-passage probability is related to the occupation probability at the output site by $P_4(t) = P_4(t-1) + F(t)$. For the first-order tree, the master equations are

$$P_1(t+1) = \frac{1}{3}P_2(t), \quad P_2(t+1) = P_1(t) + P_3(t), \quad P_3(t+1) = \frac{1}{3}P_2(t), \quad F(t+1) = \frac{1}{3}P_2(t).$$

For a particle that is initially at site 1, the corresponding master equations for the generating functions, $P_i(z) = \sum_{t=0}^{\infty} P_i(t)z^t$ and $F(z) = \sum_{t=0}^{\infty} F(t)z^t$, are

$$P_1(z) = aP_2(z) + 1, \quad P_2(z) = 3aP_1(z) + 3aP_3(z), \quad P_3(z) = aP_2(z), \quad F(z) = aP_2(z), \tag{5.2.1}$$

where $a = z/3$ and the factor of 1 on the right-hand side of the first equation arises from the initial condition. Solving for $F(z)$ yields

$$F(z) = \frac{3a^2}{1-6a^2} = \frac{z^2/3}{(1-2z^2/3)}. \tag{5.2.2}$$

From this generating function, it is easy to obtain all first-passage properties. The series expansion of the generating function in powers of z is

$$F(z) = \frac{z^2}{3}\left[1 + \frac{2}{3}z^2 + \frac{4}{9}z^4 + \ldots + \left(\frac{2}{3}\right)^n z^{2n} + \ldots\right],$$

from which the first-passage probability at time t is

$$F(t) = \frac{1}{3}\left(\frac{2}{3}\right)^{(n-2)/2}. \tag{5.2.3}$$

Finally, the mean first-passage time is

$$\langle t\rangle = \sum tF(t) = z\frac{d}{dz}F(z)\Big|_{z=1} = 6. \tag{5.2.4}$$

5.2.2 Exact Renormalization for the $N^{\rm th}$-Order Tree

We can calculate the first-passage probability in higher-order trees by solving the master equations for all the site probabilities and then computing the flux leaving the system. This is tedious and does not take advantage of the hierarchical organization. It is much better to perform the calculation iteratively by eliminating the master equations associated with occupation probabilities of the $N^{\rm th}$-order sites in the $N^{\rm th}$-order tree to give renormalized equations for a tree of one lower order. This process preserves the form of the master equations and leads to the exact solution.

For the second-order tree ($N = 2$ in Fig. 5.2), we first eliminate the variables associated with the second-order sites in the tree (open circles) to obtain renormalized master equations for the first-order sites (filled symbols) and then solve these renormalized equations. The master equations for the generating functions on the second-order tree are

$$\begin{aligned}
P_1(z) &= aP_2(z) + 1,\\
P_2(z) &= 3aP_1(z) + 3aP_3(z) + aP_4(z),\\
P_3(z) &= aP_2(z),\\
P_4(z) &= aP_2(z) + aP_5(z) + aP_8(z),\\
P_5(z) &= aP_4(z) + 3aP_6(z) + 3aP_7(z),\\
P_6(z) &= aP_5(z),\\
P_7(z) &= aP_5(z),\\
P_8(z) &= aP_4(z) + 3aP_9(z),\\
P_9(z) &= aP_8(z),\\
F(z) &= aP_8(z).
\end{aligned} \tag{5.2.5}$$

We now eliminate the equations for the second-order sites, namely, 2, 3, 5, 6, 8, and 9, and identify the remaining sites 1, 4, 7, and 10, as the renormalized first-order sites $1'$, $2'$, $3'$, and $4'$, respectively. We thereby obtain the renormalized master equations

$$P_{1'} = a'P_{2'} + c, \quad P_{2'} = 3a'P_{1'} + 3a'P_{3'}, \quad P_{3'} = a'P_{2'}, \quad F' = \frac{a'}{c}P_{2'}, \tag{5.2.6}$$

with $a' = a^2/(1-6a^2)$ and $c = (1-3a^2)/(1-6a^2)$. These have the same form as the first-order master equations, Eqs. (5.2.1), except that the hopping rate has been renormalized and the quantity c appears as both the initial condition factor in the equation for $P_{1'}$ and as an overall factor in the equation for F'. These two factors cancel in solving for the first-passage probability, and we find $F' = 3a'^2/(1-6a'^2)$. This has the same form as Eq. (5.2.2) for the first-passage probability on the first-order tree! Thus the master equations on the tree renormalize exactly. Now we may iteratively eliminate all lower-order sites to yield the first-passage probability on an $N^{\rm th}$-order tree

$$F^{(N)}(z) = \frac{3(a^{(N)})^2}{1-6(a^{(N)})^2}, \quad \text{where} \quad a^{(N)} = \frac{(a^{(N-1)})^2}{1-6(a^{(N-1)})^2}, \tag{5.2.7}$$

and $a^{(0)} = z/3$. We combine these two equations to give a renormalization equation in terms of F only

$$F^{(N)}(z) = \frac{\frac{1}{3}(F^{(N-1)})^2}{1-\frac{2}{3}(F^{(N-1)})^2}. \tag{5.2.8}$$

Because a single-parameter renormalization gives the first-passage probability, a single time scale accounts for all the moments of the first-passage time.

We now study the asymptotics of this first-passage probability. By definition, $F^{(N)}(z)$ increases monotonically in z, with $F^{(N)}(z=1) = 1$, because the probability of eventually hitting the output site equals one. Because of the finiteness of the tree, $F^{(N)}(t)$ must decay exponentially with time as $t \to \infty$, with a decay time $\tau^{(N)}$ that grows with N. We write this as

$$F^{(N)} \sim e^{-t/\tau^{(N)}} \sim (\mu^{(N)})^t, \tag{5.2.9}$$

with $\mu^{(N)} \sim 1 - (1/\tau^{(N)})$ approaching one from below as N increases.

The corresponding generating function is

$$F^{(N)}(z) = \sum_{t=0}^{\infty} F^{(N)}(t) z^t \sim \frac{A}{(1-\mu^{(N)} z)} \equiv \frac{A}{(1 - z/z_c(N))}, \tag{5.2.10}$$

where A is a constant as $\mu \to 1$ from below. Thus the location of the closest pole to $z = 1$ in the generating function $F^{(N)}(z)$ determines the decay time. Substituting this asymptotic form into Eq. (5.2.8), we find that this pole is located at $\sqrt{3/2} = 1.2247\ldots$, $1.0320\ldots$, and $1.0052\ldots$, for $N = 1$, 2, and 3, respectively. In general, $z_c^{(N)}$ is determined by the recursion formula

$$z_c^{(N)} = \sqrt{3 z_c^{(N-1)}/(1 + 2 z_c^{(N-1)})}. \tag{5.2.11}$$

Since $z_c^{(N)}$ is close to one, we define $z_c^{(N)} \equiv 1 + \epsilon_N$, with $\epsilon_N \ll 1$, and substitute this into Eq. (5.2.11) to find $\epsilon_N = \frac{1}{6}\epsilon_{N-1}$. Thus $F^{(N)}(z)$ has a simple pole at $z_c^{(N)}$ that asymptotically approaches one from above as 6^{-N}. This corresponds to the characteristic time $\tau^{(N)}$ in the exponential decay of $F^{(N)}(t)$ increasing as 6^N.

5.2.3 Reflection in the Three-Tree

We now consider the reflection process, in which a random walk starts at the left edge of the tree (site 1 of Fig. 5.2) and is absorbed upon return to this starting point. All other endpoints of the tree are reflecting. We use the simplifying device of first solving for the occupation probabilities and then exploiting the basic relation between occupation and first-passage probabilities Eq. (1.1.2) to extract the latter. The master equations on the reflecting tree are nearly identical to those in the transmission problem, Eqs. (5.2.5), except that we must now include an equation for the rightmost (reflecting) site of the tree (Fig. 5.2). For the second-order tree, for example, the rightmost site is #10 and its master equation is $P_{10}(z) = aP_8(z)$.

Following the same renormalization as in transmission and after some algebra, the generating function for the occupation probability at the origin on an N^{th}-order tree is given by

$$P_1^{(N)}(z) = \frac{1 - 6(a^{(N-1)})^2}{1 - 9(a^{(N-1)})^2} \prod_{k=0}^{N-2} \frac{1 - 3(a^{(k)})^2}{1 - 6(a^{(k)})^2} \equiv \frac{1}{\mathcal{Q}^{(N)}(1 - 9(a^{(N-1)})^2)}, \tag{5.2.12}$$

with $a^{(N)}$ defined in Eq. (5.2.7) and $a^{(0)} \equiv a = z/3$. The reason for the peculiar definition in the second line will become clear momentarily. To find the moments of the return time to the origin we start with basic relation between the first-passage and occupation probabilities

$$\begin{aligned} F^{(N)}(z) &= 1 - \frac{1}{P_1^{(N)}(z)} \qquad \text{from Eq. (1.1.2)} \\ &\equiv 1 - \mathcal{Q}^{(N)}\,(1 - 9(a^{(N-1)})^2). \end{aligned} \tag{5.2.13}$$

The mean return time is given formally by

$$\langle t^{(N)} \rangle = z \frac{dF^{(N)}(z)}{dz}\Big|_{z=1}, = \Big[1 - (1 - 9(a^{(N-1)})^2)\mathcal{Q}^{(N)}\Big]'\Big|_{z=1} = +18\mathcal{Q}^{(N)}\, a^{(N-1)}\, a^{(N-1)\prime}\Big|_{z=1}. \tag{5.2.14}$$

Using the chain rule repeatedly, together with the facts that the factor $1 - 9(a^{(N-1)})^2$ vanishes at $z = 1$ and that $a^{(k)} = 1/3$ at $z = 1$ for all k, we may easily compute the derivative of $a^{(k)}$. We thus find

$$\langle t^{(N)} \rangle = 2 \times 3^N. \tag{5.2.15}$$

The second moment $\langle (t^{(N)})^2 \rangle$ may be computed similarly (but more tediously) and gives asymptotically

$$\langle (t^{(N)})^2 \rangle \propto \times 2^N \times 3^{2N}. \tag{5.2.16}$$

The important feature is that the second moment is much larger than the first moment squared:

$$\langle (t^{(N)})^2 \rangle \propto 2^N \langle t^{(N)} \rangle^2 \gg \langle t^{(N)} \rangle^2. \tag{5.2.17}$$

In general, $\langle (t^{(N)})^k \rangle \propto 2^{(k-1)N} \times 3^{kN}$. Thus each moment of the return time scales independently. This property arises because of the intermediate-time power law decay in the distribution of return times.

We can infer the exponent of this power law in the first-return probability from the disparity between the first and the second moments together with simple reasoning. On physical grounds, the first-return probability has the form

$$F^{(N)}(t) \sim t^{-\mu} e^{-t/\tau^{(N)}},$$

where μ must be greater than one for the distribution to be normalizable when $N \to \infty$ and $\tau^{(N)}$ correspondingly diverges. This fact means that the exponential plays a subdominant role in the normalization integral, $\int_0^\infty F^{(N)}(t)\, dt = 1$, so that there is no power-law prefactor that involves $\tau^{(N)}$ in $F^{(N)}(t)$. With this form for $F^{(N)}(t)$, we then deduce

$$\langle t^{(N)} \rangle \sim \int_0^\infty t^{1-\mu} e^{-t/\tau^{(N)}}\, dt \sim (\tau^{(N)})^{2-\mu} \quad \langle (t^{(N)})^2 \rangle \sim \int_0^\infty t^{2-\mu} e^{-t/\tau^{(N)}}\, dt \sim (\tau^{(N)})^{3-\mu}. \tag{5.2.18}$$

In these formulae, the cutoff time $\tau^{(N)}$ for an $N^{\rm th}$-order tree is 6^N, as determined by our previous results about transmission mode. Comparing this with the previously-derived moments $\langle t^{(N)} \rangle \propto 3^N$ and $\langle (t^{(N)})^2 \rangle \propto 2^N \times 3^N$, we infer that the decay exponent μ is given by

$$\mu = 2 - \frac{\ln 3}{\ln 6} \approx 1.3868\ldots. \tag{5.2.19}$$

5.3 Hydrodynamic Transport

We now study the first-passage properties in media in which the flow is hydrodynamically driven by an external pressure drop. This leads to a heterogeneous flow field because of the local disorder of the medium. A crucial element in such systems is the interplay between convection and molecular diffusion. In the spirit of preceding sections, we study first passage on simple but prototypical systems.

5.3.1 Single-Sidebranch Network

As a preliminary, we consider the role of a single sidebranch on first-passage characteristics (Fig. 5.3).

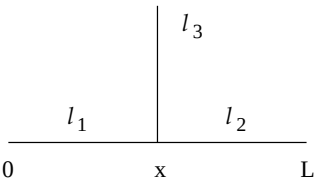

Figure 5.3: A linear system of length $L = \ell_1 + \ell_2$, with a sidebranch of length ℓ_3 attached at $x = \ell_1$. There is a current input at 0 and an output at L. The end of the sidebranch is reflecting.

To find the first-passage probability, we solve the diffusion equation in each backbone segment $(0, x)$ and (x, L), as well as in the sidebranch, subject to appropriate boundary conditions at the input, output, junction point, and at the end of the sidebranch. In terms of Laplace transforms, these boundary conditions are

$$\begin{array}{ll} j_1(x,s) = 1 & \text{at } x = 0, \\ j_3(y,s) = 0 & \text{at } y = \ell_3, \\ c_2(x,s) = 0 & \text{at } x = L, \\ c_1(x,s) = c_2(x,s) = c_3(x,s) & \text{at junction}, \\ j_1(x,s) - j_2(x,s) - j_3(y,s) = 0 & \text{at junction}. \end{array} \tag{5.3.1}$$

The solution to the diffusion equation in the $i^{\rm th}$ bond ($i = 1, 2, 3$) has the general form $c_i(x,s) = A_i e^{x\sqrt{s/D}} + B_i e^{-x\sqrt{s/D}}$, where A_i and B_i are determined by the boundary conditions. The absorbing boundary condition at $x = L$ reduces c_2 to $c_2(x,s) = A_2 \sinh\sqrt{\frac{s}{D}}(L-x)$. Similarly, the reflecting boundary at the end of the sidebranch implies that c_3 has the form $c_3(y,s) = A_3 \cosh\sqrt{\frac{s}{D}}(\ell_3 - y)$. Then the condition $j_1(x=0,s) = 1$ reduces c_1 to $c_1(x,s) = A_1\cosh\sqrt{\frac{s}{D}}x + \frac{1}{\sqrt{sD}}e^{-x\sqrt{s/D}}$. Finally, continuity of the concentration and conservation of flux at the junction provide three more equations to determine the remaining coefficients A_i and thereby the concentration in each bond. For the unit flux initial condition, the first-passage probability is just the outgoing flux at $x = L$, $j_2(x,s)$. From the equation for c_2, this flux is merely $A_2\sqrt{sD}$. By solving for the A_i, the Laplace transform of the first-passage probability is

$$j_2(L,s) = \left(\cosh\sqrt{\frac{s}{D}}L + \cosh\sqrt{\frac{s}{D}}\ell_1 \sinh\sqrt{\frac{s}{D}}\ell_2 \tanh\sqrt{\frac{s}{D}}\ell_3\right)^{-1}. \tag{5.3.2}$$

If the sidebranch is absent ($\ell_3 = 0$), the first-passage probability reduces to that of a linear chain, $j_2(L,s) = \operatorname{sech}(L\sqrt{s/D})$. By expanding $j_2(x,s)$ in a power series in s, we obtain the mean and the mean-square first-passage times

$$\langle t\rangle = \frac{1}{D}\left(\frac{1}{2}L^2 + \ell_2\ell_3\right), \quad \langle t^2\rangle = \frac{1}{D^2}\left[\frac{5}{12}L^4 + \ell_2\ell_3\left(\ell_1^2 + \frac{5}{3}\ell_2^2 + \frac{2}{3}\ell_3^2 + 4\ell_1\ell_2\right)\right]. \tag{5.3.3}$$

Notice that $\langle t\rangle$ is a *linear* function of the sidebranch length ℓ_3.

It is instructive to study the single-sidebranch network when there is a constant bias along the backbone. Thus for bonds 1 and 2 we solve the convection diffusion equation,

$$\frac{\partial c(x,t)}{\partial t} + v\frac{\partial c(x,t)}{\partial x} = D\frac{\partial^2 c(x,t)}{\partial x^2},$$

where v is the bias velocity, while for bond 3 we solve the diffusion equation. Now the general forms for the bond concentrations are $c_i(x,s) = A_i e^{\alpha_+ x} + B_i e^{\alpha_- x}$, for $i = 1$ and 2, with $\alpha_\pm = (v \pm \sqrt{v^2 + 4Ds})/2D$, while for bond 3, the general solution has a similar form with v set to zero. Applying the boundary conditions of Eqs. (5.3.1) leads, after tedious steps, to probability

$$j_2(x,s) = -\frac{\sqrt{v^2+4Ds}\; e^{-\alpha_-\ell_1}\left(1 + \frac{s}{D\alpha_+}\right)u(\ell_1)}{su(\ell_1)u(-\ell_2) + \sqrt{sD}\tanh\sqrt{\frac{s}{D}}\ell_3\, u'(\ell_1)u(-\ell_2) + Du'(\ell_1)v(\ell_2)}, \tag{5.3.4}$$

where $u(\ell) \equiv e^{\alpha_+\ell} - e^{\alpha_-\ell}$ and $v(\ell) \equiv \alpha_- e^{\alpha_+\ell} - \alpha_+ e^{\alpha_-\ell}$, and $u'(\ell)$ denotes differentiation with respect to ℓ.

For large bias the first-order expansion in s for j gives the extraordinarily simple result

$$j_2(x,s) = 1 - s\left(\frac{\ell_1+\ell_2+\ell_3}{v} - \frac{3D}{2v^2} + \mathcal{O}(e^{-Pe})\right) + \ldots,$$

where $Pe = vL/2D$ is the Péclet number. Thus, as $v \to \infty$, the mean first-passage time approaches

$$\langle t\rangle \to \frac{\ell_1+\ell_2+\ell_3}{v}. \tag{5.3.5}$$

That is, the mean first-passage time is simply the system volume divided by the flow velocity, independent of any other geometrical features of the system!

5.3.2 Single-Junction Network

We can give a deeper meaning to the single sidebranch result by considering the related single-junction network (Fig. 5.4). The interesting situation is that of a large overall pressure drop ΔP, but where the bias in one of the two bonds in parallel, either 2 or 3, is vanishingly small. While the convection time across this slow bond becomes large, the entrance probability correspondingly becomes small in such a way

that the mean time to traverse the network becomes independent of the slow bond. This occurs because when the convection time across the slow bond becomes equal to the diffusion time, the entrance probability and the local transit time both "stick" at their values at the diffusive-convective crossover. Because of this mechanism, the first-passage time across the single-junction network continues to satisfy the equal-time theorem even when there is a slow bond. This picture holds more generally when there is at least one fast path through the network where the Péclet number is large. The single-junction network allows us to understand this physical picture analytically.

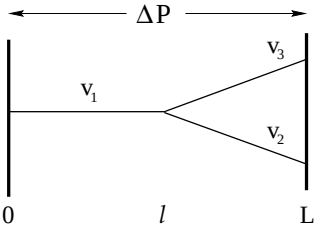

Figure 5.4: A three-bond single-junction network with an overall pressure drop ΔP that leads to local bias velocities $v_1 = v$, v_2, and v_3. There is a unit flux input at 0 and an output at L.

We now solve the convection-diffusion equations for the single-junction network. We assume bias velocities $v_1 = v$, v_2, and v_3, with $v_2 + v_3 = v$ for flux conservation. The convection-diffusion equations for each bond are supplemented by the boundary conditions

$$\begin{array}{ll} j_1(x,s) = 1 & \text{at } x = 0, \\ c_2(x,s) = c_3(y,s) = 0 & \text{at } x = L, \\ c_1(x,s) = c_2(x,s) = c_3(x,s) & \text{at junction}, \\ j_1(x,s) - j_2(x,s) - j_3(y,s) = 0 & \text{at junction}. \end{array}$$

From the general solution to the convection-diffusion equation, the absorbing boundary conditions at $x = L$ imply that the concentrations in bonds 2 and 3 have the general form $c_i(x,s) = A_i[e^{\alpha_i(x-L)} - e^{\beta_i(x-L)}]$ for $i = 1, 2$, where $\alpha_i, \beta_i = (v_i \pm \sqrt{v_i^2 + 4Ds})/2D$ and $\ell \le x \le L$. Similarly, the condition of unit flux input implies that c_1 has $c_1(x,s) = A_1[\alpha_1\, e^{\alpha_1 x} - \beta_1\, e^{\beta_1 x}] + \frac{1}{D\alpha_1} e^{\beta_1 x}$ for $0 \le x \le \ell$. Finally, we apply the remaining boundary conditions of continuity of the flux and the concentration at $x = \ell$ to fix the remaining constants.

Consider the splitting probability, namely, the probability that a particle reaches the output via bond 2 or via bond 3. By definition, the time-integrated output flux via bond i is simply $j_i(L, s = 0)$. The $s = 0$ limit of the flux can still be easily obtained by hand calculation, and the result is

$$j_2(L,0) = \frac{v_2(e^{-Pe_3} - 1)}{v_2(e^{-Pe_3} - 1) + v_3(e^{-Pe_2} - 1)}, \quad j_3(L,0) = \frac{v_3(e^{-Pe_2} - 1)}{v_2(e^{-Pe_3} - 1) + v_3(e^{-Pe_2} - 1)}, \tag{5.3.6}$$

where the local Péclet numbers are defined as $Pe_i = v_i(L - \ell)/D$, for $i = 2, 3$. When the bias in both downstream bonds is large, these fluxes reduce to the obvious result $j_2 = v_2/(v_2 + v_3)$ and $j_3 = v_3/(v_2 + v_3)$, while if the bias in both bonds vanishes, then $j_2 = j_3 = 1/2$.

The most interesting situation is the case in which, say $v_3 \to 0$ while v_2 remains large. Then the ratio of exit probabilities via each bond is

$$\frac{j_3}{j_2} \to \frac{D}{v_2(L - \ell)} = \frac{(L - \ell)/v_2}{(L - \ell)^2/D} \equiv \frac{\tau_{3,D}^{-1}}{\tau_{2,c}^{-1}}. \tag{5.3.7}$$

The physical meaning of these results is simple yet far-reaching. At the junction, the ratio of entrance probabilities into the two bonds is just the flux ratio. When one bond becomes slow, the entrance probability decreases linearly with the local bond velocity. However, when this bond becomes so slow that the diffusive rate τ_D^{-1} of entering this bond becomes comparable to the convective entrance rate τ_c^{-1}, then the entrance probability sticks at the limiting value determined by the diffusive flux. Thus the entrance probability into

a slow bond cannot become arbitrarily small. The other fundamental result is that as long as the Péclet number is large throughout at least one path through the network, $\langle t \rangle$ approaches the system volume divided by the total current.

Chapter 6

SPHERICALLY SYMMETRIC SYSTEMS

6.1 First Passage to a Sphere

6.1.1 Image Solution

We now consider the problem of *where* a diffusing particle hits the surface of an absorbing sphere (Fig. 6.1). In Section 1.3, we showed that this probability is the same as the electric field at the impact point $\vec{r}$ when a point charge of magnitude $q = 1/(\Omega_d D)$ is at the starting point $\vec{r}_0$ and the surface of the sphere is grounded.

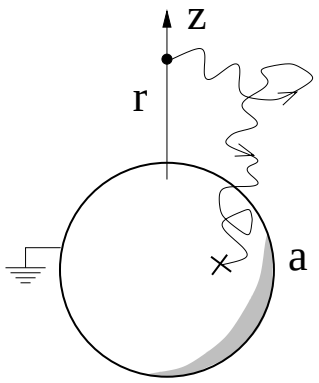

Figure 6.1: A diffusing particle starts at radius r_0 on the z axis and hits the point (a, θ, ϕ) on the sphere surface.

We may solve this problem easily by the image method. For $d > 2$ and with a point charge q located at $\vec{r}_0$ exterior to the sphere, the electrostatic potential at $\vec{r}$ is

$$\Phi(\vec{r}) = \frac{q}{|\vec{r} - \vec{r}_0|^{d-2}} + \frac{q'}{|\vec{r} - \vec{r}_0\,'|^{d-2}}, \tag{6.1.1a}$$

where q' and $\vec{r}_0\,'$ are the magnitude and the location of the image charge, respectively. The potential at any point on the surface of the sphere will be zero if

$$q' = -q\left(\frac{a}{r_0}\right)^{d-2} \qquad \text{and} \qquad r_0' = \frac{a^2}{r_0}.$$

Similarly, for $d = 2$ the electrostatic potential generically has the form

$$\Phi(\vec{r}) = q \ln|\vec{r} - \vec{r}_0| + q' \ln|\vec{r} - \vec{r}_0\ '| + A \tag{6.1.1b}$$

where the constant A is non-zero. For this potential to vanish everywhere on the surface of the grounded circle, we must choose $q' = -q$ and $r_0' = a^2/r_0$, and $A = q \ln(a/r_0)$.

Let us use these results to find the probability that the particle hits a given point on the sphere. Without loss of generality, we assume that the particle is initially on the z-axis. The hitting probability then depends only on the polar angle of the impact point and the electrostatic potential for $d > 2$ is

$$\Phi(\vec{r}) = q \left[\frac{1}{(r^2 + r_0^2 - 2rr_0\cos\theta)^{(d-2)/2}} - \frac{(a/r_0)^{d-2}}{(\frac{a^4}{r_0^2} + r^2 - 2\frac{a^2 r}{r_0}\cos\theta)^{(d-2)/2}} \right]. \tag{6.1.2}$$

Taking the radial component of the electric field, using $q = 1/(\Omega_d D)$, and multiplying by $-D$ to compute the flux, we find that the hitting probability to a point (a, θ) on the surface is

$$\mathcal{E}(\theta) = \frac{(d-2)}{\Omega_d} \frac{1}{a r_0^{d-2}} \frac{(1 - \frac{a^2}{r_0^2})}{(1 - \frac{2a}{r_0}\cos\theta + \frac{a^2}{r_0^2})^{d/2}}, \qquad d > 2, \tag{6.1.3a}$$

while for $d = 2$, the corresponding hitting probability is

$$\mathcal{E}(\theta) = \frac{1}{2\pi a} \frac{(1 - \frac{a^2}{r_0^2})}{(1 - \frac{2a}{r_0}\cos\theta + \frac{a^2}{r_0^2})}, \qquad d = 2. \tag{6.1.3b}$$

The integral of the hitting probability over the sphere surface equals one for $d = 2$ and equals $(a/r_0)^{d-2}$ for $d > 2$; these reproduce our previous results about exit probabilities. More interesting is the angular dependence of hitting probability. For example, the ratio of the probabilities of hitting the north pole (most likely) and the south pole (least likely) is

$$\frac{\mathrm{FPP}_{\max}}{\mathrm{FPP}_{\min}} = \left(\frac{1 + a/r_0}{1 - a/r_0} \right)^d$$

For example, in $d = 3$, if $r_0 = 2a$, the particle is 27 times more likely to hit the north pole rather than the south pole.

The same image approach also gives the hitting probability to any point on the sphere when a particle starts in the interior. By inversion symmetry, the electrostatic potential interior to a grounded sphere due to a point charge q that is located at $|\vec{r}_0| < a$ on the z-axis is the sum of the potential of this point charge and that of a larger image charge $q' = -q(a/r_0)^{d-2}$ that is located at $r_0' = a^2/r_0$. With this fact, the hitting probability is again given by Eqs. (6.1.3a) and (6.1.3b) for $d > 2$ and $d = 2$ respectively.

6.1.2 Efficient Simulation of Diffusion-Limited Aggregation

Our results about the hitting probability provides an elegant and efficient way to simulate diffusion-limited aggregation (DLA). Our discussion also illustrates an important maxim about simulations of diffusion. It is almost always pointless to simulate diffusion by the step-by-step motion of discrete random walks. Especially for processes with absorbing boundaries, such simulations can be performed more elegantly by exploiting first-passage ideas.

DLA is a non-equilibrium growth process that is defined by the following simple rules:

1. Start with a single "sticky" seed particle at the origin.
2. From afar, launch a diffusing particle. On touching the aggregate, the particle is incorporated and also becomes sticky.
3. Repeat step 2, until an aggregate of a desired size is grown.

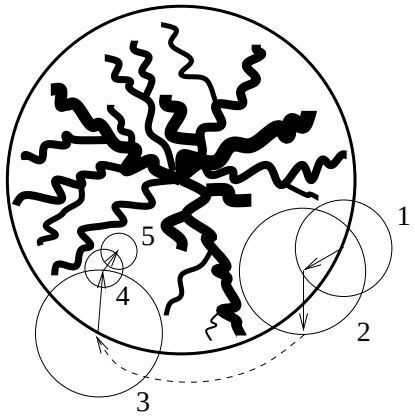

Figure 6.2: Illustration of a "good" DLA growth algorithm. Shown is a trajectory of a diffusing particle that is about to be incorporated into the aggregate. When the particle strays outside the circumscribing circle it is returned to this circle by implementing Eq. (6.1.3*b*). When the particle is within a fjord, it is efficient to move the particle to the circumference of the largest circle that is centered at the current particle position that does not touch the DLA.

These rules lead to a ramified structure, as crudely illustrated in Fig. 6.2. Although the growth algorithm is extremely simple, it is also grossly inefficient. In the early days of DLA simulations, this led to sometimes misguided efforts at improvement. These issues provide a natural segue to the use of first-passage ideas to construct an efficient simulation.

The first problem with the above algorithm is the notion of launching a particle from afar. How far is far? Clearly, we may launch a particle equiprobably from any point on the surface of smallest sphere of radius $R_{\rm circ}$ that circumscribes the aggregate. A more serious issue is what to do if the particle wanders far outside the circumscribing sphere. Since the average time for a diffusing particle to reach an absorbing sphere is infinite for $d = 2$ and, even worse, a particle has a finite probability of not hitting the sphere for $d > 2$, a naive simulation should get bogged down in following a particle that strays infinitely far from the aggregate. In early simulations, this pathology was avoided by terminating the random walk if it reached an arbitrarily determined outer radius and re-injecting the particle at $R_{\rm circ}$.

We can avoid this uncontrolled procedure by using the hitting probability of Eq. (6.1.3*a*) to move a particle that strays outside the circumscribing sphere back to the sphere surface *in a single step*. Additionally, we can speed up the motion of a particle that is inside the circumscribing circle by moving the particle equiprobably to the surface of the largest inscribed circle centered at the particle that does not touch the aggregate. Thus the particle makes large-distance hops when it is in the mouth of a wide "fjord" of the aggregate and much smaller hops once deep inside the fjords (Fig. 6.2). When these simple tricks are implemented, the best DLA simulations now appear to be memory limited, rather than CPU-time limited.

In fact, when the particle is close to the aggregate, it is even more efficient to use an off-center inscribed circle with the maximum possible radius such that the particle is included in this circle and the aggregate is not touched. We can use the image method to determine where on the surface the particle hits this inscribed circle. This ensures that the average step length of the particle step length is always as large as possible.

6.2 Reaction Rate Theory

We now turn to the relation between first passage to a sphere and the von Smoluchowski rate theory for the kinetics of diffusion-controlled reactions. In such processes, two molecules react immediately when they approach within a reaction radius and the overall process is limited by their encounter rate. A generic example is diffusion-controlled single-species annihilation, $A + A \to 0$. The evolution of the reactant density,

$\rho_A(\vec{r},t)$, may be described by the diffusion-reaction equation

$$\frac{\partial \rho_A(\vec{r},t)}{\partial t} = D\nabla^2 \rho_A(\vec{r},t) - k\rho_A(\vec{r},t)^2, \tag{6.2.1}$$

where the second term accounts for the annihilation in a homogeneous system. The reaction rate k quantifies the efficiency of an encounter between reactants. The goal of the Smoluchowski theory is to compute this rate.

This rate may be re-framed as the following idealized first-passage process. Fix one particle (a sphere of radius a) as the "target". In the rest frame of the target, the other reactants diffuse and are absorbed if they hit the target. The density is taken to be small, so that reactions among the background mobile particles can be ignored. We then identify the flux to the target as the reaction rate k. To compute this flux, we first determine the concentration around an absorbing target particle by solving the diffusion equation

$$\frac{\partial c(\vec{r},t)}{\partial t} = D\nabla^2 c(\vec{r},t), \tag{6.2.2}$$

subject to the initial condition $c(\vec{r},t=0) = 1$ for $r > a$ and the boundary conditions $c(r=a,t) = 0$ and $c(r\to\infty,t) = 1$. The reaction rate is then the integral of the flux over the sphere surface,

$$k(t) = -D\int_S \Big|\frac{\partial c(\vec{r},t)}{\partial r}\Big|_{r=a}\, d\Omega. \tag{6.2.3}$$

There are two regimes of behavior. For $d > 2$, a diffusing particle is transient and the relatively slow loss of reactants by trapping at the target is compensated for by their re-supply from infinity. Thus a steady-state is reached and the reaction rate k is finite. Conversely for $d \le 2$, diffusing particles are sure to hit the target and a depletion zone grows continuously about the trap. Correspondingly, the flux and thus the reaction rate both decay in time. Although a reaction rate does not strictly exist within the Smoluchowski theory for $d \le 2$, it is still meaningful to think of the theory as providing a time-dependent reaction rate.

6.2.1 Time-Dependent Solution for General d

We now solve Eq. (6.2.2) with the specified initial and boundary conditions. The Laplace transform is $sc - 1 = D\nabla^2 c$, where the factor -1 accounts for the constant initial condition $c(r,t=0) = 1$. A particular solution is simply $c = 1/s$, and to complete the solution we need to solve the homogeneous equation

$$c'' + \frac{d-1}{r}c' - \frac{s}{D}c = 0,$$

where the prime denotes differentiation with respect to r.

The elemental solutions to this equation are $r^\nu\, I_\nu(r\sqrt{s/D})$ and $r^\nu\, K_\nu(r\sqrt{s/D})$ with $\nu = 1 - d/2$, where I_ν and K_ν are the modified Bessel functions of order ν. Since the solution must be finite as $r\to\infty$, only the K_ν term contributes. The general solution to the diffusion equation therefore is

$$c(r,s) = \frac{1}{s} + Ar^\nu\, K_\nu(r\sqrt{s/D}).$$

Imposing the absorbing boundary condition at $r = a$ then gives

$$c(r,s) = \frac{1}{s}\left[1 - \Big(\frac{r}{a}\Big)^\nu \frac{K_\nu(r\sqrt{s/D})}{K_\nu(a\sqrt{s/D})}\right]. \tag{6.2.4}$$

To determine the flux, we separately treat the cases of: (i) $\nu < 0$ ($d > 2$) and (ii) $\nu \ge 0$ ($d \le 2$).

For $\nu < 0$, we define $\mu = -\nu = d/2 - 1 > 0$. In this regime, a steady-state concentration profile exists that we obtain by taking the $s\to 0$ limit of Eq. (6.2.4). This gives the electrostatic solution (that we could have written with no calculation)

$$c(r, s\to 0) = \frac{1}{s}\left[1 - \Big(\frac{a}{r}\Big)^{d-2}\right].$$

We now use $K_{-\nu} = K_\nu$ and the recursion formula $K_\nu(x)' = -K_{\nu-1}(x) - \nu K_\nu(x)/x$ in Eq. (6.2.4) to give the flux to any point on the absorbing sphere,

$$\phi \equiv -D\frac{\partial c}{\partial r}\Big|_{r=a} = \frac{2D\nu}{as} + \sqrt{\frac{D}{s}}\frac{K_{\mu-1}(a\sqrt{s/D})}{K_\mu(a\sqrt{s/D})}.$$

Since the leading behavior is proportional to $1/s$, the flux approaches a constant at long times. This is expected since the concentration itself approaches a steady state. There are now two interesting subcases that depend on whether $\mu - 1 \gtrless 0$. For $\mu - 1 > 0$, corresponding to $d > 4$, the small-argument asymptotics of K_μ gives

$$\phi = -\frac{2D\mu}{as} + \frac{a}{2}\frac{\Gamma(\mu-1)}{\Gamma(\mu)} + \ldots$$

Here the second term corresponds to a $1/t$ leading correction to the steady-state flux. We may obtain the total current, or reaction rate k, by integrating the flux over the surface of the sphere. This then gives

$$k = (d-2)\Omega_d\ Da^{d-2} + \frac{\text{const.}}{t} + \ldots, \qquad d > 4. \tag{6.2.5a}$$

On the other hand, for $\mu - 1 < 0$ (and $\mu > 0$), corresponding to $2 < d < 4$, we write $K_{\mu-1} = K_{1-\mu}$ to facilitate taking the $s \to 0$ limit. Then we find

$$\phi = -\frac{2D\mu}{as} + \sqrt{\frac{D}{s}}\frac{\Gamma(1-\mu)}{\Gamma(\mu)}\left(\frac{a\sqrt{s/D}}{2}\right)^{2\mu-1} + \ldots = -\frac{2D\mu}{as} + \text{const.} \times s^{(d-4)/2} + \ldots$$

Now the second term corresponds to a correction that varies asymptotically as $t^{1-d/2}$. Thus

$$k = (d-2)\Omega_d\ Da^{d-2} + \text{const.} \times t^{1-d/2} \qquad 2 < d < 4. \tag{6.2.5b}$$

In the special and physically most relevant case of $d = 3$ ($\mu = 1/2$) the ratio $K_{\mu-1}/K_\mu$ cancels, and this gives the exact result for the flux

$$\phi = \frac{D}{as} + \sqrt{\frac{D}{s}},$$

from which we immediately obtain the classical Smoluchowski formula for the reaction rate,

$$k = 4\pi aD\left(1 + \frac{a}{\sqrt{\pi Dt}}\right). \tag{6.2.5c}$$

Notice that this rate is proportional to the diffusion coefficient D times a^{d-2}. Their product then has units of (volume/time), as follows from Eq. (6.2.1). More importantly, the reaction rate is pathological for $d < 2$ because the rate *increases* as the size of the trap *decreases*. This peculiarity strongly hints that there is a fundamental difference between the kinetics of diffusion-controlled reactions in $d > 2$ and $d \leq 2$.

In the more pathological case of $\nu \geq 0$ (or $d \leq 2$), there is a fortuitous cancellation of two terms in evaluating the derivative of Eq. (6.2.4) and the flux is now given by

$$\phi = -\frac{D}{s}\frac{K_{1-\nu}(a\sqrt{s/D})}{K_\nu(a\sqrt{s/D})}, \qquad d < 2.$$

In the $s \to 0$ limit, this expression reduces to

$$\phi \to \left(\frac{2}{a}\right)^{d-1}\left(\frac{D}{s}\right)^{d/2}.$$

Thus the time dependence of the total current is

$$k \propto \frac{(Dt)^{d/2}}{t} \propto \frac{1}{t^{1-d/2}}, \tag{6.2.6}$$

where the first expression emphasizes the correct units of k.

For $\nu = 0$, or $d = 2$, the flux is

$$\phi = -\frac{D}{s}\frac{K_1(a\sqrt{s/D})}{K_0(a\sqrt{s/D})} \sim \frac{4}{a}\frac{1}{s\ln s}, \qquad s \to 0.$$

As $t \to \infty$, this corresponds to the total current having the time dependence

$$k \sim \frac{4\pi D}{\ln t} \qquad d = 2. \tag{6.2.7}$$

Notice that the reaction rates for $d \leq 2$ are independent of the radius of the target sphere! This is yet another manifestation of the recurrence of diffusion for $d \leq 2$ – even an infinitely small trap is sure to capture all particles, so that the flux, and hence the reaction rate, eventually vanishes. This is the mechanism that ultimately leads to the slow kinetics of diffusion-controlled reactions for spatial dimension $d \leq 2$.

6.2.2 Elementary Time-Dependent Solution for $d = 3$

An intriguing aspect of the Smoluchowski theory is that in the physical case of three dimensions the rate can be expressed in terms of elementary functions. This simplification hinges on the fact that the radial part of the Laplacian operator in three dimensions only is related to the one-dimensional Laplacian by

$$\nabla^2_{3d}\left(\frac{u}{r}\right) = \frac{1}{r}\nabla^2_{1d}u. \tag{6.2.8}$$

With this trick, we express the solution of a spherically symmetric three-dimensional system in terms of a corresponding one-dimensional system. Thus the solution to the diffusion equation in three dimensions, $\frac{\partial c}{\partial t} = D\nabla^2_{3d}c$, can be written in terms of the solution to the one-dimensional diffusion equation for the function $u(r,t) = rc(r,t)$, namely, $\frac{\partial u}{\partial t} = D\nabla^2_{1d}u$.

We now determine the reaction rate by this equivalence. As a preliminary, we solve the one-dimensional problem

$$\frac{\partial c}{\partial t} = D\frac{\partial^2 c}{\partial x^2},$$

subject to $c(x, t = 0) = 1$, $c(0,t) = 0$, and $c(x \to \infty, t) = 1$. The Laplace transform of this equation is $sc(x,s) - 1 = c''(x,s)$. The particular solution is $1/s$, and the homogeneous solution is $A\,e^{-x\sqrt{s/D}}$. The positive exponential does not appear because of the boundary condition at $x = \infty$. The boundary condition at $x = 0$ then gives

$$c(x,s) = \frac{1}{s}\left(1 - e^{-x\sqrt{s/D}}\right), \tag{6.2.9}$$

from which

$$c(x,t) = \mathrm{erf}\left(\frac{x}{\sqrt{4Dt}}\right). \tag{6.2.10}$$

Finally the current to the origin is

$$k = -D\frac{\partial c}{\partial x}\Big|_{x=0} = \sqrt{\frac{D}{\pi t}} \qquad d = 1. \tag{6.2.11}$$

To infer the three-dimensional solution, we now define $u = rc$. In terms of u, the initial condition is now $u = r$ (corresponding to a constant initial concentration in three dimension) and the absorbing boundary condition must be imposed at $r = a$, rather than at $r = 0$, to correspond to a sphere with a finite radius in three dimensions. With these features, the solution for u in one dimension is

$$u(r,s) = \frac{1}{s}\left(r - ae^{-(r-a)\sqrt{s/D}}\right),$$

from which the concentration in three dimensions equals

$$c(r,t) = \left[(1 - \frac{a}{r}) + \frac{a}{r}\mathrm{erf}\left(\frac{(r-a)}{\sqrt{4Dt}}\right)\right]. \tag{6.2.12}$$

The radial derivative at $r = a$ is simply

$$-\frac{\partial c}{\partial r}\Big|_{r=a} = \frac{1}{a} + \frac{1}{\sqrt{\pi D t}},$$

and the current $k = -4\pi a^2 D \frac{\partial c}{\partial r}$ reproduces Eq. (6.2.5c).

Chapter 7

WEDGE DOMAINS

7.1 Two-Dimensional Wedge

We solve the diffusion equation in the wedge to determine the survival probability of a diffusing particle. While the exact Green's function for this system is well known, we adopt the strategy of choosing an initial condition that allows us to eliminate angular variables and deal with an effective radial problem. This is suitable if we are interested only in asymptotic first-passage properties.

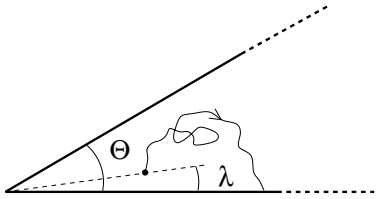

Figure 7.1: A two-dimensional wedge of opening angle Θ with absorbing boundaries. For a diffusing particle initially at angle λ, the horizontal boundary is eventually hit with probability λ/Θ and the other boundary is hit with probability $1-\lambda/\Theta$.

It is natural to write the diffusion equation for the two-dimensional wedge geometry in polar co-ordinates,

$$\frac{\partial c}{\partial t} = D\left(\frac{\partial^2 c}{\partial r^2} + \frac{1}{r}\frac{\partial c}{\partial r} + \frac{1}{r^2}\frac{\partial^2 c}{\partial \theta^2}\right), \tag{7.1.1}$$

where $c = c(r,\theta,t)$ is the particle concentration at (r,θ) at time t, D is the diffusion coefficient, and the boundary conditions are $c = 0$ at $\theta = 0, \Theta$. We reduce this system to an effective one-dimensional radial problem by noting that the exact Green's function may be written as an eigenfunction expansion in which the angular dependence is a sum of sine waves, with an integer number of half-wavelengths within $(0,\Theta)$ to satisfy the absorbing boundary conditions. These sine waves are $\sin(n\pi\theta/\Theta)$, with n an integer, and they represent the Fourier series expansion of the Green's function.

In this series, each sine wave is multiplied by a conjugate decaying function of time, in which the decay rate increases with n. In the long time limit, only the lowest term in this expansion dominates the survival probability. Consequently, we may obtain the long-time behavior by choosing an initial condition whose angular dependence is a half sine-wave in the wedge. Then the time-dependence will contain only this single term in the Fourier series.

We thus define $c(r,\theta,t=0) = \frac{\pi}{2\Theta r_0}\delta(r-r_0)\sin(\pi\theta/\Theta)$. With this initial distribution and after the Laplace transform is applied, the diffusion equation becomes

$$sc(r,\theta,s) - \frac{\pi}{2\Theta r_0}\delta(r-r_0)\sin(\pi\theta/\Theta) = D\left(\frac{\partial^2 c}{\partial r^2} + \frac{1}{r}\frac{\partial c}{\partial r} + \frac{1}{r^2}\frac{\partial^2 c}{\partial \theta^2}\right),$$

where $c = c(r,\theta,s)$. We substitute the ansatz $c(r,\theta,s) = R(r,s)\sin(\pi\theta/\Theta)$ to separate the angular dependence and thus reduces the system to an effective one-dimensional radial problem. Then introducing the dimensionless co-ordinate $x = r\sqrt{s/D}$, we find the modified Bessel equation for the remaining radial co-ordinate,

$$R''(x,s) + \frac{1}{x}R'(x,s) - \left(1 + \frac{\nu^2}{x^2}\right) R(x,s) = -\frac{\nu}{2Dx_0}\delta(x - x_0), \tag{7.1.2}$$

where $\nu = \pi/\Theta$ and the prime now denotes differentiation with respect to x.

The general solution for $x \neq x_0$ is a superposition of modified Bessel functions of order ν. Since the domain is unbounded, the interior Green's function ($x < x_0$) involves only I_ν, since K_ν diverges as $x \to 0$, while the exterior Green's function ($x > x_0$) involves only K_ν, since I_ν diverges as $x \to \infty$. By imposing continuity at $x = x_0$, we find that the Green's function has the symmetric form $R(x,s) = AI_\nu(x_<)K_\nu(x_>)$, with the constant A determined by the joining condition that arises by integrating Eq. (7.1.2) over an infinitesimal radial range that includes r_0. This gives

$$R'_> \,|_{x=x_0} - R'_< \,|_{x=x_0} = -\frac{\nu}{2Dx_0},$$

from which $A = \nu/2D$. Therefore the radial Green's function in the wedge is

$$R(x,s) = \frac{\nu}{2D}\, I_\nu(x_<)\, K_\nu(x_>), \tag{7.1.3}$$

and its Laplace inverse has the closed form

$$R(r,t) = \frac{\nu}{4Dt}\, e^{-(r^2+r_0^2)/4Dt}\, I_\nu\left(\frac{rr_0}{2Dt}\right). \tag{7.1.4}$$

With this radial Green's function, the asymptotic survival probability is

$$S(t) \sim \int_0^\Theta \sin(\nu\theta)\, d\theta \int_0^\infty r\, R(r,t)\, dr. \tag{7.1.5}$$

We may easily estimate the long-time behavior of this integral by first integrating over θ and then using the asymptotic approximations $e^{-r_0^2/4Dt} \to 1$ and $I_\nu(x) \sim \left(\frac{x}{2}\right)^\nu/\Gamma(\nu+1)$, to give

$$S(t) \sim \frac{2}{\nu\Gamma(\nu+1)} \int_0^\infty \frac{r}{2Dt}\left(\frac{rr_0}{8Dt}\right)^\nu e^{-r^2/4Dt}\, dr = \frac{2}{\nu}\left(\frac{r_0}{\sqrt{16Dt}}\right)^\nu \propto \left(\frac{r_0}{\sqrt{Dt}}\right)^{\pi/\Theta}. \tag{7.1.6}$$

Alternatively, we may estimate this integral by noting that the radial distance over which the concentration is appreciable extends to the order of $\sqrt{Dt}$. This provides the cutoff $r \approx \sqrt{Dt}$ in the radial integral in Eq. (7.1.5), within which the Gaussian factors in $R(r,t)$ can be replaced by one. Using the small-argument expansion of the Bessel function, we then obtain

$$S(t) = \int_0^\Theta \sin(\nu\theta)\, d\theta \int_0^\infty r\, R(r,t)\, dr \propto \int_0^{\sqrt{Dt}} \frac{1}{Dt}\left(\frac{rr_0}{Dt}\right)^\nu r\, dr \propto \left(\frac{r_0}{\sqrt{Dt}}\right)^{\pi/\Theta}. \tag{7.1.7}$$

We conclude that the survival probability of a diffusing particle in a wedge of opening angle Θ decays as

$$S(t) \sim t^{-\pi/2\Theta}. \tag{7.1.8}$$

7.2 Three-Dimensional Cone

For the corresponding three-dimensional problem of diffusion within an absorbing cone, the diffusion equation can again be separated into a Bessel equation for the radial co-ordinate and a non-integer Legendre equation for the angular co-ordinate. The solution to the diffusion equation can then be written as an eigenfunction expansion, in which the angular factors are the non-integral Legendre functions, $P_\nu(\cos\theta)$. Here θ is the

polar angle, with $0 < \theta < \Theta/2$, and the discrete set of indices ν are determined by the boundary conditions. For the asymptotic survival probability, we again retain only the first term in this eigenfunction expansion, corresponding to one half-wavelength of the Legendre function inside the cone. This is in the same spirit as the wedge solution. This leading term has the form

$$P(r,\theta,t) \propto \frac{1}{4\pi Dt\sqrt{rr_0}}\, e^{-(r^2+r_0^2)/4Dt}\,(2\nu+1) I_{\nu+\frac{1}{2}}\left(\frac{rr_0}{2Dt}\right)\, P_\nu(\cos\theta). \tag{7.2.1}$$

We now estimate the survival probability by using the same heuristic approach as that used in two dimensions. Namely, we cut off the radial integral at $\sqrt{Dt}$, set the Gaussian factors to one for $r < \sqrt{Dt}$, and finally use the small-argument expansion of the Bessel function. This gives

$$\begin{aligned} S(t) &= \int d\Omega \int_0^\infty \frac{e^{-(r^2+r_0^2)/4Dt}}{4\pi Dt\sqrt{rr_0}}(2\nu+1) I_{\nu+\frac{1}{2}}\left(\frac{rr_0}{2Dt}\right)\, P_\nu(\cos\theta)\, r^2\, dr \\ &\approx \int_0^{\sqrt{Dt}} \frac{1}{4\pi Dt\sqrt{rr_0}} \left(\frac{rr_0}{2Dt}\right)^{\nu+\frac{1}{2}}\, r^2\, dr \propto \left(\frac{r_0}{\sqrt{Dt}}\right)^{\nu_0}, \end{aligned} \tag{7.2.2}$$

where the integral $\int d\Omega$ is over the solid angle of the cone.

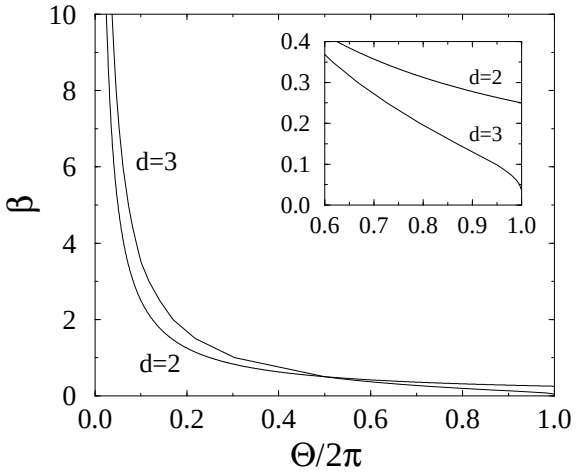

Figure 7.2: Comparison of the survival probability exponent β for a diffusing particle in an absorbing wedge (two dimensions) and in an absorbing cone (three dimensions). The exponents have similar dependences on wedge angle, except as $\Theta \to 2\pi$, where $\beta_{3d} \to 0$ while β_{2d} remains finite. The inset shows details for $0.6 \le \Theta/2\pi \le 1.0$.

To obtain numerical results, we require the lowest index of the non-integral Legendre function that vanishes at the cone boundaries (Fig. 7.2). The limiting forms of this index are

$$\nu \approx \begin{cases} \dfrac{4.91}{\Theta} - \dfrac{1}{2}, & \Theta \to 0; \\[2ex] \dfrac{1}{2\ln\frac{4}{2\pi-\Theta}}, & \Theta \to 2\pi. \end{cases}$$

For small opening angle, the survival probability exponents for both the two-dimensional wedge and the three-dimensional cone both vanish as the inverse of the opening angle (Fig. 7.2). However, as $\Theta \to 2\pi$ (absorbing needle), the exponent of $S(t)$ in two dimensions remains finite, while the exponent in three dimensions goes to zero. This means that $S(t)$ decays slower than a power law in the presence of an absorbing needle in three dimensions – an intriguing manifestation of the difference between recurrence and transience of diffusion in two and three dimensions.

7.3 Conformal Transformations and Electrostatic Methods

The connection between first-passage properties and electrostatics takes on added significance in two dimensions, where conformal transformation methods can be used. We will exploit conformal transformations to obtain time-integrated first-passage properties for diffusion within the wedge. This formulation also provides interesting results about *where* on the boundary a diffusing particle gets absorbed. For example, a diffusing particle is likely to be absorbed very close to the tip of an absorbing needle precisely because the electric field is relatively strong near the tip. Conversely, it is very improbable that a diffusing particle will penetrate and get absorbed deep within a narrow crack. As a final introductory note, conformal transformation methods can provide the first-passage characteristics in *any* geometry that is amenable to conformal analysis. Our treatment of the wedge geometry represents a small subset of what can be accomplished by such methods.

7.3.1 Point Source and Line Sink

To set the stage for the wedge geometry, consider the first-passage probability to an absorbing infinite line in two dimensions. We already obtained this result in Section 3.1 by applying the image method. For a particle that starts at (x_0, y_0) and an absorbing line $y = 0$, the probability that a diffusing particle is ultimately trapped at x is given by the Cauchy distribution,

$$\mathcal{E}(x; x_0, y_0) = \frac{1}{\pi}\frac{y_0}{(x-x_0)^2 + y_0^2}. \tag{7.3.1}$$

As mentioned in Section 3.1, the x^{-2} large-x decay of this distribution (Fig. 7.3) implies that the mean position of the probability density trapped along the absorbing line, $\langle x\rangle = \int_0^\infty x\mathcal{E}(x; x_0, y_0)\, dx$, is infinite. In fact, all moments $\langle x^n\rangle$ with $n \geq 1$ are infinite, while moments with $n < 1$ are finite.

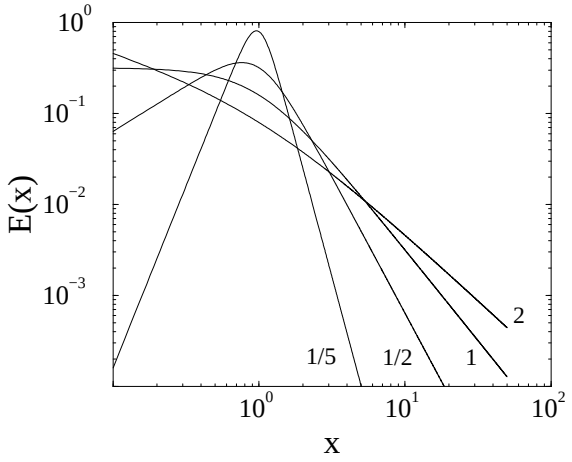

Figure 7.3: Probability for a diffusing particle to eventually hit a point a distance x from the wedge apex for different wedge angles Θ. Shown are the cases $\Theta/\pi = 1/5$, $1/2$, 1 (absorbing line), and 2 (absorbing needle or half-line). The initial particle position is a unit distance from the wedge apex along its bisector. For large x, $\mathcal{E}(x)$ decays as $x^{-1-\pi/\Theta}$, while for small x, $\mathcal{E}(x)$ varies as $x^{\pi/\Theta-1}$.

This problem may also be solved more elegantly by the electrostatic formulation of Section 1.3. In this approach, the time-integrated concentration $\mathcal{C}(x, y) = \int_0^\infty c(x, y, t)\, dt$ obeys the Laplace equation

$$\nabla^2\mathcal{C}(z) = -\frac{1}{2\pi D}\delta(z - z_0),$$

where $z = (x, y)$ is the complex co-ordinate and the factor $1/(2\pi D)$ ensures the correct normalization. Using

the image method for two-dimensional electrostatics, the complex potential is

$$\mathcal{C}(z) = \frac{1}{2\pi D}\ln\frac{z-z_0}{z-z_0^*} = \frac{1}{2\pi D}\ln\frac{x-x_0+i(y-y_0)}{x-x_0+i(y+y_0)}, \tag{7.3.2}$$

where the asterisk denotes complex conjugation. Finally, the total flux absorbed at x coincides with the electric field at this point. This is

$$\begin{aligned}\mathcal{E}(x;x_0,y_0) = -D\,\frac{\partial\mathcal{C}(x,y)}{\partial y}\bigg|_{y=0} &= \frac{1}{2\pi}\left(\frac{1}{y_0+i(x-x_0)}+\frac{1}{y_0-i(x-x_0)}\right)\\ &= \frac{1}{\pi}\frac{y_0}{(x-x_0)^2+y_0^2},\end{aligned} \tag{7.3.3}$$

which reproduces Eq. (7.3.1). This same approach may be extended in an obvious way to the semi-infinite slab geometry to reproduce Eq. (3.1.19).

There are several useful implications of this result. For example, the probability that a particle that starts at (x_0, y_0) eventually hits a point on the positive x-axis is just the integral of the local hitting probability over this domain. This is

$$\begin{aligned}\mathcal{E}_+(x_0,y_0) = \int_0^\infty \mathcal{E}(x;x_0,y_0)\,dx &= \frac{y_0}{\pi}\int_0^\infty \frac{dx}{(x-x_0)^2+y_0^2}\\ &\equiv 1-\frac{1}{\pi}\tan^{-1}(y_0/x_0).\end{aligned} \tag{7.3.4}$$

More generally, Eq. (7.3.4) gives the probability for a particle that starts at (x_0, y_0) to hit an arbitrary interval that subtends the angle $\theta_2-\theta_1$ (Fig. 7.4). From Eq. (7.3.4), the probability to hit the interval $[x_1,\infty]$ is $1-(\theta_1/\pi)$, while the probability to hit the interval $[x_2,\infty]$ is $1-(\theta_2/\pi)$. Consequently, the probability of hitting the finite interval $[x_1, x_2]$ is

$$\mathcal{E}_{\rm interval} = \frac{\theta_2-\theta_1}{\pi}. \tag{7.3.5}$$

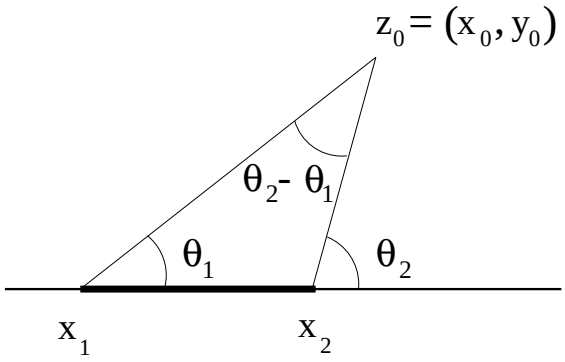

Figure 7.4: Geometry for the probability of a hitting segment that subtends the angle $\theta_2-\theta_1$. In making a correspondence to Eq. (7.3.4), the point x_1 is considered the origin, while for Eq. (7.3.5), x_1 and x_2 are arbitrary.

7.3.2 General Wedge Angles

We now use a conformal transformation to extend our hitting probability results for the half plane to the corresponding hitting probabilities in the wedge. Consider the transformation $w = f(z) = z^{\pi/\Theta}$ that maps

the interior of the wedge of opening angle Θ to the upper half plane. In complex co-ordinates, the electrostatic potential in the wedge is

$$\mathcal{C}(z) = \frac{1}{2\pi} \ln \frac{z^{\pi/\Theta} - z_0^{\pi/\Theta}}{z^{\pi/\Theta} - (z_0^*)^{\pi/\Theta}}. \tag{7.3.6}$$

From this expression, we can extract time-integrated first-passage properties in the wedge. For example, the probability of being absorbed at a distance x from the wedge apex, when a particle begins at a unit distance from the apex along the wedge bisector, is just the electric field at this absorbing point

$$\mathcal{E}(x; x_0, y_0) = \frac{1}{\Theta} \frac{x^{\pi/\Theta - 1}}{1 + x^{2\pi/\Theta}}. \tag{7.3.7}$$

For large x, this hitting probability varies as $x^{-(1+\pi/\Theta)}$, as shown in Fig. 7.3. Thus for $\Theta < \pi$, the probability of being ultimately being trapped a distance x from the wedge apex decays more rapidly than x^2 and the mean distance from the wedge apex for the distribution of trapped particles is finite. Another interpretation of the case $\Theta < \pi$ is that if a diffusing particle starts somewhere in an absorbing crack the particle is very unlikely to penetrate any deeper. This is simply a consequence that the electric field is very small deep inside a narrow crack when the boundary is a grounded conductor. Conversely for $\Theta > \pi$, the hitting probability diverges as $x^{\pi/\Theta - 1}$ as $x \to 0$. This means that a diffusing particle is most likely to hit near the tip of a thin needle. This is the source of the generic tip instability of diffusion-controlled growth processes in two dimensions. Another feature of a wedge with opening angle $\Theta > \pi$ is that the hitting probability at large distances x from the tip decays more slowly than x^2. Consequently the mean distance from the wedge apex for the distribution of trapped particles is infinite.

Another simple but useful application of conformal mapping is to the splitting probability. In the wedge geometry, we are interested in the probability that a particle ultimately gets trapped on the horizontal generator or on the inclined generator of the wedge as a function of its starting position. From the conformal transformation $w = z^{\pi/\Theta}$, the probability $\mathcal{E}_+^{\rm wedge}$ that a diffusing particle that starts at $z_0 = Ae^{i\lambda}$ in the wedge, hits the positive x axis is the same as the probability that a particle that starts at $w_0 = A^{\pi/\Theta} e^{i\lambda\pi/\Theta}$ in the upper half-plane, hits the positive x axis. This equivalence immediately gives

$$\mathcal{E}_+^{\rm wedge} = 1 - \lambda/\Theta. \tag{7.3.8}$$

7.4 First-Passage Times

We now investigate the time until a diffusing particle hits the boundary of an absorbing wedge or cone. For the infinite wedge, this exit time may be finite or infinite, depending on the wedge opening angle. We can understand this transition in a revealing way by studying the exit time in a pie wedge, in which r is restricted to $(0, R)$ with an absorbing boundary condition at $r = R$. While the exit time in this system is always finite, for wedge angles $\Theta < \pi/2$ the exit time remains finite as $R \to \infty$, while for $\Theta \geq \pi/2$, the exit time diverges as $R \to \infty$. This is a harbinger of the transition in the exit time for the infinite wedge.

It is worth noting that the equation for the exit time in the pie wedge is identical in form to the equation for the velocity field of viscous fluid flow in an infinite pipe with the same pie wedge cross-section. The transition in the behavior of the exit time translates to a corresponding pathology for the flow problem. Namely, for $\Theta < \pi/2$ the flow velocity $r = 0$ remains finite as $R \to \infty$, while for $\Theta > \pi/2$, the velocity near $r = 0$ diverges as the distant boundary $R \to \infty$!

7.4.1 Infinite Two-Dimensional Wedge

Let us begin by determining the mean time for a diffusing particle to hit the sides of an infinite two-dimensional wedge of opening angle Θ. It is convenient to orient the wedge bisector along the $\theta = 0$ axis, with the two wedge generators at $\theta = \pm\Theta/2$. For a particle that starts at $\vec{r}$, the (unrestricted) mean exit time $t(\vec{r})$ to hit anywhere on the boundary obeys the Poisson equation $D\nabla^2 t(\vec{r}) = -1$, subject to the boundary conditions $t = 0$ for $\theta = \pm\Theta/2$, corresponding to an exit time of zero for a particle that starts at the

boundary. In polar co-ordinates, this equation is

$$D\left(\frac{\partial^2 t}{\partial r^2}+\frac{1}{r}\frac{\partial t}{\partial r}+\frac{1}{r^2}\frac{\partial^2 t}{\partial \theta^2}\right)=-1. \tag{7.4.1}$$

By dimensional analysis, $t(r,\theta)$ must have the units of r^2/D. This suggests that the exit time can be written in the scaling form,

$$t(r,\theta)=\frac{r^2}{D}f(\theta), \tag{7.4.2}$$

with f a function of θ only. To determine $f(\theta)$ we substitute this ansatz into Eq. (7.4.1) and find that f satisfies $4f+f''=-1$. where prime means differentiation with respect to θ. The general solution to this equation is $f(\theta)=A\cos(2\theta)+B\sin(2\theta)-\frac{1}{4}$ and imposing the boundary conditions $t(\pm\Theta/2)=0$ gives

$$t(r,\theta)=\frac{r^2}{4D}\left(\frac{\cos(2\theta)}{\cos\Theta}-1\right). \tag{7.4.3}$$

As expected, the exit time scales as r^2/D. For fixed r, this time is obviously maximal for a particle starting along the wedge bisector and smoothly goes to zero as the initial location approaches the wedge.

More intriguingly, $t(r,\theta)$ diverges as $\Theta\to\pi/2$! This feature also follows from that fact that the survival probability $S(t)$ decays as $t^{-\pi/2\Theta}$ (Eq. (7.1.7)). As a result, the mean exit time, $t=\int_0^\infty S(t')\,dt'$, is divergent for $\Theta\geq\pi/2$. To understand the meaning of this divergence, we consider the exit time in a pie wedge with finite outer radius R and then take the limit $R\to\infty$.

7.4.2 Pie Wedge in Two Dimensions

For a pie wedge with opening angle $\Theta<\pi/2$ and outer radius R, the dependence of the exit time on R must yield a finite limit when $R\to\infty$. On the other hand, for $\Theta\geq\pi/2$, the exit time must diverge as $R\to\infty$. The formal way to understand this phenomenon is to solve the Poisson equation in the pie wedge. That is, we solve $D\nabla^2 t(r,\theta)=-1$ subject to $t=0$ on the boundaries. The general solution to this equation is

$$t(r,\theta)=\frac{r^2}{4D}\left(\frac{\cos 2\theta}{\cos\Theta}-1\right)+\sum_{n=0}^{\infty}A_n r^{\lambda_n}\cos(\lambda_n\theta), \tag{7.4.4}$$

where the series represents the general solution to the homogeneous problem. Here $\lambda_n\Theta/2=(2n+1)\pi/2$ for $n=0,1,2,\ldots$, to satisfy the boundary condition on the sides of the wedge. The boundary condition $t=0$ for $r=R$ then leads to

$$A_n=\frac{(-1)^{n+1}4R^{2-\lambda_n}}{D\Theta\lambda_n(\lambda_n^2-4)}.$$

The leading behavior of the solution in Eq. (7.4.4) is ultimately determined by the lowest angular eigenvalue λ_0. If $\lambda_0>2$ then the particular solution dominates and we recover the infinite wedge result, Eq. (7.4.3). This range of λ corresponds to a wedge angle $\Theta<\pi/2$. However, for $\lambda_0\leq 2$, corresponding to wedge angle $\Theta\geq\pi/2$, then the eigenfunction expansion dominates the solution for large R. In this case, the leading behavior of the solution for small r is

$$t(r,\theta)\sim r^{\pi/\Theta}R^{2-\pi/\Theta}. \tag{7.4.5}$$

In the context of the exit time problem, this means that a particle starting near the wedge apex takes an infinite time to exit the wedge as $R\to\infty$. In the corresponding viscous fluid-flow problem in an infinite pipe with a pie-wedge cross section of opening angle Θ, this translates to a pathology in the flow field near the wedge apex. For opening angle $\Theta<\pi/2$, the velocity near the apex converges as $R\to\infty$, while for $\Theta\geq\pi/2$, the velocity near the apex diverges as $R\to\infty$!

These anomalous properties for the pie wedge with $\Theta\geq\pi/2$ can also be obtained by a simple physical argument that relies on the power-law decay of the survival probability. In an infinite wedge with $\Theta<\pi/2$, the survival probability decays faster than t^{-1}, so that the mean exit time $t=\int_0^\infty S(t')\,dt'$ converges. In this case, the role of the circumferential boundary is irrelevant. On the other hand, for $\Theta>\pi/2$, $S(t)$ decays more slowly than t^{-1} and the integral for an infinite system is formally divergent. To compute the exit time

in a finite pie wedge, however, we should include a finite-size exponential cutoff in $S(t)$ for $t > R^2/D$. Thus the exit time should scale as

$$t(r,\theta;\Theta > \pi/2) = \int_0^\infty S(t')\,dt' \sim \int^{R^2/D} (t')^{-\pi/2\Theta}\,dt' \propto R^{2-\pi/\Theta}. \tag{7.4.6}$$

Here, we replace the exponential cutoff in $S(t)$ by a sharp cutoff at $t = R^2/D$; this construction still gives the correct asymptotic behavior. By dimensional analysis, t must be a quadratic function of length. Since the only other length in the problem is the starting location r, we infer that $t \propto r^{\pi/\Theta}R^{2-\pi/\Theta}$, in agreement with Eq. (7.4.5).

With this crude approach, we can also determine the behavior of the exit time in the borderline case $\Theta = \pi/2$. Here the integral in Eq. (7.4.6) diverges logarithmically and it is necessary to include both a short-time and a long-time cutoff to get a dimensionally correct result. Clearly, the lower cutoff should be of the order of r^2/D, where r is the starting radial coordinate of the particle. Thus

$$t(r,\theta;\Theta = \pi/2) = \int_0^\infty S(t')\,dt' \sim \int_{r^2/D}^{R^2/D} (t')^{-1}\,dt' \propto \ln(R/r). \tag{7.4.7}$$

Then by dimensional analysis, the mean exit time varies as $t \propto r^2\ln(R/r)$ for the case $\Theta = \pi/2$.

7.5 Extension to Time-Dependent First-Passage Properties

Although the electrostatic formulation ostensibly gives only time-integrated first-passage properties, we now adapt it to also give time-dependent features. By our approach, we can obtain the asymptotic time dependence of the diffusion equation merely by solving the time-independent Laplace equation and applying basic physical intuition about the relation between Laplacian and diffusive solutions. The wedge geometry provides a nice illustration of this approach.

This adaptation of the time-integrated approach is based on the following re-interpretation of the equivalence between electrostatics and diffusion. We previously learned that an electrostatic system with a point charge and specified boundary conditions is identical to a diffusive system in the same geometry and boundary conditions, in which a continuous source of particles is fed in at the location of the charge. Suppose now that the particle source is "turned on" at $t = 0$. Then, in a near zone that extends to a distance of the order of $\sqrt{Dt}$ from the source, the concentration has sufficient time to reach its steady-state value. In this zone, the diffusive solution converges to the Laplacian solution. Outside this zone, however, the concentration is very close to zero. More relevant to our discussion is that this almost-Laplacian solution provides the time integral of the survival probability up to time t. We then deduce the survival probability by differentiating the concentration due to this finite-duration source.

As a concrete example, suppose that a constant source of diffusing particles at the point z_0 within the wedge is turned on at $t = 0$. Then within the region $|z_0| < |z| < \sqrt{Dt}$, the density profile is approximately equal to the Laplacian solution, $\mathcal{C}(z) \sim |z|^{-\pi/\Theta}$. We can neglect the angular dependence of $\mathcal{C}(z)$ in this zone, as it is immaterial for the survival probability. Conversely, for $|z| > \sqrt{Dt}$, the particle concentration is vanishingly small. From the general discussion in Section 1.3, the near-zone density profile is just the same as the time integral of the diffusive concentration. Thus, using the equivalence between the spatial integral of this near-zone concentration in the wedge and the time integral of the survival probability, we have

$$\int_0^t S(t')\,dt' \approx \int_0^{\sqrt{Dt}} r^{-\pi/\Theta}\,r\,dr \sim t^{1-\pi/2\Theta}. \tag{7.5.1}$$

Since the total particle density injected into the system is t, the survival probability in the wedge is roughly $\int_0^t S(t')\,dt'/t \sim t^{1-\pi/2\Theta}/t$. This gives $S(t) \sim t^{-\pi/2\Theta}$, thus reproducing the known result.

Chapter 8

APPLICATION TO SIMPLE REACTIONS

8.1 Reunions and Reactions of Three Diffusing Particles

We now study reunions and reactions of three particles in one dimension. This system is surprisingly rich, but can be understood simply and completely in terms of the first-passage of a diffusing particle in a wedge, as discussed in the previous chapter. The three-particle system also provides an important building block toward understanding diffusion-controlled reactions in one dimension. For other situations it is useful to view one particle as a "prey" that is killed whenever it meets either of the other two mutually independent "predators". In the context of tracking the relative particle positions it is useful to view all three particles as independent. We will investigate the following basic questions:

- What is the survival probability of the prey as a function of time and the initial condition?
- What is the *first-meeting* probability? More precisely, label the particles as 1, 2, and 3, with initial positions $x_1 < x_2 < x_3$. Either 1 and 2, or 2 and 3 meet first (see Fig. 8.1). What is the probability for these events to occur as a function of the initial particle positions?
- What is the *lead probability* – the probability that the rightmost particle remains in the lead? A related question is: what the probability that each particle is *never* in the lead? More stringently, we may ask: what is the probability that the particles maintain their order, that is, none of the particles ever meet?

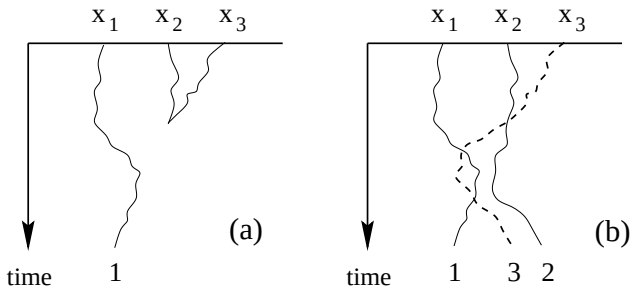

Figure 8.1: Space-time trajectories of three diffusing particles in one dimension. (a) A configuration that contributes to the probability that 2 and 3 meet first. (b) A configuration that contributes to the probability that particle 1 never leads. The trajectory of 3 is dashed for visual contrast.

We answer these questions by mapping the three-particle system in one dimension to a "compound" diffusing particle in an appropriately-defined two-dimensional wedge. We start by viewing the coordinate

x_i of each particle on the line as a Cartesian component of a three-dimensional diffusion process. Since the overall length scale is irrelevant, we can then project onto a two-dimensional subspace of relative co-ordinates. The order constraints outlined above correspond to this diffusion process being confined to a suitably-defined absorbing wedge of the plane, with the process terminating when the sides of the wedge are hit. Since we know the dependence of the survival probability in the wedge as a function of the wedge angle (Chap. 7), we thus infer 1survival probabilities in the three-particle system. This simple approach can still be applied when the diffusion coefficient D_i of each particle is distinct. In this case, we merely redefine the co-ordinate of the i^{th} particle as $y_i = x_i/\sqrt{D_i}$. In the y_i co-ordinates the diffusion process is once again isotropic, so that mapping to the wedge geometry can be used to solve the particle kinetics.

8.1.1 Prey Survival Probability

We first determine the survival probability of a prey as a function of its initial position. There are two independent cases: (i) "surrounded" prey, or (ii) a "chased" prey – prey on one side of both predators.

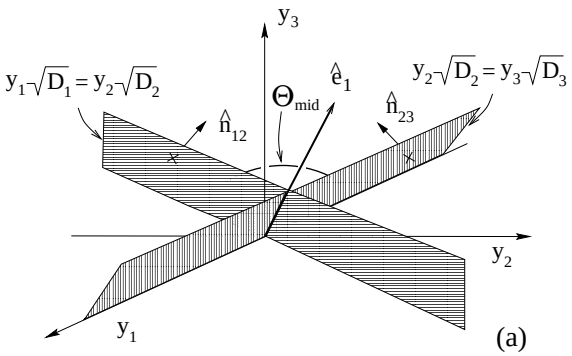

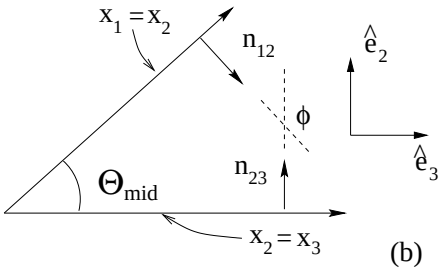

A surrounded prey survives if the co-ordinates satisfy the inequalities $x_1 < x_2$ – particles 1 and 2 do not meet, *and* $x_2 < x_3$ – particles 2 and 3 do not meet. In the isotropic y_i system these constraints for the compound particle are $y_1\sqrt{D_1} < y_2\sqrt{D_2}$ and $y_2\sqrt{D_2} < y_3\sqrt{D_3}$ (Fig. 8.2(a)). If the compound particle hits one of the planes, then it is absorbed. In the original one-dimensional system, this corresponds to particle 2 hitting either particle 1 (if $y_2\sqrt{D_2} = y_1\sqrt{D_1}$) or particle 3 (if $y_2\sqrt{D_2} = y_3\sqrt{D_3}$).

The survival probability of the surrounded prey is determined by the opening angle of the accessible wedge for the compound particle, Θ_{mid}. To compute Θ_{mid}, we use the fact that the unit normals to the planes $y_1\sqrt{D_1} = y_2\sqrt{D_2}$ and $y_2\sqrt{D_2} = y_3\sqrt{D_3}$ are, respectively,

$$\hat{n}_{12} = (-\sqrt{D_1}, \sqrt{D_2}, 0)/\sqrt{D_1 + D_2}, \quad \hat{n}_{23} = (0, -\sqrt{D_2}, \sqrt{D_3})/\sqrt{D_2 + D_3}.$$

The angle ϕ between these two normals is related to the wedge angle by $\Theta_{\text{mid}} = \pi - \phi$ (Fig. 8.2(b)). Thus

$$\Theta_{\text{mid}} = \cos^{-1}(D_2/\sqrt{(D_1 + D_2)(D_2 + D_3)}).$$

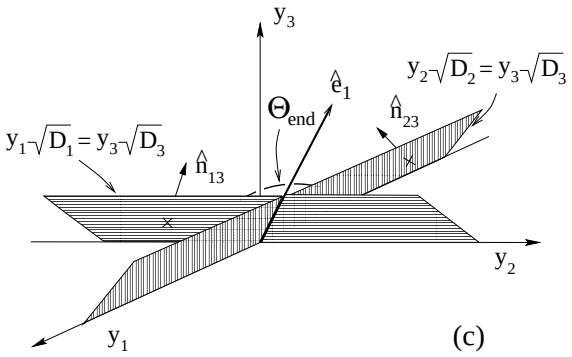

Figure 8.2: Mapping of three diffusing particles on the line to a single isotropically diffusing compound particle in the three-space $y_i = x_i/\sqrt{D_i}$. (a) For a surrounded prey, its co-ordinates are subject to the constraints $y_2\sqrt{D_2} > y_1\sqrt{D_1}$ and $y_2\sqrt{D_2} < y_3\sqrt{D_3}$. The compound particle survives if it remains within the indicated wedge-shaped region of opening angle $\Theta_{\rm mid}$. (b) Projection of this wedge onto a plane perpendicular to the $\hat{e}_1 = (1,1,1)/\sqrt{3}$ axis. (c) For a chased prey, its co-ordinates are subject to the constraints $y_1\sqrt{D_1} > y_3\sqrt{D_3}$ and $y_2\sqrt{D_2} < y_3\sqrt{D_3}$, leading to an allowed wedge of opening angle $\Theta_{\rm end} > \Theta_{\rm mid}$.

From Eq. (7.1.8), the corresponding survival probability exponent is

$$\beta_{\rm mid} = \frac{\pi}{2\Theta_{\rm mid}} = \frac{\pi}{2\cos^{-1}\left(\dfrac{D_2}{\sqrt{(D_1+D_2)(D_2+D_3)}}\right)}. \tag{8.1.1}$$

To understand these results, consider the following illustrative examples:

- If $D_1 = D_2 = D_3$, the wedge angle is $\Theta_{\rm mid} = \pi/3$, giving $\beta_{\rm mid} = 3/2$. This provides basic results for aggregation in one dimension. In aggregation, particles that do not undergo any reaction are monomers. Therefore the monomer density and indeed the densities of aggregates of any fixed mass all decay as $t^{-3/2}$.
- If $D_2 = 0$ (stationary prey), then $\Theta_{\rm mid} = \pi/2$. This gives $\beta_{\rm mid} = 1$, independent of D_1 and D_3. In this limit, the survival probability factorizes into the product of the survival probabilities of the 12 and the 23 reactions. Since the survival probability for each two-particle system is proportional to $t^{-1/2}$, independent of the particle diffusivities, the survival probability of the middle particle in the combined system decays as $(t^{-1/2})^2 = t^{-1}$. This factorization does *not* apply when $D_2 > 0$, as the motions of the two predators are correlated in the rest frame of the prey.
- Finally for $D_2 \gg D_1 = D_3 \equiv \delta$, the wedge opening angle vanishes as $\Theta_{\rm mid} \to \sqrt{2\delta/D}$ and the decay exponent therefore diverges as $\beta_{\rm mid} \to \frac{\pi}{2}\sqrt{D/2\delta}$.

Here, the optimal survival strategy for a surrounded prey is to remain stationary.

For the chased prey – defined to be particle 3 – to survive, both pairs 1 and 3, and 2 and 3 must not meet, while meetings of particles 1 and 2 are immaterial. This gives the simultaneous constraints $y_3\sqrt{D_3} > y_1\sqrt{D_1}$ and $y_3\sqrt{D_3} > y_2\sqrt{D_2}$ that define another wedge in the space of the compound particle (Fig. 8.2(c)). With the same reasoning as that for the surrounded prey, the wedge opening angle for the chased prey is now

$$\Theta_{\rm end} = \pi - \cos^{-1}\frac{D_3}{\sqrt{(D_1+D_3)(D_2+D_3)}},$$

and the corresponding survival exponent is

$$\beta_{\rm end} = \frac{\pi}{2\Theta_{\rm end}} = \left(2 - \frac{1}{\pi}\cos^{-1}\frac{D_3}{\sqrt{(D_1+D_3)(D_2+D_3)}}\right)^{-1}. \tag{8.1.2}$$

We again consider several illustrative cases:

- When $D_1 = D_2 = D_3$, the wedge angle is $\Theta_{\rm end} = 2\pi/3$, corresponding to $\beta_{\rm end} = 3/4$. As we expect naively, for equal diffusivities of all particles, a prey initially at one end is much more likely to survive than a prey between two predators ($\beta_{\rm mid} = 3/2$).

- For $D_3 = 0$ (stationary prey), the problem reduces to two independent one-dimensional survival problems on the semi-infinite line and $\beta_{\rm end} = 1$.

- Finally, for $D_3 \gg D_1, D_2$, the motion of the other two particles becomes irrelevant and the survival probability reduces to that of a particle with an immobile absorbing boundary, for which $\beta_{\rm end} = 1/2$.

Here the optimal survival strategy for a chased prey is to diffuse as rapidly as possible.

8.1.2 Pair Meeting Probabilities

We now determine which of the two particle pairs, 12 or 23, meets first, as a function of their initial positions. To solve this problem, we again translate the initial positions x_1, x_2, and x_3 of the particles on the line to the initial position of the compound particle within the wedge. A given particle pair reacting in one dimension corresponds to the compound particle hitting one of the generators of the wedge. This latter meeting probability is trivial to compute in the wedge geometry (Eq. 7.3.8).

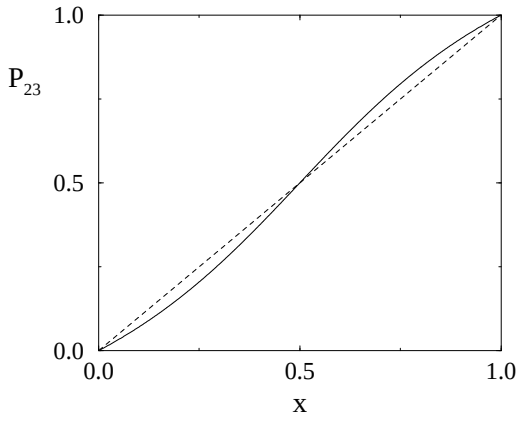

Figure 8.3: Probability P_{23} that the middle particle, in a group of three particles initially at 0, x, and 1, first meets its right neighbor as a function of x. The diffusivities of the three particles are $D_2 = 0$ and $D_1 = D_3$, where P_{23} exhibits the greatest deviation from linearity. For comparison, a line of unit slope – the meeting probability for the case $D_1 = D_3 = 0$ and D_2 non-zero – is also shown (dashed).

To avoid unilluminating complications, consider for the moment equal particle diffusivities, $D_i = D$, $\forall i$. The compound particle then lies within the wedge of opening angle $\pi/3$ defined by $x_1 < x_2$ and $x_2 < x_3$. The apex of the wedge is generated by the unit vector $\hat{e}_1 \equiv (1,1,1)/\sqrt{3}$, and two convenient perpendiculars to this generator are $\hat{e}_2 = (0,-1,1)/\sqrt{2}$ and $\hat{e}_3 = (-2,1,1)/\sqrt{6}$ (Fig. 8.2(b)). For the initial state $\vec{x} = (x_1, x_2, x_3)$, the corresponding components in the co-ordinate system perpendicular to the wedge apex are $z_2 = \vec{x}\cdot\hat{e}_2 = (x_3 - x_2)/\sqrt{2}$ and $z_3 = \vec{x}\cdot\hat{e}_3 = (x_2 + x_3 - 2x_1)/\sqrt{6}$. Consequently the inclination angle of this initial point with respect to the plane $x_2 = x_3$ in plane-polar co-ordinates is

$$\lambda = \tan^{-1}\frac{z_2}{z_3} = \tan^{-1}\left(\frac{\sqrt{3}(x_3 - x_2)}{x_2 + x_3 - 2x_1}\right). \tag{8.1.3}$$

From Eq. 7.3.8, the probability that the plane $x_2 = x_3$ is eventually hit, or equivalently, that particle 2 meets particle 3, is simply $1 - \lambda/\Theta$. Therefore this eventual meeting probability is

$$P_{23} = 1 - \frac{3}{\pi}\tan^{-1}\left(\sqrt{3}\,\frac{1-x}{1+x}\right), \qquad D_1 = D_2 = D_3. \tag{8.1.4a}$$

where we now write $x_1 = 0$, $x_2 = x$, and $x_3 = 1$ without loss of generality.

For general particle diffusivities $D_1 = D_3 = D = \eta D_2$, the counterpart of Eq. (8.1.4a) is

$$P_{23} = 1 - \frac{1}{\cos^{-1}(\frac{1}{1+\eta})}\tan^{-1}\left(\sqrt{\eta^2+2\eta}\,\frac{1-x}{1+\eta x}\right). \tag{8.1.4b}$$

In the limit $\eta \to \infty$, corresponding to the middle particle stationary, this reduces to

$$P_{23} = 1 - \frac{2}{\pi}\tan^{-1}\left(\frac{1-x}{x}\right), \qquad D_2 \ll D_1, D_3, \tag{8.1.4c}$$

while for reference, if $D_2 \gg D_1, D_3$, that is, a diffusing particle in a fixed absorbing interval, the 23 meeting probability is simply

$$P_{23} = x, \qquad D_2 \gg D_1, D_3. \tag{8.1.4d}$$

A plot of the 23 first-meeting probability as a function of x, for the case of a stationary middle particle or, equivalently, infinitely mobile predators ($\eta = \infty$), is shown in Fig. 8.3. This is the case in which P_{23} has the largest deviation from a linear dependence. Even so, this deviation is only barely perceptible. Here $|P_{23} - x|$ attains a maximum value of approximately 0.0453 at $|x - \frac{1}{2}| = 0.262$.

8.1.3 Lead and Order Probabilities

Finally, we study the evolution of the relative particle positions by exploiting the wedge mapping. We treat the case of equal particle diffusivities; the generalization to arbitrary diffusivities is immediate. In the three-space defined by the x_i, the constraints $x_i = x_j$ for $i \neq j$ generate the three planes shown in Fig. 8.4. By projecting onto the subspace perpendicular to the $(1,1,1)$ axis, the constraint planes symmetrically divide the subspace into six regions, each of which corresponds to the co-ordinate orderings indicated. From this categorization, the probability that the compound particle remains within a particular wedge corresponds to the particles on the line satisfying a corresponding set of constraints. From this connection, general order probabilities can be deduced easily.

The general result is that the possible wedge angles are $n\pi/3$, with $n = 1, 2, \ldots, 5$, corresponding to survival probabilities $t^{-3/2n}$, $n = 1, 2, \ldots, 5$. All that remains is to ascribe a physical meaning to these different wedge angles in terms of the relative positions of the particle on the line. For example, the probability that a given particle on the line maintains its lead corresponds to the compound particle remaining within a wedge of opening angle $2\pi/3$ (Fig. 8.4). Therefore the single-particle lead probability decays as

$$P_{\rm lead}(t) \sim t^{-3/4}. \tag{8.1.5a}$$

A specific particle *never* being in the lead is equivalent to the compound particle remaining within a wedge of opening angle $4\pi/3$. Consequently, this no lead probability decays as

$$P_{\text{no lead}}(t) \sim t^{-3/8}. \tag{8.1.5b}$$

The condition that the initial ordering of the co-ordinates never gets reversed corresponds to the compound particle remaining within a wedge of opening angle $5\pi/3$. This "no-reversal" probability therefore decays as

$$P_{\text{no reverse}}(t) \sim t^{-3/10}. \tag{8.1.5c}$$

Finally, we can ask for the probability that the particles *always* maintain their relative positions. That is, if initially $x_1 < x_2 < x_3$, what is the probability that this inequality is always maintained up to time t? According to Fig. 8.4(b), this is equivalent to the compound particle remaining within a single elemental wedge of opening angle $\pi/3$. Consequently, the order probability decays as

$$P_{\rm order}(t) \sim t^{-3/2}. \tag{8.1.5d}$$

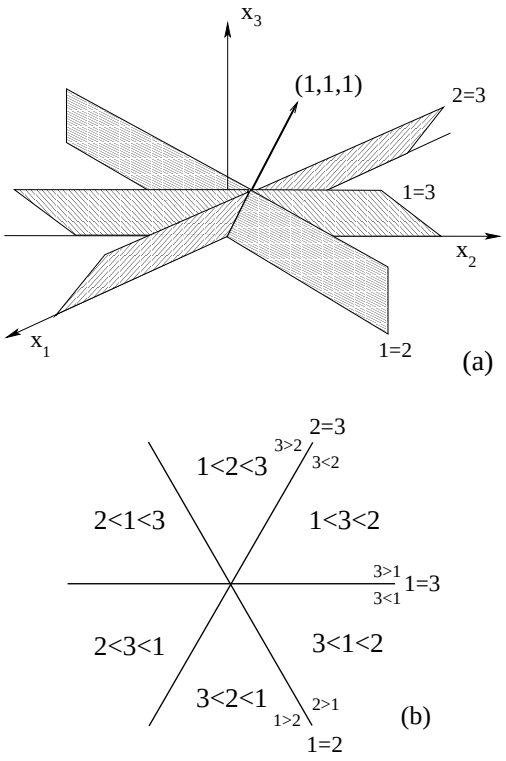

Figure 8.4: (a) The three constraint planes $x_1 = x_2$, $x_1 = x_3$, and $x_2 = x_3$ for the compound particle. (b) Their projection onto the two-space perpendicular to $(1, 1, 1)$ axis. Each $\pi/3$ wedge corresponds to the specific particle ordering indicated.

8.2 Diffusion-Controlled Reactions

We now investigate the diffusion-controlled reactions of capture, coalescence, annihilation, and aggregation in one dimension, where first-passage ideas provide key insights for the kinetics (Fig. 8.5).

8.2.1 The Capture Reaction, $p + P \to P$

We begin with the capture reaction, in which a single prey p is "stalked", and ultimately killed upon contact, by independent diffusing predators P, as represented by $p + P \to P$. We focus on the most interesting situation of predators all to one side of the prey in one dimension. By making a correspondence with the survival of a diffusing particle near an advancing, absorbing boundary, we will show that the prey survival probability in the presence of $N \gg 1$ predators decays as $t^{-\beta(N)}$, where $\beta(N)$ grows logarithmically with N.

In principle, the prey-predator capture reaction is soluble by mapping the $N + 1$-particle system onto diffusion within an absorbing wedge region in $N + 1$ dimensions. For $N = 1$ and 2, the decay exponents may be deduced from our previous discussions of first passage in few-particle systems. From Section 4.4, $\beta_1 = 1/2$ for a diffusing prey and a single diffusing predator, independent of their diffusion coefficients. From Section8.1, $\beta_2 = 3/4$ for equally mobile prey and predators, while for an arbitrary diffusivity ratio $r = D_{\rm prey}/D_{\rm P}$, Eq. (8.1.2) gives

$$\beta_2(r) = \left[2 - \frac{2}{\pi}\cos^{-1}\frac{r}{1+r}\right]^{-1}. \tag{8.2.1}$$

As $D_{\rm prey}/D_{\rm P} \to \infty$, the advantage of two predators versus one is largely negated by their inertness (Fig. 8.7).

For arbitrary N, the rightmost predator typically approaches the prey, even though each predator undergoes isotropic diffusion (Fig. 8.8). We can then apply our results from Section 4.4 to determine the

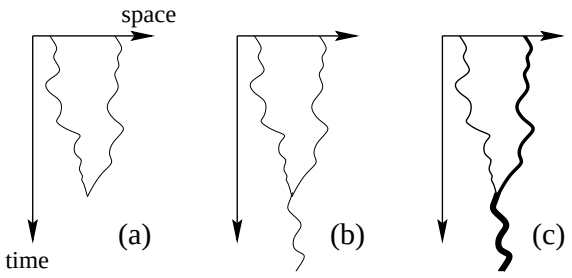

Figure 8.5: Space-time cartoon of the trajectory of a pair of particles in: (a) diffusion-controlled annihilation, $A + A \to 0$, (b) coalescence, $A + A \to A$, and (c) aggregation, $A_i + A_j \to A_{i+j}$. In (c), the thickness of the trajectory indicates the (conserved) aggregate mass

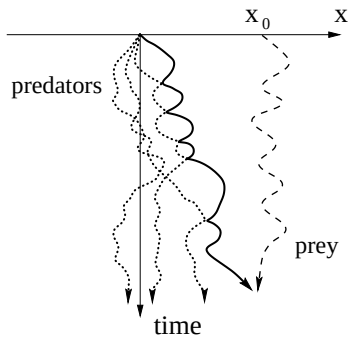

Figure 8.6: Space-time evolution in one dimension of $N = 4$ diffusing predators (dotted curves) that all start at $x = 0$ and a single diffusing prey (dashed curve) that starts at $x = x_0$. The trajectory of the closest ("last") predator, whose individual identity may change with time, is indicated by the heavy solid path.

prey survival probability due to this approaching absorbing boundary. To determine the location of this last predator, $x_{\rm last}(t)$, suppose initially that all the predators are at the origin. We estimate $x_{\rm last}(t)$ by the extreme statistics condition

$$\int_{x_{\rm last}(t)}^{\infty} \frac{1}{\sqrt{4\pi D_{\rm P} t}}\, e^{-x^2/4D_{\rm P}t}\, dx = \frac{1}{N}, \tag{8.2.2}$$

that states that there is one predator from the initial group of N that lies in the range $[x_{\rm last}(t), \infty]$. The asymptotic behavior of this integral can be expressed in terms of the complementary error function, but we can estimate it directly. Since the integral is non-zero only in a very small range beyond $x_{\rm last}$, we write $x = x_{\rm last}(t) + \epsilon$ and expand the integrand for small ϵ to find

$$\int_{x_{\rm last}}^{\infty} \frac{1}{\sqrt{4\pi D_{\rm P} t}}\, e^{-x_{\rm last}^2/4D_{\rm P}t}\, e^{-x_{\rm last}\epsilon/2D_{\rm P}t}\, e^{-\epsilon^2/4D_{\rm P}t}\, d\epsilon = \frac{1}{N}.$$

Over the range of ϵ for which the second exponential factor is non-negligible, the third exponential factor may be set to one. The resulting integral is then elementary, with the result

$$\frac{1}{\sqrt{4\pi D_{\rm P} t}}\, e^{-x_{\rm last}^2/4D_{\rm P}t}\, \frac{2D_{\rm P}t}{x_{\rm last}} \approx \frac{1}{N}. \tag{8.2.3}$$

Defining $y = x_{\rm last}/\sqrt{4D_{\rm P}t}$, this condition can be simplified to $ye^{y^2} = N/\sqrt{4\pi}$, with the solution

$$y = \sqrt{\ln N/\sqrt{4\pi}}\,\Big(1 - \frac{1}{4}\frac{\ln(\ln N/\sqrt{4\pi})}{\ln N/\sqrt{4\pi}} + \ldots\Big).$$

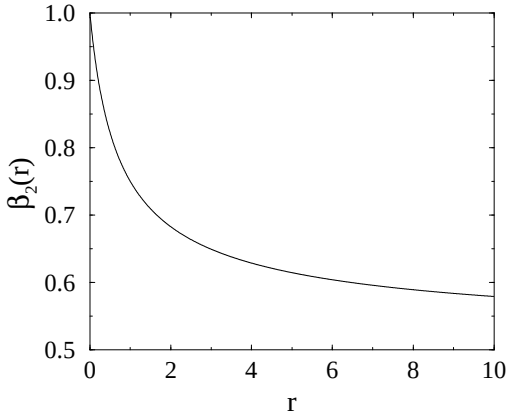

Figure 8.7: The survival exponent $\beta_2(r)$ given by Eq. (8.2.1) versus diffusivity ratio r.

To lowest order, this gives

$$x_{\rm last}(t) \sim \sqrt{4D_{\rm P} \ln N\, t} \equiv \sqrt{A_N t} \tag{8.2.4a}$$

when the number of predators is finite.

For $N = \infty$ it is not sensible to pack all the predators at a single point as $x_{\rm last}(t)$ would identically equal t. A more suitable initial condition is a uniform concentration c_0 of predators that extends from $-\infty$ to 0. Now only $N \propto \sqrt{c_0^2 D_{\rm P} t}$ of the predators are "dangerous," that is, within a diffusion distance from the edge of the pack and thus potential killers of the prey. Consequently, for $N \to \infty$, the leading behavior of $x_{\rm last}(t)$ becomes

$$x_{\rm last}(t) \sim \sqrt{2D_{\rm P} \ln(c_0^2 D_{\rm P} t)\, t}\,. \tag{8.2.4b}$$

Since the last predator advances toward the prey as $\sqrt{A_N t}$ for N finite and as $\sqrt{2D_{\rm P} \ln(c_0^2 D_{\rm P} t) t}$ for $N = \infty$, this suggests that we use the method of Section 4.4 for the survival probability of a diffusing particle near an approaching, absorbing boundary. This method becomes more accurate for large N, as the distribution of $x_{\rm last}$ becomes both smoother and sharper (albeit slowly) as N increases (Fig. 8.8). In the large-N limit, we therefore replace the stochastically moving absorbing boundary induced by the last predator with the smoothly moving boundary whose position is given by Eq. (8.4.2). Then we may transcribe our results from Section 4.4 to determine the prey survival probability. For finite N, this gives the survival exponent

$$\beta_N(r) \sim A_N/16D_{\rm prey} \sim \ln(Nr)/4r, \tag{8.2.5}$$

while for $N \to \infty$, the survival probability decays as

$$S_\infty(t) \sim \exp(-\ln^2 t/8r). \tag{8.2.6}$$

However, different asymptotic behavior should arise in the extreme limits of $r \to 0$ and $r \to \infty$. In the limit of a stationary prey, we know that $S_N \sim t^{-N/2}$, while for an infinitely mobile prey, the survival probability should simply decay as $t^{-1/2}$. By matching these with Eq. (8.2.5), we infer that the full dependence of β_N on the diffusivity ratio r is

$$\beta_N(r) = \begin{cases} N/2 & r \ll 1/N; \\ \ln(4Nr)/4r & 1/N \ll r \ll \ln N; \\ 1/2 & r \gg \ln N. \end{cases} \tag{8.2.7}$$

The result for the intermediate regime of $1/N \ll r \ll \ln N$ represents the generalization of the three-particle exponents in Eqs. (8.1.2) to arbitrary N.

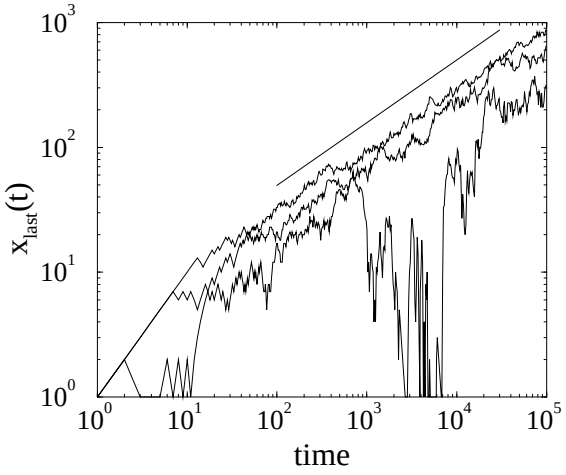

Figure 8.8: Time dependence of $x_{\rm last}$ for a single realization of $N = 4$, 64, and 1028 nearest-neighbor random walks starting from $x = 0$ (bottom to top). The straight line of slope 1/2 indicates the expected long-time behavior.

The actual value of the survival exponent merits comment. As in the approaching cliff problem of Section 4.4, the exponent in Eq. (8.2.7) is not particularly accurate for intermediate values of N, although the correct asymptotic behavior for $N \to \infty$ is reproduced. For example, for the case $r = 1$, estimates for β_N from numerical simulations are $\beta_3 \approx 0.91$, $\beta_4 \approx 1.032 \pm 0.01$, and $\beta_{10} \approx 1.4$. In contrast, the asymptotic formula $\beta_N = \frac{1}{4}\ln(N)$ gives $\beta_3 = 0.274\ldots$, $\beta_4 = 0.346\ldots$, and $\beta_{10} = 0.575\ldots$.

8.2.2 Coalescence, $A + A \to A$

The kinetics of the coalescence reaction $A + A \to A$ is particularly simple because it can be reduced to an effective one-body system. This stems from the fact that the particles are indistinguishable so that each particle sees only the "cage" formed by its two nearest neighbors. It is immaterial that these neighbors may coalesce with more distant particles (Fig. 8.9). Consequently, the kinetics of each particle involves only itself and its two nearest neighbors.

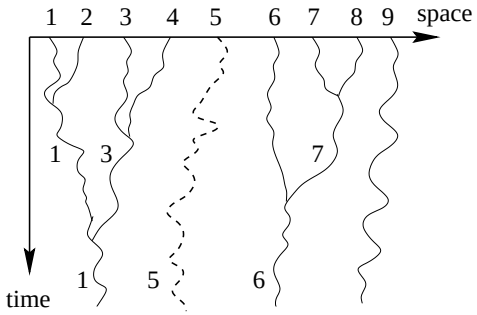

Figure 8.9: Space-time particle trajectories for $A + A \to A$ in one dimension showing the propagation of the particle numbers. The trajectories of the nearest neighbors to particle 5 (dashed) form a cage whose boundaries diffuse even as reactions between these neighbors and more distant particles occur. Particle 5 and the two cage particles can be treated independently of the rest of the system.

To implement the reduction of coalescence to a one-body problem, it is convenient to define a particle as

"killed" if it meets its left neighbor, while the particle continues to "live" if it meets its right neighbor. This identifies the labels of the surviving particles unambiguously. To determine the fate of any particle, we need consider only a particle and its left neighbor; the latter continues to diffuse even if it experiences additional coalescence events. Suppose that the initial separation of the particle and its left neighbor is x_0. Since both the particle and its neighbor have diffusion coefficients D, the two-particle system is equivalent to a single particle with diffusivity $2D$ that diffuses and is ultimately trapped at a stationary absorbing point.

The probability $\rho(x,t)$ that the separation between the two particles equals x at time t therefore obeys the diffusion equation, subject to an absorbing boundary condition at $x=0$. The Green's function for this diffusion equation is simply the image solution given in Eq. (3.1.1) but with $D \to 2D$. Therefore

$$\rho(x,t) = \int_0^\infty G(x,x_0,t)\rho(x_0,0)\,dx_0, \tag{8.2.8}$$

with

$$G(x,x_0,t) = \frac{1}{\sqrt{8\pi Dt}}\left[e^{-(x-x_0)^2/8Dt} - e^{-(x+x_0)^2/8Dt}\right] \underset{t\to\infty}{\longrightarrow} \frac{1}{\sqrt{8\pi Dt}}\,\frac{xx_0}{2Dt}\,e^{-(x^2+x_0^2)/8Dt}. \tag{8.2.9}$$

From the distance distribution $\rho(x,t)$, the particle survival probability $S(t)$ is just the probability that the interparticle distance remains positive at time t. This gives

$$S(t) = \int_0^\infty \rho(x,t)\,dx, \tag{8.2.10}$$

and the particle concentration is simply given by $c(t) = c_0 S(t)$. The distance distribution of the surviving particles at time t, $p(x,t)$, is then given by

$$p(x,t) = \rho(x,t)/S(t). \tag{8.2.11}$$

As long as the probability distribution of initial distances x_0 decays rapidly for large x_0, the long-time behavior of the distance distribution and the particle concentration are *independent* of the initial condition. For a bounded initial distance distribution, we may set $e^{-x_0^2/8Dt} \to 1$ in the Green's function of Eq. (8.2.9) as $t\to\infty$. In this case $\rho(x,t)$ becomes

$$\rho(x,t) \sim \frac{1}{\sqrt{8\pi Dt}}\int_0^\infty \frac{x}{2Dt}e^{-x^2/8Dt}\,[x_0\rho(x_0,0)]\,dx_0. \tag{8.2.12}$$

Notice the separation of the dependences on x and x_0 and, more importantly, that the integral is just the first moment of the initial distribution of separations. By definition, this is just the inverse of the initial concentration $1/c_0$. We therefore obtain

$$\rho(x,t) \sim \frac{1}{\sqrt{8\pi Dt}}\frac{x}{2Dt}e^{-x^2/8Dt}\,\frac{1}{c_0}. \tag{8.2.13}$$

Now, integrating over all x, we find that the survival probability is

$$S(t) \sim \frac{1}{\sqrt{2\pi Dt}}\frac{1}{c_0}. \tag{8.2.14}$$

In summary, the concentration at long times is

$$c(t) = c_0 S(t) \sim \frac{1}{\sqrt{2\pi Dt}}, \tag{8.2.15}$$

while the probability that two nearest-neighbor particles are separated by a distance x is

$$p(x,t) = \rho(x,t)/S(t) \sim \frac{x}{4Dt}e^{-x^2/8Dt}, \tag{8.2.16}$$

independent of the initial conditions.

8.2.3 Annihilation, $A + A \to 0$

At first sight, the annihilation reaction $A+A \to 0$ seems more difficult to treat than coalescence, $A+A \to A$, as the surrounding cage of a specific particle sometimes diffuses and occasionally increases in size suddenly if one of the cage particles is annihilated (Fig. 8.10). Because of this sporadic motion, the single-particle picture that provided the solution for coalescence is not appropriate for annihilation. We treat this reaction by noting that the motion of reactants in $A+A \to 0$ is identical to the motion of ferromagnetic domain walls in the kinetic Ising-Glauber model at zero temperature. By this equivalence, we can obtain the solution for the particle concentration in $A + A \to 0$ merely by transcribing the appropriate results from the Glauber solution of the kinetic Ising model.

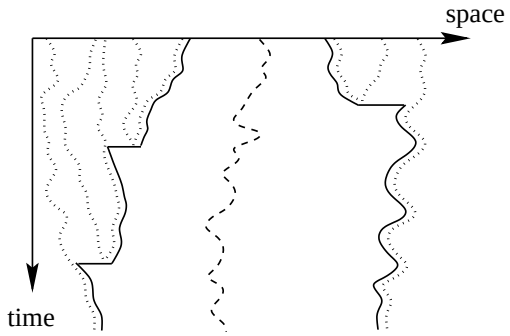

Figure 8.10: Space-time particle trajectories for $A + A \to 0$ in one dimension. The boundaries of the "cage" that surrounds the dashed particle trajectory is shown solid.

The starting point for this equivalence is the identification of domain walls in the Ising-Glauber model with reactants in the annihilation process. For the Ising model at low temperature, the spins organize into aligned domains (Fig. 8.11) that are separated by domain-wall particles. The zero-temperature Glauber kinetics is equivalent to a process in which domain-wall particles diffuse freely and annihilate whenever they meet – that is, $A + A \to 0$.

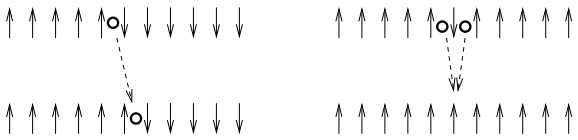

Figure 8.11: Equivalence between Ising spins in one dimension and $A+A \to 0$. Nearest-neighbor antiparallel spins define a domain-wall particle (heavy dot) that hops to a nearest-neighbor site whenever a spin flips. If the target site is already occupied, annihilation occurs.

To exploit this correspondence, consider the two-spin correlation function in the Ising system $c_k = \langle \sigma_i \sigma_{i+k} \rangle$ (see Section 4.2), where σ_i is the spin at site i takes the values ± 1 and $\langle \cdots \rangle$ denotes the thermal average. For a translationally invariant system, this correlation function depends only on the separation k between the two spins. We can also use this correlation function to count the number of domain-wall particles. When spins i and $i+1$ are antiparallel, $(1 - \sigma_i \sigma_{i+1})/2$ equals 1, while this quantity equals 0 if the spins are antiparallel. The average number of domain-wall particles in the spin system, or equivalently, the number of A's in the reactive system, is then $A(t) = (1 - \langle \sigma_i \sigma_{i+1} \rangle)/2 = (1 - c_1)/2$. Since the exact behavior of the two-spin correlation function is known for any initial condition, we can transcribe this result to obtain the particle density in $A + A \to 0$.

From the original Glauber solution, the two-spin correlation function at zero temperature is

$$c_k(t) = 1 + e^{-2t} \sum_{m=1}^{\infty} [c_m(0) - 1][I_{k-m}(2t) - I_{k+m}(2t)], \tag{8.2.17}$$

where $I_n(z)$ is the modified Bessel function of the first kind of order n. For a random initial spin state with $\langle \sigma_i \rangle = m_0$, the initial value of the nearest-neighbor correlation function is $c_1(0) = m_0^2$. Then, using the fact that the modified Bessel function satisfies $I_n(z) = I_{-n}(z)$ for integer n, we find that most of the terms in the infinite series of Eq. (8.2.17) for $c_1(t)$ cancel in pairs and we are left with

$$c_1(t) = 1 - e^{-2t}(1 - m_0^2)[I_0(2t) + I_1(2t)], \tag{8.2.18}$$

from which the density of domain walls is

$$A(t) = (1 - c_1(t))/2 = \frac{1}{2}(1 - m_0^2)e^{-2t}[I_0(2t) + I_1(2t)] \sim \frac{1 - m_0^2}{\sqrt{4\pi t}} + \mathcal{O}(t^{-3/2}). \tag{8.2.19}$$

Amusingly, for $m_0 = 0$ the asymptotic density is independent of the initial particle density, while for $m_0 \neq 0$, the asymptotic density depends on this initial density. Intuitively, this arises because a non-zero magnetization corresponds to particles in the initial state that are more likely to be arranged in pairs.

8.2.4 Aggregation, $A_i + A_k \to A_{i+j}$

Finally, we study the kinetics of irreversible aggregation, $A_i + A_j \to A_k$, with $k = i + j$. Here A_i denotes a cluster of mass i, and in a reaction between an i-cluster and a j-cluster, the result is a cluster of mass $k = i+j$. The basic physical observables in aggregation are the concentrations of clusters of mass k at time t, $c_k(t)$. Parallel to our treatments of coalescence and annihilation, we consider aggregation in one dimension, where insights from first-passage phenomena help determine the kinetics. For simplicity, we assume that aggregates are always structureless point clusters; thus by ignoring the cluster masses, aggregation reduces to the coalescence reaction. We also assume that the diffusion coefficients of the aggregates are independent of their mass. Although this latter assumption is generally not true, this idealization allows us to recast aggregation as a classical first-passage problem. The extension to general mass-dependent diffusion and mass-dependent reaction rates represents a challenging open problem.

Amazingly, the concentration of k-clusters at any time has exactly the same form as the first-passage probability for diffusion in one dimension with absorption at $k = 0$. For example, for the monomer-only initial condition $c_k(t = 0) = \delta_{k,1}$,

$$c_k(t) = \frac{k}{\sqrt{4\pi D t^3}}\, e^{-k^2/4Dt}. \tag{8.2.20}$$

The simple behavior ultimately stems from the fact that, in one dimension, the mass contained inside a fixed-length interval undergoes a diffusion process. This mass can change either by a cluster just inside the interval hopping out, or by a cluster just outside the interval hopping in. The equation of motion that describes the mass evolution in the interval also satisfies an absorbing boundary for intervals of zero length. It is these two attributes that lead to an equivalent first-passage description for $c_k(t)$.

To solve for the cluster concentrations, we first consider the quantity $A_{i,j}^M$, defined as the set of states in which there is a total mass M in the site interval (i, j) (Fig. 8.12). It is convenient to view the mass as being located at the midpoints between sites so as to include the possibility of a zero-length interval (i, i) that necessarily contains zero mass. In an interval that is part of $A_{i,j}^M$, the mass may be distributed arbitrarily among clusters as long as the total mass equals M.

We now enumerate the possibilities that contribute to the change of the mass in this interval. The crucial point is that in terms of the sets $A_{i,j}^M$ a simple diffusion equation emerges whose solution immediately gives the concentration of clusters of a given mass.

- Gain terms: These are illustrated on the left-hand side of Fig. 8.13 from top to bottom.

1. Mass M in $(i, j-1)$ and an arbitrary-mass k-cluster in $(j-1, j)$ leaves the interval by hopping to the right. Thus mass M exists in $(i, j-1)$ but not in (i, j) – this is the state set $A_{i,j-1}^M - A_{i,j}^M$.

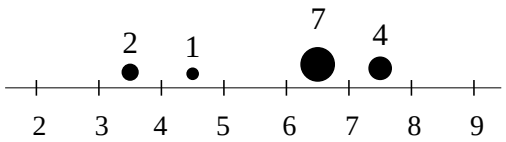

Figure 8.12: Example configuration that contributes to $A^{14}_{3,8}$ – four clusters within $(3, 8)$ whose total mass is 14. The numbers over the dots denote the individual cluster masses.

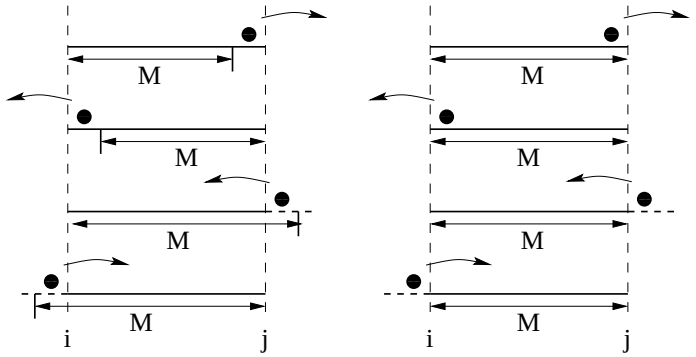

Figure 8.13: Configurations that contribute to the change in the set of states with mass M in the interval (i, j). The left-hand side shows the four processes that lead to a gain in A^M_{ij}, and the right-hand side shows the four loss processes.

2. M in $(i + 1, j)$ and a k-cluster in $(i, i + 1)$ hops to the left – state set $A^M_{i+1,j} - A^M_{i,j}$.

3. M in $(i, j + 1)$ and a k-cluster in $(j, j + 1)$ hops left to enter (i, j) – state set $A^M_{i,j+1} - A^M_{i,j}$.

4. M in $(i - 1, j)$ and a k-cluster in $(i - 1, i)$ hops right to enter (i, j) – state set $A^M_{i-1,j} - A^M_{i,j}$.

- Loss terms: Right-hand side of Fig. 8.13 from top to bottom.

1. M in (i, j) and a k-cluster in $(j - 1, j)$ hops right to leave (i, j) – state set $A^M_{i,j} - A^M_{i,j-1}$.

2. M in (i, j) and a k-cluster in $(i, i + 1)$ hops left to leave (i, j) – state set $A^M_{i,j} - A^M_{i+1,j}$.

3. M in (i, j) and a k-cluster in $(j, j + 1)$ hops left to enter (i, j) – state set $A^M_{i,j} - A^M_{i,j+1}$.

4. M in (i, j) and a k-cluster in $(i - 1, i)$ hops right to enter (i, j) – state set $A^M_{i,j} - A^M_{i-1,j}$.

The probability for each of these composite configurations can be expressed in terms of elemental configurations. For example, consider the probability $P(A^M_{i,j-1} - A^M_{i,j})$ to have mass M in $(i, j - 1)$ but not in (i, j). By straightforward counting, the probability for these states to occur equals $P^M_{i,j-1} - P(A^M_{i,j}|0)$. Here the first term is the probability that mass M occupies $(i, j - 1)$ *without* any occupancy restrictions on the boundary and the second term is the probability that mass M occupies (i, j) *and* $(j - 1, j)$ is unoccupied.

By adding all the processes enumerated above, we obtain the diffusion-like equation of motion

$$\frac{\partial P^M_{i,j}}{\partial t} = r(P^M_{i+1,j} + P^M_{i-1,j} + P^M_{i,j+1} + P^M_{i,j-1} - 4P^M_{i,j}), \tag{8.2.21}$$

where r is the hopping rate for each cluster per unit time. For a translationally invariant system, $P^M_{i,j}$ is just a function of $x = j - i$. We simplify further by taking the continuum limit in which the lattice spacing δx

and hopping rate r simultaneously go to zero such that their ratio $D = r(\delta x)^2/2$ remains constant. Then the equation of motion reduces to

$$\frac{\partial P^M(x,t)}{\partial t} = D\frac{\partial^2 P^M(x,t)}{\partial x^2}, \tag{8.2.22}$$

that is valid for all $M \geq 0$.

Thus the interval occupation probabilities are governed by the diffusion equation! Again, this occurs because the mass can change only by local hopping events at the boundary of any interval. The boundary conditions for this diffusion equation are $P^0(0,t) = 1$, $P^M(0,t) = 0$, and $P^M(x,t) \to 0$ as $x \to \infty$. The former two are the continuum limits of the condition that there cannot be any mass in an interval of zero length. The last condition states that the mass in an infinitely long interval cannot remain finite.

Finally, to determine the density of clusters of fixed mass, we start with the fact that $P^M_{i,i+1}$ is the probability that a cluster of mass M occupies $(i, i+1)$. In the continuum limit, we write $i \to x$, $i+1 \to x+\delta x$, so that $P^M_{i,i+1} \to P^M(\delta x) = P^M(0) + \delta x \frac{\partial P^M}{\partial x} + \ldots$. The zeroth-order term in this expansion is zero by definition. Then, by equating the first derivative to the probability that a cluster of mass M occupies a region of size δx, we obtain

$$c_k(t) = \frac{\partial P^k}{\partial x}\Big|_{x=0}. \tag{8.2.23}$$

For a lattice system in which each site is initially occupied by a single particle, $P^M(x) = \delta(x - M)$, since there is exactly a mass M inside an interval of length M. With this initial condition and with absorbing boundary conditions, Eq. (8.2.22) is equivalent to the motion of a particle that starts at $x = k$, diffuses on the positive line, and is absorbed whenever $x = 0$ is reached. The solution to this diffusion problem with an absorbing boundary is just our familiar image solution given in Eq. (3.1.1), from which the corresponding flux at the origin is just the cluster concentration quoted in Eq. (8.2.20).